Guanosine nucleotides link cell wall metabolism and protein synthesis during entry into quiescence

Simon Diez

Submitted in partial fulfillment of the
requirements for the degree of
Doctor of Philosophy
under the Executive Committee
of the Graduate School of Arts and Sciences

COLUMBIA UNIVERSITY

2021

© 2021

Simon Diez

All Rights Reserved

Abstract

Guanosine nucleotides link cell wall metabolism and protein synthesis during entry into quiescence

Simon Diez

Quiescence, a transitory period of non-growth, is a ubiquitous aspect that is present in all organisms. In addition to being present in all forms of life, quiescence is a feature that has been observed in cells that are important for human health, including stem cells in mammals and antibiotic tolerant cells in bacteria. In bacteria, quiescence per se has recently been suggested to underlie the transient tolerance to a wide range of antibiotics. Furthermore, most microbial life exists in a quiescent state. Despite their prevalence and importance, relatively little is known about the physiology of quiescent bacteria. One aspect of bacterial quiescence that has been repeatedly observed is their lowered metabolic activity compared to actively growing bacteria. How do cells that grow and divide enter into a temporary state of non-growth? In particular, how are the energy-intensive processes that are required for growing cells regulated during a non-growing state? The main subject of this thesis is to investigate how protein synthesis, the most energy-intensive process in growing bacterial cells, is regulated during entry into a quiescent phenotype (stationary phase).

I first investigate how protein synthesis is regulated using a single cell method that fluorescently tags nascent polypeptide chains. In chapter 3, I show that during entry into stationary phase, protein synthesis is downregulated heterogeneously with one group of cells having comparatively low protein synthesis, resulting in a population that is approximately bimodal. I further show that this bimodality is dependent on a signaling system (PrkC and its partner phosphatase PrpC) that senses cell wall metabolism. I connect signaling from this system to the expression of an enzyme (SasA) that produces a group of nucleotides that are major regulators of

growth in bacteria ((pp)pGpp). Lastly, I show that the bimodality is dependent on the three enzymes that synthesize (pp)pGpp.

In chapter 4, I explore in detail how the bimodality in protein synthesis is generated. This heterogeneity requires the production of (pp)pGpp by three synthases: SasA, SasB, RelA. I first show that these enzymes differentially affect this bimodality: RelA and SasB are necessary to generate the sub-population exhibiting low protein synthesis, whereas SasA is necessary to generate cells exhibiting comparatively higher protein synthesis. The RelA product (pppGpp) allosterically activates SasB, and I find that the SasA product (pGpp) competitively inhibits this activation. I provide *in vivo* evidence that this antagonistic interaction mediates the observed heterogeneity in protein synthesis. This chapter, therefore, identifies the mechanism underlying the generation of phenotypic heterogeneity in the central physiological process of protein synthesis.

In chapter 5, I next turn to understand the biochemical mechanism by which cells with comparatively low levels of protein synthesis down-regulate this process. I first show that ppGpp is sufficient to inhibit protein synthesis *in vivo*. I then show that ppGpp inhibits protein synthesis by inhibiting translation initiation directly by binding to the essential GTPase, Initiation Factor 2 (IF2). In collaboration with Ruben Gonzalez's lab, we also show that ppGpp prevents the allosteric activation of IF2. Finally, I demonstrate that the observed attenuation of protein synthesis during the entry into quiescence is a consequence of the direct interaction of (pp)pGpp and IF2.

Table of Contents

List of Figures and Tables

Acknowledgments

I would like to thank my mentor during my Ph.D., Dr. Jonathan Dworkin. In particular, I would like to thank him for his constant support of my interest and creativity. Additionally, I would like thank Jonathan for his genuine enthusiasm in my research. I would also like to thank the several other members of the Dworkin lab. I would like to specifically thank Dr. Heather Feaga for her support throughout the entirety of my Ph.D. Her suggestions and advice were instrumental to the development of the work presented in this thesis. I would also like to thank Abigail Whalen for generating the RelA^{Y308A} strain and for helping me with the experiments used to dissect the role of the three (pp)pGpp synthetases presented in Chapter 4. I would also like to thank Dr. Krithika Rajagopalan for helping to train me during my early years in the Dworkin Lab.

Additionally, I would like to thank Dr. Ruben L. Gonzalez Jr. and the members of his lab for working with us to investigate the structural aspects of ppGpp's inhibition of IF2, which are presented in Chapter 5. Specifically, I would like to thank Dr. Ruben L. Gonzalez Jr. for helping to conceptualize the specific question we explored and for helping to design the experiments. I would also like to thank Jaewook Ryu and Dr. Kelvin Caban for performing the experiments and analyzing the data.

I would like to thank Dr. Max E. Gottesman, Dr. Ruben L. Gonzalez Jr., and Dr. Lars E. Dietrich for serving on my committee. Their guidance and constructive suggestions were essential for solidifying the work presented here. I would also like to thank Dr. Luke E. Berchowitz for serving as the outside member during my thesis defense.

Dedication

This thesis is dedicated to my parents and my brother, who take me as I am.

Chapter 1

1 Introduction

1.1 Quiescence

1.1.1 A reversable state of non-growth

Essential to the survival of every form of life is the generation of new cells that will carry on the organism's genome. Equally ubiquitous, however, are cells that do not grow or divide. These cells are described as either senescent and quiescent, based on their ability to re-enter into active growth and division. Senescence is defined as a period of terminal non-growth and division that occurs via direct processes that respond to damage that make a cell unable to generate new cells (1). For example, cells that have sustained significant damage to their telomeres or are incapable of repairing their telomeres due to non-functional telomerase enter into a terminal state of non-growth and division (2). Quiescence, the other form of non-growth, describes cells that enter into a non-growing period, remain viable for a time, and at some point return into active cycles of growth and division (3). Since quiescent cells can re-enter into growth, it is only logical that the stimuli that send them into this state do not constitute fatal errors in the important processes for producing functional cells. However, the signals that cause a cell to become quiescent are less clear than the signals that induce senescence (4).

Another understudied aspect of quiescent cells is their metabolic state. The conversion of energy and nutrients into cellular components (cell wall, proteins, nucleic acids) is of utmost importance for a cell to increase in size and divide (5). What is the state of these processes during quiescence? Quiescent cells of a wide range of organisms have low rates of active processes, which are required for growth, and it is widely believed that their metabolic rate is decreased compared to actively growing cells (6). For example, bacterial cells in quiescent states, such as during

nutrient limitation, have decreased ATP levels (7) and lower rates of protein synthesis (8, 9). Quiescence in yeast, such as occurs during nutrient deprivation, is accompanied by a decrease in transcription rates (10), a lowered translation rate (11), and the generation of a subpopulation of cells in which the cycle is arrested (12). Although quiescent cells have lowered metabolism, they are not believed to be completely metabolically inactive like cells that have entered into a dormant phenotype such as bacterial spores. That is, although they clearly have lower levels of the processes that require energy, they maintain these processes at lower levels, and there is evidence to suggest that they are necessary for quiescent cell survival. For example, inhibition of protein synthesis negatively affects viability of bacterial cells that have already entered into starvation induced quiescence (13), suggesting that although quiescent cells have lowered protein synthesis and metabolism, some level of these processes is still necessary.

Presumably, it would not be advantageous for a quiescent cell to maintain a highly active cellular program. A cell that expends limited energy and resources and does not generate a new viable cell that passes on the genetic material is at a disadvantage to a cell that does. In addition, if a quiescent cell does not dilute newly generated cellular components through growth or division, then the cell has a limited volume to store them. Ultimately, unregulated accumulation of one or more cellular components without commensurate growth could lead to lysis of the cell. Quiescent cells, therefore, represent a basic biological problem: How are the energy-consuming processes of growing cells down-regulated upon entry into quiescence?

1.1.2 A functional aspect of important cell types

In addition to being universal, quiescence has been postulated to be an essential aspect of biology in that it serves as a regulator of exponential growth. The argument for quiescence is best put in terms of a simple single-celled organism. Given the growth rate of a single cell of

Escherichia coli (*E. coli*) under optimal conditions, the entire biomass of the earth would be quickly taken up were it not for a mechanism that limited exponential growth (14). Following this argument strictly, there must be a way for life to regulate its rate of expansion, or it risks using up all of its available resources and dies. But in any real environment, a single *E. coli* cell will only have access to a limited number of resources within spatial proximity. These resources flow in and out at rates that can be unpredictable. This reality again brings up the problem of unregulated exponential growth. A cell that uses up all the available nutrients within its vicinity may be left without nutrients for an undetermined period of time. For this reason, it is believed that quiescence is not just advantageous to survival but may be an essential mechanism of life.

Quiescence is also a feature of cells that are important for human health. A well-studied example of quiescent cells is the adult stem cells (ASCs) that constitute the reservoir of human cells with the potential to replenish other cell types in adults. The extent to which ASCs are quiescent and how this contributes to their function has been the subject of major study for several decades (4). ASCs exist in both actively dividing and quiescent states (15), but the role of the quiescent reservoir of ASCs has remained unclear. Quiescence has been observed in stem cells that are important for the regeneration of tissues following an injury, those that are central for hematopoiesis, and the cells that are important for epithelial renewal (3). Recent evidence has led to the idea that quiescence may not just be a feature of certain stem cells but could also be an important determinant of how certain stem cells are able to serve as a reserve pool for actively dividing stem cells, especially during tissue injury (16, 17). The function of quiescence in certain stem cells, therefore, would be to serve as a backup to either replenish the actively dividing subset of ASCs or to provide extra support during stress.

1.1.3 Persistence

The emergence of antibiotic-resistant bacteria is a major topic of biological, public health, and economic discussion (18). Most attention has centered on the dissemination of genetic changes that allow specific strains of bacteria to continue to grow in the presence of the antibiotic agent (19). Another form of antibiotic treatment evasion occurs when a small fraction of a growing bacterial population stochastically enters into a quiescent phenotype with comparatively low levels of processes like protein translation, cell wall synthesis, transcription, and DNA replication. As a consequence, these cells exhibit increased tolerance to antibiotics that target active processes in bacterial cells. For example, if a population of cells is treated with a β–lactam (the most widely used class of antibiotics) such as penicillin, the penicillin will covalently bind to a group of essential proteins that are involved in the formation of the polymer that makes up the bacterial cell wall (peptidoglycan) (20). These proteins, called penicillin binding proteins (PBPs), carry out the transpeptidase and carboxypeptidase activity required to generate and remodel peptidoglycan (21). Penicillin, therefore, inhibits active bacterial cell growth. Its clinical success, however, is often dependent on the presence of cells with active cell wall synthesis. A cell with very little or no cell wall synthesis will not have active PBPs whose function can be impeded by penicillin. The presence of these cells within a bacterial population would therefore provide a reservoir of survivors cells that, if they remain viable until the antibiotic is removed, could reinstate the bacterial population.

These survivor cells were first described by Bigger in 1944 (22). Bigger followed up on observations by Hobby et al. in 1942, who first showed that a small proportion of *Staphylococcus aureus* (*S. aureus*) cultures (less than 1% of cells) are able to resist treatment with penicillin (23). Bigger confirmed this result and further showed that upon recovery, the small number of cells that

survive have the same growth characteristics as the original population. That is, the cells that somehow survived the penicillin treatment do not exhibit a growth pattern that would suggest that they had acquired any genotypic difference that would account for the survival of the original penicillin treatment. Furthermore, when Bigger used these survivors to repopulate a bacterial culture and again treated with penicillin, the proportion of cells that survived the treatment was indistinguishable from the original experiment. This observation confirmed that the ability to survive the antibiotic treatment was not due to a genotypic difference between susceptible and survivor cells but that the difference between these cell types was phenotypic. Bigger termed this kind of antibiotic tolerance as bacterial persistence, and he carefully denoted the difference between persistent bacteria (phenotypic survivors) and resistant bacteria (genotypic survivors). Since these observations, persistent bacterial cells have been the subject of major study. Despite a large body of work, the molecular mechanisms that generate persistent cells are unclear, and no single mechanism(s) has been definitively shown to be essential for persister formation.

Bigger also originally tied these phenotypic survivors to quiescence. When trying to understand the nature of persistent cells, Bigger tested whether persistence was affected by growth status in *S. aureus* (22). This was motivated by previous observations that suggested that penicillin affected cell division (24). Bigger reasoned that if persister cells were not affected by penicillin, then maybe their divisional status might differ from cells that died in the presence of penicillin. Bigger showed that cultures of *S. aureus* in a static (non-growing and non-dividing) state had higher proportions of persisters than those that were actively growing and dividing (22). Periods of non-growth in bacterial cultures are a ubiquitous condition called stationary phase. While bacteria are capable of very rapid growth (called exponential growth) when nutrients are replete, all bacteria enter into stationary phase in response to limiting nutrients (9). However, rather than a

simple exit from rapid growth as a consequence of the absence of a building block important for generating a new cell, stationary phase is a directed process that ensures survival in the absence of nutrients (9). Stationary phase is accompanied by changes gene expression as well as a reduction in energy intensive processes such as RNA and protein synthesis (25).

Recent work suggests that perhaps no single mechanism is directly responsible for persistence, but rather that these mechanisms contribute to a cellular state that itself makes a cell transiently tolerant to antibiotics. In 2019 Pontes and Groisman provided evidence that certain mechanisms (Toxin Anti-toxin (TA) systems and (pp)pGpp) that inhibit cell growth and can increase persistence are not essential for the presence of tolerant cells under conditions where growth is already slowed. They further showed that inhibiting growth on its own using various methods is sufficient to increase the number of cells that survive antibiotic treatment. This led them to propose that slow growth itself is the mediator of persistence and that specific cellular processes are linked to persistence in that reduce the growth rate decrease (26).

A complete understanding of the biology of bacterial persistence remains elusive, but the threat that it poses in the fight against bacterial infections is more tangible. Firstly, bacterial persistence is generally believed to underlie certain chronic infections, which are damaging to health and costly (27, 28). Mounting evidence shows that the cells from chronic bacterial infections exhibit slow growth like persister cells (29). Treatment of chronic infections by repeated cycles of antibiotic treatment can have potential consequences (30). For example, persistent cells within a bacterial population that survive multiple rounds of antibiotic exposure have recently been linked to the rise of genetic resistance (31).

1.2 Heterogeneity

1.2.1 Role of heterogeneity

Heterogeneity in isogenic populations of bacteria is well documented. For example, *Pseudomonas aeruginosa* (*P. aeruginosa*) biofilms display differential gene expression and antibiotic tolerance depending on where they reside within the biofilm (32, 33). *B. subtilis* developmental states, such as competence, occur in only a subpopulation of cells during stationary phase (34). But why is heterogeneity advantageous for the survival of bacterial populations? To answer this question, it is essential to thoroughly consider the native environment in which communities of bacteria reside.

Unlike exponential growth in a laboratory environment, most microbial life exists in nutrient limited environments. Optimal growth is dependent on the right combination of nutrients (carbon, phosphate, nitrogen), temperature, pH, and salinity. Bacteria also face danger from antibiotic molecules (either generated by other organisms or those applied clinically). Furthermore, infection by phage is a major threat to all bacteria outside of the laboratory. A bacterial cell that does not accurately adjust to a change in any of these environmental factors not only risks being at a disadvantage to ones that do but even losing viability altogether. Furthermore, environmental conditions are unpredictable and can cycle between being optimal for growth to poorly sustaining life at inconsistent rates. For example, rapid and slow growth can both be advantageous for bacteria infecting a human host depending on whether antibiotic treatment is applied. But a bacterial community has no way to predict if this will be the case. An alternative strategy for a group of isogenic cells is to display both slow and fast growing phenotypes. This way, some members of the community will be well adapted to any situation. This hypothesis is backed up by simulations of bacterial assemblages, which show that a population of isogenic cells can actually achieve a

higher net growth rate by generating heterogeneity under fluctuating environmental conditions (35).

Mounting evidence suggests that heterogeneity is advantageous in clonal bacterial populations (36, 37). But is phenotypic heterogeneity achieved passively, as a result of imprecise systems, or do direct mechanisms mediate the generation of heterogeneity? It is unlikely that a single biological mechanism could be so precise as to yield a distinct output with very low variance when applied to a population of thousands to millions of cells (38). This biological variance could itself generate groups of cells that differ slightly from each other, and if the system is imprecise enough, then the cells on either extreme could display significantly different phenotypes(38). But more extreme forms of heterogeneity exist. For example, populations of isogenic bacteria often do not display phenotypes centered around a single mean but rather two.

1.2.2 Bimodality

Bimodal distributions of gene expression and physiological state are readily observable in bacteria. One common example, which I have already discussed, is antibiotic persistence. When Bigger first explained tolerance to penicillin by a small number of cells within a population of non-resistant cells, he also presented the first piece of evidence that temporary tolerance to antibiotics is, on a population level, bimodal. He noted that in cultures of *S. aureus* treated with penicillin, not only do most cells die and a few survive, but also that the rate of death occurred in a biphasic fashion. That is, whereas most of the cells (99% of the population) died within the first 6 hours, the rest of the population died over a much larger time window (over 72 hours). This evidence, which has been confirmed many times since then, suggests that on a population level, tolerance to penicillin is bimodal. This phenomenon was confirmed 60 years later, and bacterial persistence has now been shown to be a phenotypic switch (39).

Bimodal phenotypes arise from mechanisms that display bi-stability in which either of two extremes represents a more energetically stable state than the ones that lie between these two states. For example, in Bigger's experiments, cells were either susceptible to penicillin or tolerant to it. How does biology generate bistable systems? Two mechanisms have been identified that generate bimodality in isogenic populations (40, 41). The first involves a master regulator whose activity is auto-activated in a non-linear fashion. The nonlinearity of activation allows for a small change in concentration of the master regulator to provide two vastly different outputs. This kind of regulation has been experimentally validated using a gene regulation circuit in *Saccharomyces cerevisiae* (*S. cerevisiae*), where a graded increase in a transcriptional activator can provide a binary response in GFP production if the transcriptional activator activates not only GFP transcription but also its own transcription (42). The second mechanism involves two mutually repressive repressors. The first repressor (R1) is inactivated if the second repressor (R2) is present. If R2 becomes inactivated for any reason, such as due to an external stimulus, then the expression of R1 is turned on. R1 then stimulates expression of itself. Finally, since R1 represses R2 expression, once R1 expression reaches a certain point, then the system tends to stay in an R1 ON state **(Figure 1.1)**.

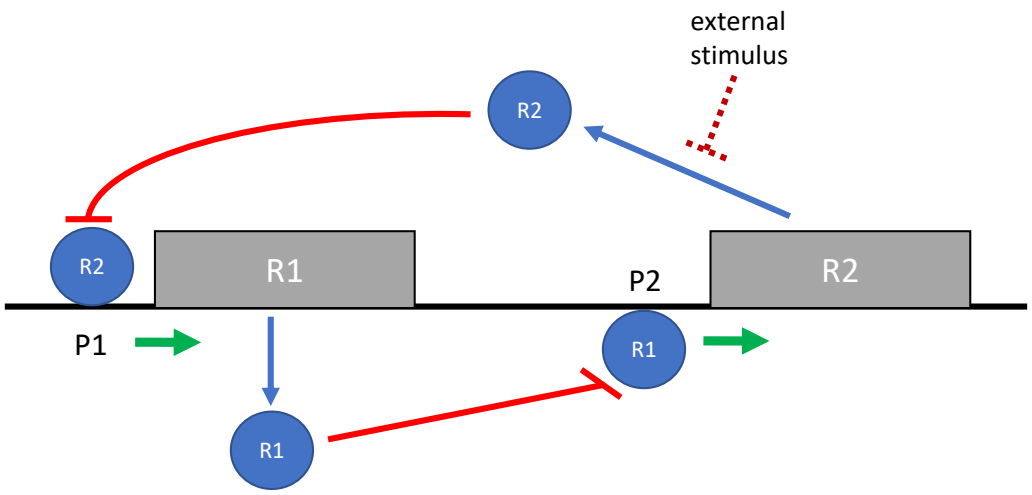

Figure 1.1 Mutually repressing repressors. Bistability in gene expression can be the product of a gene network where two genes act as repressors of each other. Expression of the first repressor, R1 is controlled by the second repressor R2 and vice versa. So under conditions where R2 is expressed, R1 expression is inhibited, and R2 expression is therefore de-repressed. If, for some reason, such as because of an external stimulus, R2 expression decreases, then R1 expression increases. At some point, the buildup of R1 is able to repress R2 expression, and R2 concentration decreases further, and the system switches from expression of R2 to R1.

An example of this mechanism is the switching between lysogeny and lysis in phage λ (43). During λ phage infection of *E. coli*, the bacteriophage decides to either enter into a lysogenic phase where it is integrated into the host chromosome or to initiate a lytic program that involves replication of its genome and eventual phage particle production by the host *E. coli* cell. Both lysogeny and lysis are stable states that both repress the progress of the other state. Lysogeny is maintained by the CI repressor, which inhibits transcription of the genes that are essential for lysis and promotes transcription of CI itself as well as lysogeny specific genes, including the lysis promoting *cro*. If, under certain circumstances, the CI repressor becomes inactivated, then expression of the lysis promoting Cro increases. Cro production stimulates expression of itself and lysis specific genes. Cro also represses CI repressor production, which further promotes induction of Cro and lytic genes. CI and Cro, therefore, represent mutually repressive repressors and these two proteins mediate the switch from lysogeny to lysis in λ phage (43).

Either of the two systems discussed above (self-activating master regulator and mutually repressive repressors) can mediate switching in bacterial populations. How are these controlled? Specifically, how does the concentration of the master regulator become upregulated past the tipping point? How does R2 become inactivated?

1.2.3 Types of switching

In theory, two extreme systems could control phenotypic switching. The first, responsive switching, describes mechanisms that generate heterogenous populations of isogenic cells in response to environmental stimuli. This kind of heterogeneity could theoretically allow a population to maximize growth when conditions are favorable by exploiting the replicative power of every single cell. Upon sensing that conditions are not sufficient to sustain growth of all cells, the community of cells would then switch to generate phenotypic heterogeneity. In order for this

type of switching to provide maximal advantage, however, ample time is required for the population to generate heterogeneity.

The second kind of switching, spontaneous stochastic switching, occurs in the absence of an environmental cue. That is, the heterogeneity is intrinsic to the population. Unlike responsive switching, this form of heterogeneity sacrifices the growth of certain members of the population even in the absence of any signal that would communicate to the population that heterogeneity would be advantageous. But, this sacrifice provides an important advantage in the form of the ability to very quickly deal with a very fast-changing environment. Unlike responsive switching, stochastic generation of variants preemptively provides the population with a reservoir of cells that can survive a rapid change in environmental conditions. For this reason, stochastic switching has been shown through modeling and simulation to be advantageous compared to responsive switching in a dynamic environment (44).

1.2.4 Sources of switching: Noise

As described above, switching between different phenotypes occurs stochastically, and this has been linked to either expression of a gene that acts to upregulate its own activity in a non-linear fashion or by expression of two mutually repressive repressors. Both of these mechanisms translate small changes in the expression of master regulators into bistable gene expression. But what causes the initial small variation? A degree of variance in the expression of any given gene product is a general characteristic of gene expression. The synthesis of an mRNA from a DNA template, followed by the translation of this mRNA into a protein, are all processes that are carried out by the biochemical activity of a relatively small number of enzymes (45). The low abundance of these enzymes means that even small variations in their absolute numbers between two cells can result in a noticeable difference in the expression of a gene in these two cells (46, 47). In

addition, their fidelity in carrying out a biochemical process is not perfect (48). The variance that both of these aspects of gene expression provide to heterogeneity between cells is termed noise and has been observed in systems including phage infection (49), *lac* operon regulation (50), and chemotactic swimming (51).

Two basic types of noise exist in gene expression. The first, intrinsic noise, refers to noise that occurs as a part of the randomness of the biochemical reactions that are a part of gene expression, such as binding of a transcription factor to a DNA element. Intrinsic noise in gene expression manifests itself as randomness that is not specific to a given gene. That is, if a cell had two genes under the same expression control (identical promoters), intrinsic noise would cause the levels of each gene to not be highly correlated even though they are under the same control. The second, extrinsic noise, affects gene expression in a manner that is not specific to a particular gene. This kind of noise arises from differences in the abundances of cellular components that are important for gene expression, such as RNA polymerase (46). Differences in extrinsic noise would cause the same two genes above to have expression levels that were highly correlated. Both of these types of gene expression have been found to be physiologically relevant experimentally, and both contribute significantly to heterogeneity in cells (52). Furthermore, noisy gene expression has been observed throughout the genome in *E. coli* (53). Intrinsic noise could explain the differences that give rise to stochastic switching that is observed in bacteria populations. But the ability to regulate the level of noise in response to specific stimuli is an appealing feature of extrinsic noise from an evolutionary standpoint. Importantly, both forms of noise are subject to selection via evolution, but extrinsic noise could adjust the level of heterogeneity in a population in response to a stimulus that reflects changes in environmental conditions.

1.3 Signaling through membrane bound kinases

1.3.1 Sensing of environmental conditions

As I discussed above, bacteria live in environments that often provide unpredictable amounts of nutrients and other factors that are necessary for growth. For this reason, mechanisms that sense the environment are essential for survival. The most well-studied sensory mechanisms used by bacteria involve transduction of a signal through two-component systems (TCS) (54). The basic architecture of a TCS involves a sensor protein, whose activity is stimulated by a specific stimulus, and a response regulator that carries out the cellular function appropriate for the environmental condition (54). The sensor modifies the response regulator and therefore changes its activity. The prototypical sensor is a histidine kinase that auto-phosphorylates on a conserved histidine residue in response to a specific signal (54). This phosphorylation is followed by transfer of this phosphoryl group to its corresponding response regulator. The phosphorylation on the response regulator occurs on a conserved aspartate residue on a signal receiver domain that activates an output domain that mediates an appropriate cellular function. The response regulator is typically a DNA-binding protein, and phosphorylation affects DNA binding resulting in transcriptional changes (54). Many sensor kinases are bi-functional, meaning they mediate the addition and removal of the phosphoryl group from the response regulator (54).

1.3.2 eSTKs in bacterial sensing

Signaling through histidine and aspartic phosphorylation by TCSs was assumed to be the only form of phosphorylation-based signaling in bacteria. This notion was upended when a protein kinase (Pkn1) with the ability to auto-phosphorylate on a serine residue was discovered in *Myxococcus xanthus* (*M. xanthus*)(55). Pkn1 is also essential for the formation of fruiting bodies, a developmental state that *M. xanthus* undergoes in response to nutrient deprivation. Since this

original observation, eSTKs have been identified in many different species, and they are now believed to be ubiquitous in bacteria. Similar to the TCSs, eSTKs have a diverse set of functions in bacteria. These include sensing and regulating cell wall synthesis and cell division in important human pathogens like *Mycobacterium tuberculosis* (*M. tuberculosis*) (56) and *Streptococcus pneumoniae* (*S. pneumoniae*) (57).

1.3.3 eSTKs as a means of regulating cellular programs

eSTKs are also important for a developmental state in the Gram-positive model organism *Bacillus subtilis* that occurs in response to nutrient deprivation (58). Under nutrient limitation, *B. subtilis* enters into a developmental state, sporulation, where a dormant cell, the spore, that is highly resistant to physical stress is generated. Spores survive in non-optimal environments and can remain viable > 100 years (59). Although spores do not grow or they divide, they retain the capability to re-enter into a vegetative state through a process called germination (60) that occurs in response to specific environmental cues that signal to the dormant cell that re-growth could be advantageous. Spores have the capability to germinate in response to nutrients availability. For example, L-alanine is a well-known germinant for *B. subtilis* spores (61).

B. subtilis spores also sense the growth of other bacteria, which serves as an indirect measure of nutrient availability. Specifically, they sense muropeptides derived from the cell wall peptidoglycan. In order for a cell to grow in size and divide, it must generate and remodel its cell wall, a mesh-like extracellular structure composed of peptidoglycan, a polymer of crosslinked glycan strands, that provides the necessary rigidity to maintain shape in the presence of turgor pressure. Remodeling of the cell wall during growth and division is accomplished by a group of proteins that insert and crosslink new peptidoglycan and hydrolyze old peptidoglycan in order to either grow the cell or aid in division (58). As a result, cell wall fragments (muropeptides) are

released into the environment (59). Since muropeptide release occurs during bacterial growth and division, environments where cells are growing contain relatively high levels of these molecules.

B. subtilis spores exploit this fact in order to decide when to germinate. Specifically, *B. subtilis* spores express an integral membrane eSTK called PrkC that senses muropeptides (60). PrkC is a PASTA (Penicillin and Ser/Thr Kinase Associated) -domain-containing eSTK (60) where the cytoplasmic kinase domain is connected via a membrane-spanning domain to the extracellular PASTA domain that binds peptidoglycan fragments (61). *B. subtilis* spores germinate in response to fragments of cell wall from diverse species in a PrkC dependent manner, suggesting that in spores, PrkC serves to sense fragments of bacterial cell wall that growing bacteria have shed in order to signal to the dormant cell that conditions are favorable for growth (60).

During peptidoglycan induced germination, PrkC phosphorylates EF-G, the essential translational GTPase involved in translocation of ribosomes on mRNAs (60). In growing cells, PrkC interacts with the essential *B. subtilis* WalRK TCS that controls expression of genes that are important for cell wall metabolism (62). WalK phosphorylates WalR on Asp-43, and, in addition PrkC also phosphorylates WalR on Thr-101 (63). This secondary phosphorylation affects the binding of WalR to DNA and affects expression of genes in its regulon (64). One of these genes is particularly interesting because its gene product is a protein that has been suggested previously to induce dormancy by generating a nucleotide second messenger (SasA). Intriguingly, expression of *sasA* is heterogeneous and is subject to extrinsic noise (64).

Phosphorylation through eSTKs also has a direct effect on energy-intensive mechanisms that are important for growth. During sporulation in *B. subtilis*, a growing cell generates a dormant spore that must undergo a shut-down of energy-intensive processes. For example, inhibition of protein synthesis via phosphorylation of an essential translation factor has been shown to be

important to effectively generate dormant spores (65). This inhibition is dependent on a sporulation-specific eSTK (YabT). YabT phosphorylates the translation factor Elongation Factor Tu (EF-Tu) that mediates delivery of aminoacylated tRNAs to the ribosome. Phosphorylation of EF-Tu inhibits its ability to hydrolyze GTP, preventing its release from the ribosome, thereby inhibiting the cycles of elongation that are necessary for protein synthesis. Interestingly, ablation of EF-Tu phosphorylation in *B. subtilis* (via deletion of the eSTKs that can phosphorylate EF-Tu) results in cultures where a higher proportion of spores show hallmarks of spontaneous germination compared to wildtype (65).

1.4 Differentially phosphorylated guanosine nucleotides

1.4.1 Nucleotide second messengers

As discussed above, kinase-dependent signal transduction can alter the cellular program by phosphorylation of key proteins. But is signal transduction through kinases restricted to post-translational modifications? More specifically, phosphorylation of translation factors can affect rates of protein synthesis during entry into quiescence. But how does signaling through these kinases communicate this information to the other cellular programs? A common theme in signal transduction is the production of nucleotide second messengers. Nucleotide second messengers have been the subject of study since the early 1950s when it was demonstrated that cyclic 3’5’ adenosine phosphate (cAMP) mediates the metabolic changes in eukaryotic cells as a response to hormone exposure (66). Sutherland and colleagues published a series of papers that identified that the activity of one of the enzymes responsible for breaking up glycogen (glycogen phosphorylase) was upregulated when cells were exposed to the hormones epinephrine and glucagon (67, 68). The link between hormone exposure and phosphorylase activity was the presence of a small cyclic nucleotide (cAMP) which would later be found to be a major second messenger molecule in both

eukaryotic and prokaryotic organisms. In bacteria, cAMP mediates catabolite repression, the mechanism by which bacteria preferentially utilize one carbon source by shutting off expression of genes required to utilize other carbon sources (69). Around the same time, important work on another nucleotide second messenger was also emerging. The nucleotides (pp)pGpp have similarly been the subject of major study in bacterial physiology. These nucleotides have been shown to be major regulators of growth in bacteria and play a central role in communicating availability of nutrients to energy-intensive processes.

1.4.2 History of (pp)pGpp

In 1952, Sands and Roberts demonstrated that bacterial cells coordinate the synthesis of important macromolecules (70) by observing a concomitant decrease in the synthesis of RNA when cells were starved for certain amino acids. This discovery, termed the stringent response, led to the identification of how and why RNA and protein synthesis was linked. An important advance was the identification of a strain that did not exhibit this tight regulation (71). This strain was found using mutations that accumulated as *E. coli* was adapted to a laboratory environment and allowed Stent and Brenner to identify the genetic determinant of this control (the "RC gene") (72). The mechanism by which this gene brought about the observed link between amino acid starvation and RNA synthesis, however, remained unknown. Cashel and Gallant observed that upon amino acid starvation, not only the synthesis of RNA but also the synthesis of phosphorylated species, including nucleoside triphosphates, was altered in an RC gene-dependent fashion. (73). They postulated that the link between decreased RNA synthesis and amino acid starvation was mediated by a molecular inhibitor that also restricted metabolic functions generally and that this inhibitor was the product of the RC gene. Deciding to investigate phosphorylated species, they observed the presence of two molecules that accumulated when cells were starved of amino acids in an RC

gene-dependent fashion. These molecules were termed “magic spots” and opened up a field of investigation on the control of metabolic functions in cells undergoing starvation conditions. The two magic spots were soon after described as two phosphorylated guanosine nucleotides, guanosine 5’triphosphate 3’diphosphate and 5’diphosphate 3’diphosphate ((pp)pGpp)) (74).

Although more than 50 years have passed since (pp)pGpp was originally observed, many questions still remain regarding its role in cellular physiology. For example, a role for (pp)pGpp in translation has been suggested and *in vitro* evidence exists that (p)ppGpp interacts with essential components of this process, direct *in vivo* evidence has not been reported (75, 76). This is due, in part, to the methods used to analyze (pp)pGpp that rely on inducing amino acid starvation in exponentially growing cells and thereby directly inhibit translation. Specifically, although (pp)pGpp was originally identified when cells were shifted to amino acid free media, the field soon moved to using molecular inhibitors of tRNA charging, such as serine hydroxamate (77). These inhibitors simulate amino acid starvation and thereby also inhibit protein synthesis directly (78). While this treatment efficiently increases cellular (pp)pGpp, it precludes any observation of (pp)pGpp’s effects on translation. Recently, (pp)pGpp synthetases have been identified in Gram-positive bacteria whose activity is controlled transcriptionally and is not dependent on amino acid starvation (79). As I will discuss, these findings make it possible to study the effects of (pp)pGpp under conditions not intrinsically limiting for protein synthesis.

1.4.3 Synthetases and the different nucleotides

Not all bacteria possess an equal breadth of (pp)pGpp synthetic enzymes. Gram-negative bacteria generally possess one long-form RelA/SpoT homologs (RSH) (with the exception of β and γ proteobacteria which have two-long form RSHs), whereas Gram-positive bacteria typically have a single bi-functional RSH enzyme and two small alarmone synthetases (SAS) (80). In most

bacteria, one of the long-form RSH enzymes is ribosome-associated, and it directly senses deacylated tRNAs in the A site of the ribosome (80). Specifically, in *E. coli,* RelA binds the deacylated tRNA by wrapping around the tRNA via its C terminus, which contains flexible arms that allow it to cradle the tRNA in the A-site of the ribosome (81). RelA also directly contacts the acceptor arm of the tRNA via its TGS domain and directly senses if the tRNA is uncharged (81). Binding of an uncharged tRNA in the A-site stimulates RelA to make (pp)pGpp via its synthetase domain, which lies at the N-terminus of the protein **(Figure 1.2 B)** (81). Unlike the RSH proteins, SAS enzymes are believed to be regulated transcriptionally, and they lack the accessory domains that are essential for RelA to associate with the ribosome and sense amino acid starvation **(Figure 1.2 B)** (80). In *B. subtilis* the long-form RSH, RelA, is the mediator of the stringent response, and RelA produces (pp)pGpp in response to deprivation of amino acids **(Figure 1.3A)** (82). The role of the SAS enzymes has been postulated to either fine-tune the stress response mediated by RelA or to respond to different environmental cues (80).

In Gram-positive bacteria the SAS proteins have been associated with cell wall stress. In *B. subtilis* expression of one of these enzymes, SasA is induced in response to treatment with antibiotics that inhibit cell wall synthesis **(Figure 1.3C)** (83). Similarly, both of the *S. aureus* SAS enzymes (RelP and RelQ) are induced by cell wall active antibiotics (84). These enzymes are also important for survival during cell wall stress because deletion of both of these enzymes negatively affects viability during exposure to vancomycin (84). One of the SAS enzymes has also been suggested to be a sensor for single-stranded RNA (ssRNA). The SAS1 enzyme of multiple species (*B. subtilis* SasB and *E. faecalis* RelQ) are active as homo-tetramers, and this tetramerization forms two allosteric binding sites for (pp)pGpp (85, 86). Both enzymes are allosterically activated by pppGpp, but this allosteric activation seems to depend on the presence of a ssRNA with a Shine-

Delgarno-like sequence (GGAGG) in the *E. faecalis* RelQ enzyme (86). This has led to the proposition that RelQ (SasB in *B. subtilis*) serves as a sensor for ssRNA but whether this is physiologically relevant remains to be shown **(Figure 1.3B).**

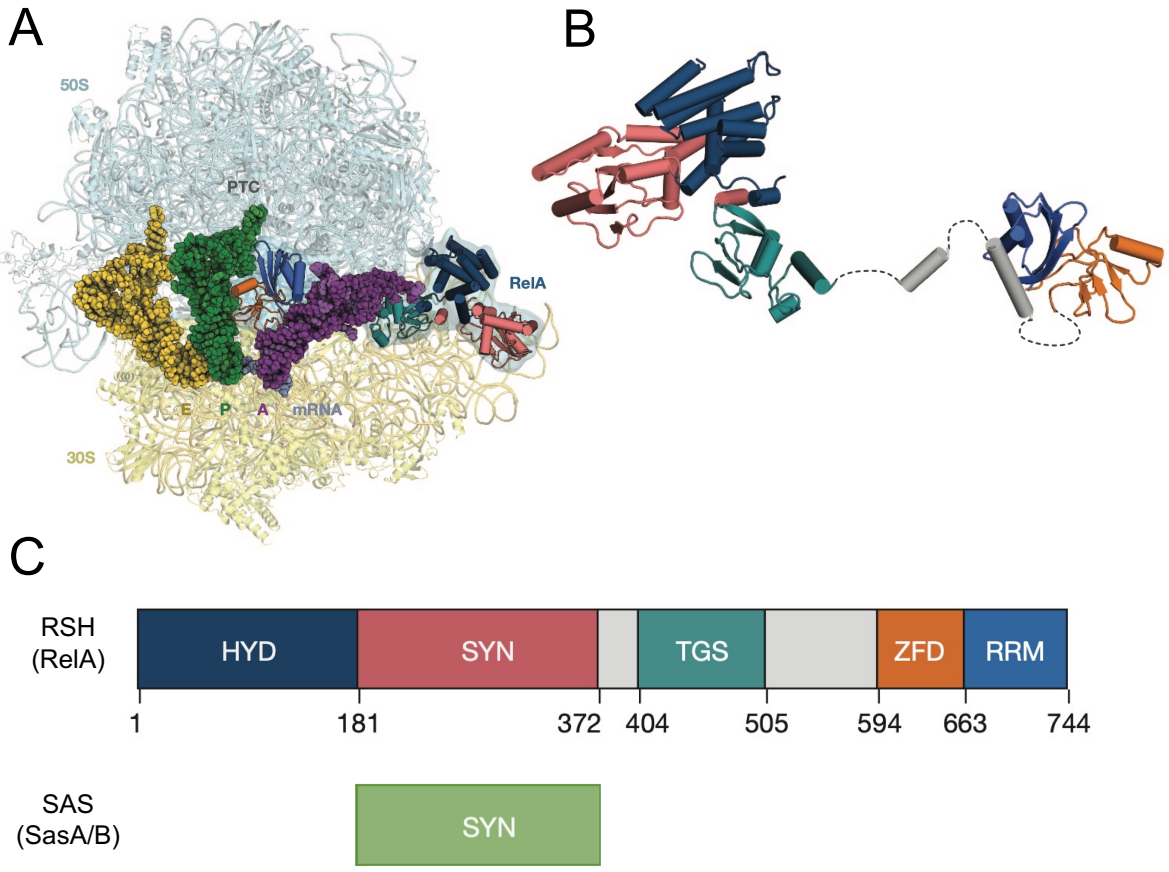

Figure 1.2 RSH enzymes but not SAS enzymes interact with the ribosome (Reproduced from *Brown et al. Nature 2016*). **(A)** Structural view of *E. coli* RelA in complex with a starved ribosome showing the interaction between the C-terminal domain of RelA with the uncharged tRNA (purple) in the A site of the ribosome. The C-terminal domain of RelA cradles the A-site tRNA and the TGS domain of RelA contacts the tRNA acceptor arm. **(B)** Ribbon structure of ribosome bound *E.coli* RelA depicting the N-terminal hydrolase domain (navy) and synthetase (red) and the tRNA contacting TGS (dark green) and the C-terminal domains that cradle the tRNA in the A-site. **(C)**. Domain architecture of RSH enzymes compared to the SAS enzymes. Whereas the RSHs are bi-functional proteins with N-terminal hydrolase and synthetase domains and C-terminal domains that interact with ribosome associated uncharged tRNAs, SAS enzymes lack both hydrolase domains and the domains necessary to interact with starved ribosomes.

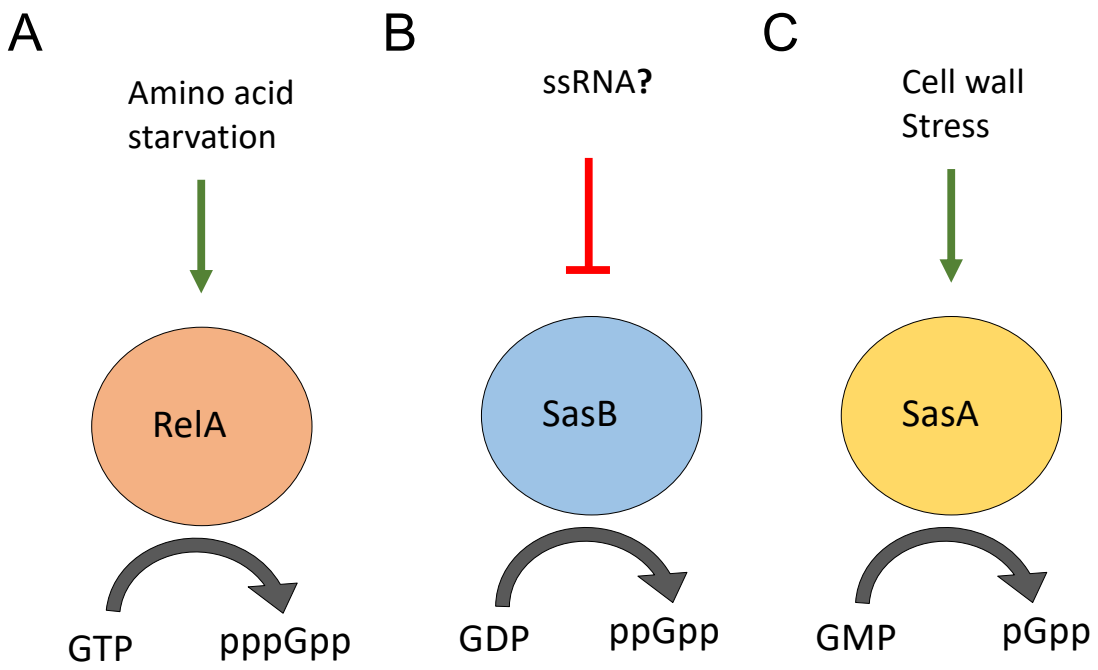

Figure 1.3. *B. subtilis* (pp)pGpp synthetases respond to different signals and generate different molecules. **(A)** *B. subtilis* RelA is the mediator of the stringent response and generates a pentaphosphorylated guanosine nucleotide (pppGpp) in response to amino acid starvation. **(B)** One of the Gram positive specific SAS enzymes present in *B. subtilis,* SasB, primarily generates a tetraphosphorylated guanosine nucleotide (ppGpp) and has been postulated to be a sensor of ssRNA because allosteric activation is inhibited by ssRNA, although the physiological relevance of this is not known. **(C)** The other SAS enzyme in *B. subtilis,* SasA, preferentially generates a 5' monophosphate 3' di-phosphate guanosine and its expression is stimulated under conditions of cell wall stress.

Apart from the breadth of enzymes which generate (pp)pGpp, the specific role of each of these closely related guanosine nucleotides is a topic of recent investigation. In *B. subtilis,* each (pp)pGpp synthetase preferentially generates a particular closely related nucleotide. The rationale for the presence of several closely related guanosine molecules is yet to be fully understood. Gram-negative bacteria have been known to generate approximately equal amounts of the tetra- and the penta-phosphorylated guanosines (82). In contrast, *B. subtilis* primarily generate the penta-phosphorylated form in response to amino acid starvation by the action of the RSH protein RelA using GTP and ATP as substrates (Figure 2A) (82). *B. subtilis* SasB (*yjbM*), preferentially utilizes GDP and ATP to generate the tetra-phosphorated guanosine *in* vivo (Figure 2B) (79). B. subtilis SasA generates a 5' monophosphate 3' di-phosphate guanosine (pGpp) using GMP and ATP as substrates *in vitro* and *in vivo* (Figure 2C) (79). pGpp was recently shown to be an alarmone in *B. subtilis* with distinct function to both ppGpp and pppGpp (87). Both the tetra- and penta-phosphorylated guanosines interact GTPases that control ribosome biogenesis, translation, and with proteins involved in regulation of purine nucleotide biosynthesis (87). pGpp, however, seems to interact with proteins involved in purine biosynthesis. Furthermore, an enzyme (NahA) that generates pGpp using both ppGpp and pppGpp is involved in the regulation of recovery from nutrient downshift because cells that lack this enzyme take longer to begin growth following re-addition of nutrients (87).

1.4.4 Role in regulating energy intensive processes

When amino acids are scarce, bacterial populations enter into a quiescent phenotype known as stationary phase. During stationary phase, bacterial growth halts, and cell division pauses. The bacterial response to nutrient deprivation has been linked to (pp)pGpp that directly binds and inhibits key proteins which catalyze energy-intensive processes, including transcription via

binding of the Gram-negative RNA polymerase (88, 89), GTP biosynthesis (via binding to the GTP biosynthetic enzymes HprT and GmK) (90), DNA replication (via binding to DNA primase) (91), ribosome assembly (via binding to several ribosome assembly factors including ObgE and RsgA) (92).

(pp)pGpp can also bind translational GTPases (93). However, other than several early, intriguing *in vitro* observations (94, 95), much less attention has been paid to the large number of fully formed active ribosomes and if a direct (pp)pGpp-dependent mechanism inhibits their activity. Furthermore, although myriad translational- and ribosome-associated GTPases have been shown *in vitro* to be inhibited by (pp)pGpp, the identification of a verified in vivo target and its role during quiescence related attenuation requires further study.

1.5 Protein synthesis

1.5.1 Translation as a regulatory step

Of the energy-intensive processes in a growing bacterial cell, protein synthesis utilizes the most energy. Specifically, during active growth in *E. coli,* protein synthesis consumes ~60 percent of the ATP that is generated (5). Because of this, regulation of translation, the most energy-intensive portion of protein synthesis (96) is an important regulatory mechanism during entry into quiescence (65). Translation proceeds in four general steps: initiation of a peptide chain, elongation of this peptide as coded by an mRNA, termination of the peptide, and recycling of the ribosome. Of these steps, the inhibition of initiation has been shown to be a common form of translational regulation (97). In eukaryotes, this occurs via phosphorylation of the initiation GTPase, which mediates binding of $tRNA^{met}$ to the ribosome, eIF2. This phosphorylation inhibits its ability to be released from the ribosome and globally shuts off translation (97). It has also been suggested, but

not demonstrated, that inhibition of initiation occurs during nutrient deprivation in bacteria via direct inhibition of the bacterial GTPase involved in initiation (Initiation Factor 2, IF2) (75).

1.5.2 Initiation

During bacterial translation initiation, the ribosome must correctly bind to a region of an mRNA upstream of the gene to be translated. The most common motif is called a Shine-Delgarno (SD) sequence consisting of a sequence of conserved nucleotides located 8-10 nucleotides upstream of the start codon (98). The SD is important for recognition of the ribosome binding site, and interactions between a complementary sequence in the 16S ribosomal RNA (the anti-SD) are important for recruitment of the 30S ribosomal subunit (98). This recognition and binding of the ribosome to the RBS occur as soon as the ribosome binding site is transcribed as transcription and translation are linked in bacteria via physical linkage between the ribosome and RNA polymerase (RNAP) (98). Accurate initiation is also promoted by the bacterial Initiation Factors 1, 2, and 3 (IF1/2/3) (98). The first of these, IF1 helps to promote the binding of IF2 and IF3 (98). IF2, a GTPase with homologous function to the eukaryotic initiation factor 5B (eIF5B), helps to recruit the initiator tRNA (fMet-$tRNA^{fMet}$) (98). This tRNA is specifically used to carry a modified methionone (*N*-Formylmethionine) which is required to initiate a peptide chain (98). The third initiation factor (IF3) functions to provide fidelity of recognition of this specific tRNA (98). If the initiator tRNA is not associated, IF3 interferes with the final step of translation initiation (association of the ribosomal subunits) (98).

At the beginning of initiation, the 30S subunit, all three initiation factors, and the fMet-$tRNA^{fMet}$ form a 30S preinitiation complex (30S PIC) (98). The three factors and the fMet-$tRNA^{fMet}$ do not need to bind to the 30S subunit in a particular sequence (98). However, from a kinetic standpoint, the following sequence is preferred (98). First IF3 binds to the 30S, followed

by IF2, IF1, and finally, the fMet-tRNA^{fMet} (98). The binding of the fMet-tRNA^{fMet} is sometimes preferentially through a complex consisting of GTP, IF2, and fMet-tRNA^{fMet}, but this is not essential (98). The unstable 30S PIC requires recruitment of an mRNA in order to form the more stable 30S initiation complex (30S IC) (98). This binding can occur to the 30S ribosome at any time regardless of initiation factors but, 30S IC formation requires all the factors to be present (98). 30S IC formation allows for the recruitment of the large ribosomal subunit (50S), and the binding of the 50S to the 30S IC brings about the disassociation of the initiation factors (98). During this step, the fMet-tRNA^{fMet} must be correctly accommodated in the peptidyl-site (P-site) of the ribosome (98). The disassociation of the initiation factors signifies the formation of the mature ribosome (70S) (98).

1.5.3 Elongation, termination, and recycling

The next steps of translation involve elongation of a peptide chain, translocation of the ribosome down the message, termination of the peptide chain, and finally recycling of the ribosome. Importantly, both elongation and translocation are energy-intensive processes that require repetitive cycles of association and then subsequent release of essential and universally conserved GTPases. During elongation, GTP bound EF-Tu delivers the amino acylated tRNAs to the ribosome so that these may be added to a growing peptide chain. Once a new amino acid has been added to the peptide chain, the ribosome must translocate down the mRNA. This is mediated by GTP bound EF-G, which binds the ribosome, and upon translocation and GTP hydrolysis releases from the ribosome. Recent research on elongation, termination, and recycling is reviewed in detail in (98) but will not be the main subject of this thesis, so they will not be covered in depth here.

1.6 Scope of this thesis

In this thesis, I will explore how protein synthesis, the most energy-intensive process in a bacterial cell, is regulated during the transition from active growth to stationary phase. I begin by observing rates of protein synthesis using a fluorescent probe that allows single-cell analysis of protein synthesis. Using this method, I first identify that populations of *B. subtilis* entering into stationary phase displays a bimodal distribution of protein synthesis (Chapter 3). Specifically, two populations arise, one with low rates of protein synthesis and one with comparatively higher rates. This bimodality suggested that an active mechanism mediated the shutdown in protein synthesis, and I proceed to explore that possibility in Chapter 4. I provide evidence that the shutdown in protein synthesis is mediated by a sensing system that is responsive to changes in cell wall synthesis. I further connect sensing through this system to the production of the nucleotide second messengers (pp)pGpp and show that the (pp)pGpp is essential for the heterogeneity observed. I continue to dissect the heterogeneity and show that crosstalk between two closely related guanosine nucleotides (pGpp and pppGpp) regulates the allosteric production of a third of these nucleotides (ppGpp) and that this crosstalk mediates the bimodality observed in protein synthesis. Lastly, I define a molecular mechanism by which ppGpp directly inhibits translation initiation and show that this mechanism mediates the shutdown in protein synthesis during entry into stationary phase.

Chapter 2

2 Materials and Methods

2.1 *B. subtilis* Bacterial Strain construction

B. subtilis strains generated in this thesis are all derived from the wildtype lab strain 168 (*trpC2*). All strains and transformation were grown in the presence of L-tryptophan (at least 50 μg/mL L-tryptophan). All strains were all generated by integrating plasmids, PCR products, or genomic DNA containing homology to a specific region of the wildtype *B. subtilis* chromosome using standard lab protocols. Briefly, *B. subtilis* strains are made competent by picking individual colonies grown overnight at 37 °C into 2 mLs SpC media (1X Tbase, 1% glucose, 0.036% $MgSO_4$, 0.4% Yeast Extract, 0.05% Casamino acids, 53.5 μg/mL L-tryptophan) and grown at 37 °C on a roller drum for 4 hours.These cultures were then transferred to 20 mLs of SpII media (1X Tbase, 0.5% glucose, 0.5mM $CaCl_2$, 0.000084% $MgSO_4$, 0.15% Yeast Extract, 0.01% Casamino acids, 80 μg/mL L-tryptophan) and grown at 37 °C on a water bath shaker for 1.5 hours. The entire culture was then spun down at 3K RCF for 10 minutes. The supernatant was transferred to a sterile container and cell pellets were re-suspended in 1.5 mLs of this supernatant. 300 uL of 50% glycerol was added and cells were aliquoted in 200 μL and frozen and stored at -80 °C.

B. subtilis competent cells were transformed by growing 100 uL of cells with 100 uL of SpIIE media (1X Tbase, 0.5% glucose, 0.084% $MgSO_4$, 0.1% Yeast Extract, 0.01% Casamino acids, 2 mM EGTA, 100 μg/mL L-tryptophan) and either 1 μL of purified plasmid DNA, 5 μLs of gel purified PCR products, or 1 μL of 1:100 diluted gDNA. Cells were incubated on a roller drum for 40 mintues at 37 °C and plated on an antibiotic plate for selection. Plates were grown overnight at 37 °C and single colonies were picked and re-streaked to single colonies. Single colonies from re-

streak plates were grown in LB without selection overnight at 37 °C and strains were stored at -80 °C in 25% glycerol.

2.2 *B. subtilis* Growth curves

Growth curves were performed in a Tecan Infinite m200 plate reader at 37 ºC with continuous shaking and OD_{600} measurements were made every five min. Cultures were grown from single colonies from fresh LB plates grown overnight at 37 ºC. Exponential phase starter cultures (OD_{600} ~ 0.5 - 1.5) were diluted to OD_{600} = 0.01 and grown in 96-well Nunclon Delta surface clear plates (Thermo Scientific) with 150 µL per well. All growth curves were done in triplicate and media-only wells were used to subtract background absorbance.

2.3 OPP labeling

Click-iT Plus OPP Protein Synthesis Assay Kit (Invitrogen) was used to label cells with OPP following manufacturer's instructions. 450 µL of cells at given time points were transferred to disposable glass tubes. OPP was added to a final concentration of 13 µM. Labelling was performed at 37 ºC on a roller drum for 20 min and all subsequent steps were done at RT. Cells were harvested by centrifugation at 16K RCF for 1 min and re-suspended in 100 µL of 3.7% formaldehyde in PBS for fixation. Cells were fixed for 10 min, harvested, and permeabilized using 100 µL of 0.5% Triton X-100 in PBS for 15 min. Cells were labelled using 100 µL of 1X Click-iT cocktail for 20 min in the dark. Cells were harvested and washed one time using Click-iT rinse buffer and then re-suspended in 20-40 µL of PBS for imaging or in 150 µL of PBS for fluorescence measurement on a Tecan Infinite m200 plate reader in 96-well flat bottom White sided plates (Greiner Bio-One). Images were analyzed using Image J.

2.4 HPG labeling

Click-iT Plus HPG Alexa Fluor 488 Protein Synthesis Assay Kit (Invitrogen) was used to label cells with HPG following manufacturer's instructions. 450 μL of cells were transferred to disposable glass tubes. HPG was added to a final concentration of 60 μM. Labelling was performed at 37 ºC on a roller drum for 20 min and all subsequent steps were done at RT. Cells were harvested by centrifugation at 16K RCF for 1 min and re-suspended in 100 μL of 3.7% formaldehyde in PBS for fixation. Cells were fixed for 10 min, harvested, and permeabilized using 100 μL of 0.5% Triton X-100 in PBS for 15 min. Cells were labelled using 100 μL of 1X Click-iT cocktail for 20 min in the dark. Cells were harvested and washed one time using Click-iT rinse buffer and then re-suspended in 150 μL of PBS for fluorescence measurement on a Tecan Infinite m200 plate reader in 96-well flat bottom White sided plates (Greiner Bio-One).

2.5 HADA labeling

HADA probe was used to label active cell wall synthesis throughout growth. 450 μL of cells were transferred to disposable glass tubes and 2.25 μL of 100 mM HADA stain was added. Cells were grown at 37° C in roller drum for 20 minutes. Cells were pelleted at 16K RCF for 1 minute and cells were then washed one time with 500 μL of 1X PBS. Cells were again pelleted at 16K RCF for 1 minute and pellets were resuspended based on OD_{600} (10 uLs for log phase, 40-50 uL for transition phase and stationary phase. 10μL of cells were spotted on an agar pad and images were taken on microscope using phase contrast and DAPI filters.

2.6 *sasB* transcriptional reporter cloning

sasB transcriptional reporter strain was constructed essentially as described in (64). Briefly, a 107 bp region encompassing the *sasB* operon promoter (P_{sasB}) was amplified and inserted into

AEC 127 using EcoRI and BamHI sites. The resulting AEC 127 P_{sasB} was integrated into *B. subtilis* 168 trpC2 at *sacA*.

2.7 F42A SasB strain construction

sasB^{F42A} strain was generated using integration of a pMINIMAD2 derivative (pMINIMAD2 *sasB*^{F42A}). Briefly, *sasB* was amplified excluding start and stop codons and the F42A mutation was introduced using overlap extension PCR. *sasB*^{F42A} was inserted into pMINIMAD2 vector using EcoRI and SalI sites. pMINIMAD2 *sasB*^{F42A} vector was transformed into *B. subtilis* 168 *trpC2* using a standard transformation protocol. Transformants were selected for erythromycin resistance at 45 ºC overnight and grown for 8 hours at room temperature in LB in liquid culture. Cultures were diluted 1:10 in LB and grown overnight. Cultures plated for single colonies and grown overnight at 45 ºC. Single colonies were checked for erythromycin sensitivity and sensitive clones were checked for *sasB*^{F42A} allele by Sanger sequencing of *sasB* amplified genomic region.

2.8 Y308A RelA strain construction

relA^{Y308A} strain was generated using integration of a pMINIMAD2 derivative (pMINIMAD2 *relA*^{Y308A}). Briefly, *relA* was amplified and the Y308A mutation was introduced using overlap extension PCR. *relA*^{Y308A} was inserted into pMINIMAD2 vector using EcoRI and BamHI sites. pMINIMAD2 *relA*^{Y308A} vector was transformed into *B. subtilis* 168 *trpC2* using a standard transformation protocol. Transformants were selected for erythromycin resistance at 45 ºC overnight and grown for 8 hours at room temperature in LB in liquid culture. Cultures were diluted 1:10 in LB and grown overnight. Cultures plated for single colonies and grown overnight at 45 ºC. Single colonies were checked for erythromycin sensitivity and sensitive clones were checked for *relA*^{Y308A} allele by Sanger sequencing of *relA* amplified genomic region.

2.9 SasB/SasA purification

Wildtype and F42A SasB and wildtype SasA proteins were expressed and purified essentially as described (85). Wildtype *sasB* and *sasA* were amplified from *B. subtilis* 168 *trpC2*. The F42A mutation was introduced using overlap extension PCR. WT and $sasB^{F42A}$ PCR products and WT were inserted into pETPHOS expression vector using EcoRI and BamHI sites. pETPHOS WT *sasB* and pETPHOS $sasB^{F42A}$ were transformed into *E.coli* BL21 and proteins were induced with 1 mM IPTG for 2 hours at OD_{600} ~0.5. Cells were harvested at 4 ºC and lysed using a Fastprep (MP biomedicals) in 50 mM Tris (pH 8.0), 250 mM NaCl, 5 mM $MgCl_2$, 2 mM BME, 0.2 mM PMSF, and 10mM imidazole. Lysates were clarified and bound to a Ni-NTA column (Quiagen) for 1 hour. Columns were washed using 20 mM imidazole. Protein was eluted using 500 mM imidazole, dialyzed into 20mM Tris, 500 mM NaCl, 5mM $MgCl_2$, 2 mM BME, and 10% glycerol and stored at -20 ºC

2.10 NahA purification

NahA protein was purified in a similar way to SasB and SasA except that NahA was induced for 1 hour at 30 ºC and NahA expressing cells (JDE3138) were lysed, washed, and eluted in 250 mM NaCl instead of 500 mM.

2.11 pGpp synthesis

pGpp was synthesized *in vitro* by purified NahA enzyme as described (87). Briefly, 10 nM purified *B. subtilis* NahA was incubated with 30 nM pppGpp (Trilink Biotechnologies) in 40 mM Tris-HCl (pH 7.5), 100 mM NaCl, 10 mM $MgCl_2$ at 37 ºC for 1 hour. Reactions were monitored for conversion of pppGpp to pGpp using thin layer chromatography on PEI-cellulose plates in 1.5 M KH_2PO (pH 3.6). Nucleotides were visualized using short wave UV light. NahA enzyme was precipitated using ice cold acetone and nucleotides were stored at -20 ºC.

2.12 SasB activity assay

SasB activity was assayed by measuring amount of ppGpp generated as described (99). Briefly, 0.8 mM purified *B. subtilis* WT or F42A SasB enzyme was incubated with 0.5 mCi of [γ-^{32}P]-ATP (PerkinElmer) and 50 mM GDP in 20 mM Tris (pH 7.5), 500 mM NaCl, 5 mM $MgCl_2$, 2mM BME. SasB was allosterically activated using 12.5 mM pppGpp (Trilink Biotechnologies) and pGpp was added to reactions as noted in figures. Reactions were performed in a total volume of 10 mL, and each reaction was incubated at 37 ºC for 1 min. Each reaction was stopped using 5 mL of ice cold acetone. Conversion of ATP to ppGpp was visualized using thin layer chromatography on PEI-cellulose plates in 1.5 M KH_2PO_4 (pH 3.6). Plates were dried completely at RT and exposed for 5 min on a phosphor storage screen and visualized (GE Typhoon). ATP and ppGpp spot intensities were quantified using ImageJ.

2.13 Single round transcription termination assays

Single round transcription termination assays were performed essentially as described in (100). Briefly, templates for single round transcription were dsDNA constructs designed to include the *D. hafniense ilvE* riboswitch starting at the predicted natural transcription site and extending 28 nucleotides beyond the terminator stem. The promoter used to enable transcription is from the *B. subtilis lysC* gene (compatible with the *E. coli* RNAP). Templates were purchased as dsDNAs (IDT) and were amplified using PCR reactions Since ppGpp is known to inhibit the *E. coli* RNA polymerase initiation, the holoenzyme was first assembles into a stalled, stable ternary complex befre ppGpp was added with the elongation mixture. 2 pmol of gel purified PCR products were added to transcription initiation mixtures (20 mM Tris·HCl (pH 7.5 at 23 °C), 75 mM KCl, 5 mM MgCl2, 1 mM DTT, 10 μg mL^{-1} BSA, 130 μM ApA dinucleotide, 1% glycerol, 0.04 U μL^{-1} E. coli RNA polymerase holoenzyme, 2.5 μM GTP, 2.5 μM 32 ATP, and 1 μM UTP. 1 μCi [α-^{32}P]-

UTP was added to 8 uL reactions and transcription mixtures were incubated at 37 °C for 10 minutes which leads to a stalled polymerase complex at the first cytidine nucleotide for each transcript. 1 uL of a 10X elongation buffer (20mM Tris·HCl (pH 7.5 at 23 °C), 75 mM KCl, 5 mM $MgCl_2$, 1 mM DTT, 2 mg mL^{-1} heparin, 1.5 mM ATP, 1.5 mM GTP, 1.5 mM CTP, and 250 μM UTP) was then added to each 8 uL reaction. Each reaction also had 1 uL of a 10X solution of each ligand (ppGpp or pGpp). Reactions were incubated at 37 °C for an additional 60 minutes.

Transcription products were run on 10% PAGE gel and exposed onto a phosphor screen and visualized (GE Typhoon). Full length (FL) fraction were calculated using the formula (FL)/(FL+T).

2.14 *E. coli* RelA purification

Purified *E. coli* RelA N-terminal mutant protein (amino acids 1-455) was used to generate radio-labelled (pp)pGpp. RelA N-terminal mutant protein was amplified from *E. coli* MG1655 strain and inserted into pETPHOS expression vector using NdeI and BamHI sites. pETPHOS *relA* was transformed into *E.coli* BL21 and proteins were induced with 1 mM IPTG for 1 hours at OD_{600} ~0.5. Cells were harvested at 4 ºC and lysed using a Fastprep (MP biomedicals) in 50 mM HEPES (pH 7.5), 1M KCl, 1mM MgOAC, 4 mM BME, 0.2 mM PMSF, and 10mM imidazole. Lysates were clarified and bound to a Ni-NTA column (Quiagen) for 1 hour. Columns were washed using 20 mM imidazole. Protein was eluted using 250 mM imidazole, dialyzed into 5mM HEPES-KOH, 1M KCl, 10mM MgOAC, 5 mM BME, and 10% glycerol and stored at -20 ºC.

2.15 Radio-labelled (pp)pGpp synthesis

Purified *E. coli* RelA N-terminal mutant protein (amino acids 1-455) was incubated overnight at 30oC with [α-^{32}P]- GTP (PerkinElmer) in 50 mM Tris (pH 8), 15 mM MgOAc, 60 mM KOAc, 30 mM NH4OAc, 0.2 mM EDTA, and 0.5 mM PMSF. Reactions were supplemented with 8 mM

cold ATP. Conversion of GTP to (pp)pGpp (>90%) was monitored by thin layer chromatography on PEI-cellulose plates in 1.5 M KH2PO4 (pH 3.6).

2.16 *B. subtilis* EF-G purification

Wildtype *B. subtilis* EF-G protein was expressed and purified essentially as described in (101). Wildtype *fusA* was amplified from *B. subtilis* 168 *trpC2*. *fusA* PCR product and was inserted into pETPHOS expression vector using NdeI and BamHI sites. pETPHOS *fusA* and was transformed into *E.coli* BL21 and protein expression induced with 1 mM IPTG for overnight at OD_{600} ~0.5 at 30 °C. Cells were harvested at 4 ºC and lysed using a Fastprep (MP biomedicals) in 20 mM Tris (pH 8.0), 300 mM NaCl, 2 mM BME, 0.2 mM PMSF, and 10mM imidazole. Lysates were clarified and bound to a Ni-NTA column (Quiagen) for 1 hour. Columns were washed using 30 mM imidazole. Protein was eluted using 250 mM imidazole and 500 mM NaCl, dialyzed into 20mM Tris, 100 mM KCl, 20mM MgOAC, 10 mM BME, and 10% glycerol and stored at -20 ºC

2.17 *B. subtilis* IF2 purification

Wildtype and G226A H230A *B. subtilis* IF2 proteins were expressed and purified essentially as described (101). Wildtype *infB* was amplified from *B. subtilis* 168 *trpC2*. The G226A H230A mutation was introduced using overlap extension PCR. WT and $infB^{G226AH230A}$ PCR products were inserted into pETPHOS expression vector using NdeI and BamHI sites. pETPHOS WT *infB* and pETPHOS $infB^{G226AH230A}$ were transformed into *E.coli* BL21 and proteins expression induced with 1 mM IPTG for 4 hours at OD_{600} ~0.5 at 37 °C. Cells were harvested at 4 ºC and lysed using a Fastprep (MP biomedicals) in 20 mM Tris (pH 8.0), 300 mM NaCl, 2 mM BME, 0.2 mM PMSF, and 10mM imidazole. Lysates were clarified and bound to a Ni-NTA column (Quiagen) for 1 hour. Columns were washed using 30 mM imidazole. Protein was eluted using 250 mM imidazole and

500 mM NaCl, dialyzed into 20mM Tris, 100 mM KCl, 20mM MgOAC, 10 mM BME, and 10% glycerol and stored at -20 ºC

2.18 Luminescence growth curves

Cultures were grown in LB from single colonies grown overnight at 37 ºC on LB plates. Cultures in exponential phase (OD_{600} ~ 0.5-1.0) were diluted to OD_{600} = 0.1 in 150 μL LB containing 4.7 mM D-luciferin (Goldbio) and grown in a 96-well flat bottom white sided plates (Greiner Bio-One) plates in triplicate. OD_{600} and luminescence measurements were made every 5 min using a Tecan Infinite m200 plate reader and media only wells were used to subtract background.

2.19 RNA quantification

RNA was quantified from cultures grown in LB as above. At given time points 14 mL of the cultures were pelleted at 8 K RCF for 10 minutes at room temperature and frozen at -80 ºC. Pellets were re-suspended in TRIzol (Invitrogen) to match based on OD_{600}. ~ 5 OD_{600} units of all cultures were lysed using a FastPrep 24 5G (MP Biomedicals). Lysates were spun down at 20 K RCF for 20 min and RNA was extracted using the Direct-Zol RNA miniprep kit (Zymo Research). RNA samples were DNAse I treated following manufactures protocol (NEB) and 1 μg of RNA was used to generate cDNA using the High Capacity cDNA Reverse Transcription Kit (Applied Biosystems). cDNAs were diluted 1:200 and used as templates for qPCR. qPCRs were preformed using SYBR green. Primers were design using the PrimeQuest Tool (IDT). No cDNA and no RT controls were used to ensure signal was specific to desired RNAs**.**

2.20 *in vitro* translation

Translation assays used the PURExpress system (NEB) following the manufacture's protocol and a plasmid encoding a CotE-FLAG fusion protein as template DNA (65). ppGpp (TriLink

Biotechnologies) at the specified concentrations was added to translation reactions. Reactions were run for 20 min each at 37 ºC and stopped by adding 2X SDS loading buffer. Synthesized proteins were separated by SDS-PAGE, transferred to PVDF membranes and visualized by probing with an anti-FLAG HRP antibody (Sigma). Mutant IF2 was assayed using a ΔIF123 PURExpress kit (NEB) supplemented with equal concentrations of purified *E. coli* IF1 and IF3. Reactions were run essentially as above but 0.47 μM of either WT or mutant *B. subtilis* IF2 was added to each reaction as the sole source of IF2. WT and mutant IF2s were purified as described (101). Band intensities were analyzed using ImageJ.

2.21 DRaCALA binding assay

Radiolabeled (pp)pGpp was generated essentially as described (92). Briefly, purified *E. coli* RelA N-terminal mutant protein (amino acids 1-455) was incubated overnight at 30ºC with [α-^{32}P]- GTP (PerkinElmer) in 50 mM Tris (pH 8), 15 mM MgOAc, 60 mM KOAc, 30 mM NH4OAc, 0.2 mM EDTA, and 0.5 mM PMSF. Reactions were supplemented with 8 mM cold ATP. Conversion of GTP to (pp)pGpp (>90%) was monitored by thin layer chromatography on PEI-cellulose plates in 1.5 M KH2PO4 (pH 3.6). DRaCALA binding assays were carried out essentially as described (92, 102). 6 μM protein was incubated with 55.5 nM [α-^{32}P]-labeled (pp)pGpp in 40 mM Tris (pH 8), 100 mM NaCl, 10 mM $MgCl_2$, and 2mM PMSF. Reactions were incubated for 5 min at RT and 2.5 μL of each reaction was spotted onto nitrocellulose membranes and dried completely at RT. Spots were exposed for 30 min on a phosphor storage screen and visualized (GE Typhoon). Inner and outer ring intensities were quantified using ImageJ. Reactions where protein was not added were used to subtract background.

2.22 smFRET experiments

All of the *E. coli* components for assembling 30S ICs, including 30S ribosomal subunits, 5'-biotinylated mRNA, Cyanine (Cy) 3-labeled fMet-tRNA^{fMet} (labeled with maleimide-derivatized Cy3 at the naturally occurring 4-thiouridine at residue position 8), IF1, and Cy5-labeled IF2 (labeled with maleimide-derivatized Cy5 at an engineered cysteine at residue position 810) were prepared as previously described (103). 30S ICs lacking IF2 and IF3 were assembled by combining 0.6 μM 30S subunits, 1.8 μM 5'-biotinylated mRNA, 0.8 μM Cy3-labeled fMet-tRNA^{fMet}, and 0.9 μM IF1 in Tris-Polymix Buffer (50 mM Tris-OAc (pH_{RT} = 7.5), 100 mM KCl, 5 mM NH_4OAc, 5 mM $Mg(OAc)_2$, 0.1 mM EDTA, 5 mM putrescine-HCl, 1 mM spermidine-free base, and 6 mM β-mercaptoethanol). The reaction was incubated at 37 °C for 10 minutes then on ice for an additional 5 minutes. Small aliquots of 30S ICs were flash-frozen in liquid nitrogen and stored at -80 °C.

To conduct smFRET experiments, 30S ICs assembled were first diluted to a final concentration of 75 pM in the presence of 2 uM IF1, 25 nM Cy5-labeled IF2, and 1 mM GTP or ppGpp. 30S ICs were then tethered to the polyethylene glycol (PEG)/biotin-PEG-derivatized surface of a microfluidic observation flowcell using a biotin-streptavidin-biotin between the 5'-biotinylated mRNA and the biotin-PEG. Untethered 30S ICs were flushed from the flowcell, and tethered 30S ICs were buffer exchanged, by washing the flowcell with Imaging Buffer (Tris-Polymix Buffer with an oxygen scavenging system composed of 2.5 mM 3,4-dihydroxybenzoic acid (PCA) and 250 mM protocatechuate 3,4-dioxygenase (PCD) and a triplet-state quencher cocktail composed of 8.4 mM 1,3,5,7-cyclooctatetraene (COT) and 8.7 mM 3-nitrobenzyl alcohol (NBA)) supplemented with 2 uM IF1, 25 nM Cy5-labeled IF2, and 1 mM GTP or ppGpp in order to enable rebinding of these components to 30SICs from which they might dissociates during the course of imaging. Finally, 30S ICs were imaged at single-molecule resolution and at a 0.1 sec per frame

acquisition time using a laboratory-built, prism-based total internal reflection fluorescence (TIRF) microscope as previously described (103). A previously described approach (104) was used to identify fluorophores and classify them into 'fluorophore' or 'background' classes; align the Cy3 and Cy5 imaging channels; fit individual Cy3 and Cy5 fluorophore to 2D Gaussians and estimate and, in the case of Cy5, bleedthrough correct the Cy3 and Cy5 fluorescence emission intensity *versus* time trajectories; and generate the E_{FRET} *versus* time trajectories. Only those trajectories exhibiting a signal-to-background (SBR) of 3.5:1 or greater as well as single-step photobleaching of Cy3 within the observation time were selected for further analyses.

In order to estimate the rate constants for the association of IF2 with the 30S IC (k_a) and for the dissociation of IF2 from the 30S IC (k_d) we began by estimating a 'consensus' hidden Markov model (HMM) of the E_{FRET} *versus* time trajectories using a slight extension of the variational Bayes approach we introduced in the vbFRET algorithm (105) Briefly, instead of using a likelihood function for each E_{FRET} *versus* time trajectory, we used a single likelihood function that simultaneously includes all of the E_{FRET} *versus* time trajectories in a dataset to arrive at a log-likelihood function given by

Eq. 1

$$\ln(\mathcal{L}) = \sum_{i \in trajectories} \ln(\mathcal{L}_i)$$

where $\mathcal{L}_i$ is the variational approximation of the likelihood function for a single trajectory. A further development of this approach in a hierarchical context underlies the hFRET algorithm that we have recently reported(106). Using this consensus HMM approach, we estimated HMMs for 1-6 states and performed model selection using the highest evidence lower bound (ELBO) as described in Bronson et al., 2009. In all cases, the 2-state HMM yielded the highest ELBO. The transition matrix obtained from this 2-state model consists of a 2 x 2 matrix in which the off-

diagonal elements correspond to the number of times a transition takes place between the IF2-free and the IF2-bound states of the 30S IC and the on-diagonal elements correspond to the number of times a transition does not take place. The 2 rows of this matrix parameterize Dirichlet distributions and, for each Dirichlet distribution, we calculated the lower bounds (2.5 %) and upper bounds (97.5 %) of the transition probability using the inverse cumulative distribution function of the corresponding Dirichlet distribution. These transition probabilities (p) were used to calculate rate constants (k) using the equation

$$k = -\frac{\ln(1-p)}{t}$$

where t is the time between successive data points (*i.e.*, the acquisition time) (t = 0.1 sec). Finally, we calculated k_a using the equation

Eq. 3

$$k_a = \frac{k'_a}{[IF2]}$$

where k'_a is the pseudo-first-order association rate constant calculated using Eq. 2 and [IF2] is the concentration of IF2, and we calculated k_d directly from Eq 2. The equilibrium dissociation constant for IF2 binding to the 30S IS (K_d) was obtained by summing the columns of the 2 x 2 transition matrix to obtain the total number of data points in which the 30S IC was either in the IF2-free state or the IF2-bound state. These sums can then be used to parameterize a Dirichlet distribution describing the fraction of 30S ICs in the IF2-bound state (f_b). The lower bounds and upper bounds of f_b were calculated using the inverse cumulative distribution function of this Dirichlet distribution, as described above, and the K_d was calculated using the equation K_d / [IF2] = $(1/f_b) - 1$.

2.23 G226A H230A IF2 strain construction

infB$^{G226\ H230A}$ strain was generated using integration of pMINIMAD2 derivatives (pMINIMAD2 *infB*$^{G226\ H230A}$). Briefly, *infB* was amplified excluding start and stop codons and G226A H230A mutation was introduced using overlap extension PCR. *infB*$^{G226\ H230A}$ was inserted into pMINIMAD2 vector using EcoRI and SalI sites. pMINIMAD2 *infB*$^{G226\ H230A}$ vector was transformed into *B. subtilis* 168 *trpC2* using a standard transformation protocol. Transformants were selected for erythromycin resistance at 45 ºC overnight and grown for 8 hours at room temperature in LB in liquid culture. Cultures were diluted 1:10 in LB and grown overnight. Cultures plated for single colonies and grown overnight at 45 ºC. Single colonies were checked for erythromycin sensitivity and sensitive clones were checked for *infB*$^{G226\ H230A}$ allele by Sanger sequencing of *sasB* amplified genomic region.

Chapter 3

3 Protein synthesis is downregulated in a (pp)pGpp dependent manner during entry into stationary phase

3.1 Protein synthesis decreases heterogeneously during entry into stationary phase

In the nutrient-rich medium LB, *B. subtilis* grows exponentially until a stereotypic cell density, presumably dictated by nutrient availability. After this point, growth occurs non-exponentially in the transition phase, culminating in the non-proliferative state of stationary phase **(Figure 3.1)**. I first wanted to understand how the dynamics of growth compared with energy-intensive processes required during exponential phase. I therefore investigated changes in protein synthesis, the most energy-intensive process during active growth, during the transition from exponential to stationary phase. I measured protein synthesis by measuring incorporation of the puromycin analog *O*-propargyl-puromycin (OPP) that can be visualized and quantified in single cells following addition of a fluorophore using click chemistry (107). Incorporation of OPP results in the accumulation of fluorescently tagged nascent polypeptide chains that directly reflect the rate of translation (107) **(Figure 3.2A)**. Importantly, OPP incorporation enables the measurement of protein synthesis under conditions where amino acids are not specifically limiting as is required during ^{35}S-Met incorporation. OPP itself does not inhibit protein synthesis under the conditions I used (OPP concentration used to label cells is ~3X lower than the IC_{50} of puromycin) because incorporation of OPP continues to increase even after cells have been exposed to it for 10 minutes **(Figure 3.2B)**. OPP incorporation is sensitive to an inhibitor of protein synthesis (chloramphenicol), consistent

with it being an appropriate measure of protein synthesis **(Figure 3.2B)**.

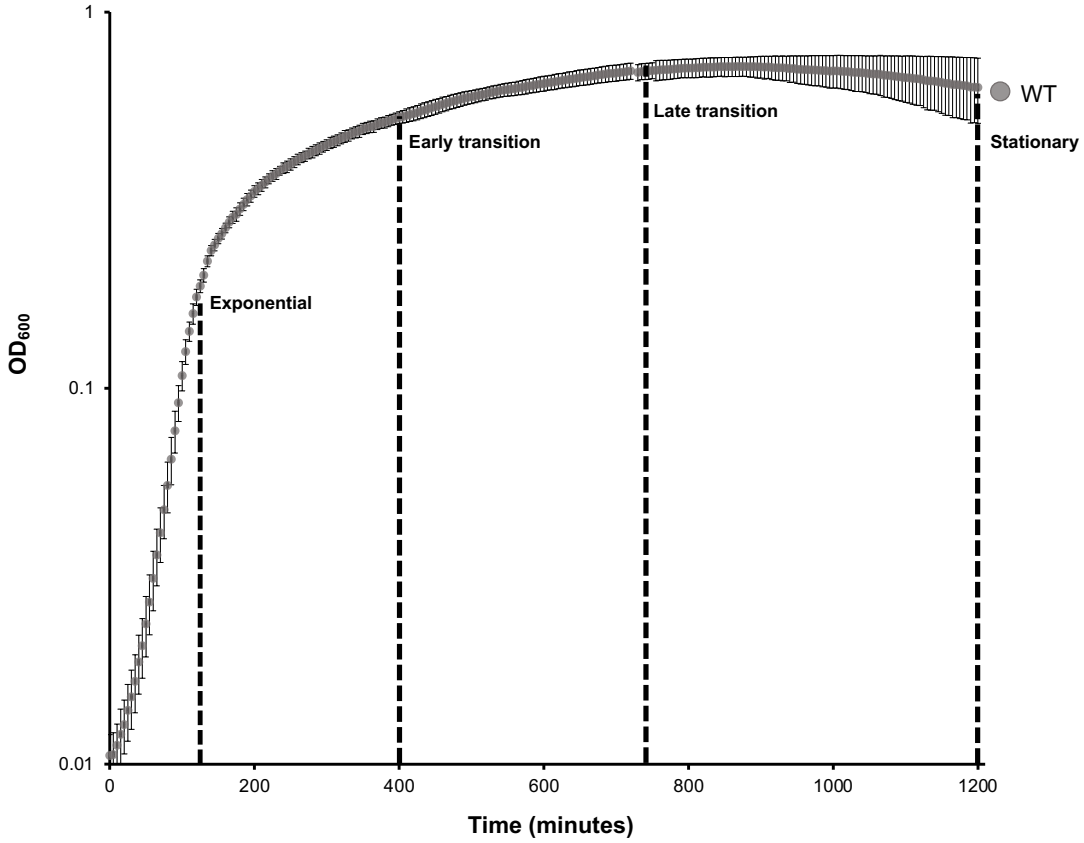

Figure 3.1 Growth of wildtype *B. subtilis.* In the nutrient rich medium LB, *B. subtilis* grows exponentially until a stereotypical cell density. After this cell density is reached, growth occurs more slowly during a period called transition phase. The cells then enter into stationary phase where the population of cells stop growing. Black dashed lines represent the time points where cells are labelled with OPP to assay protein synthesis.

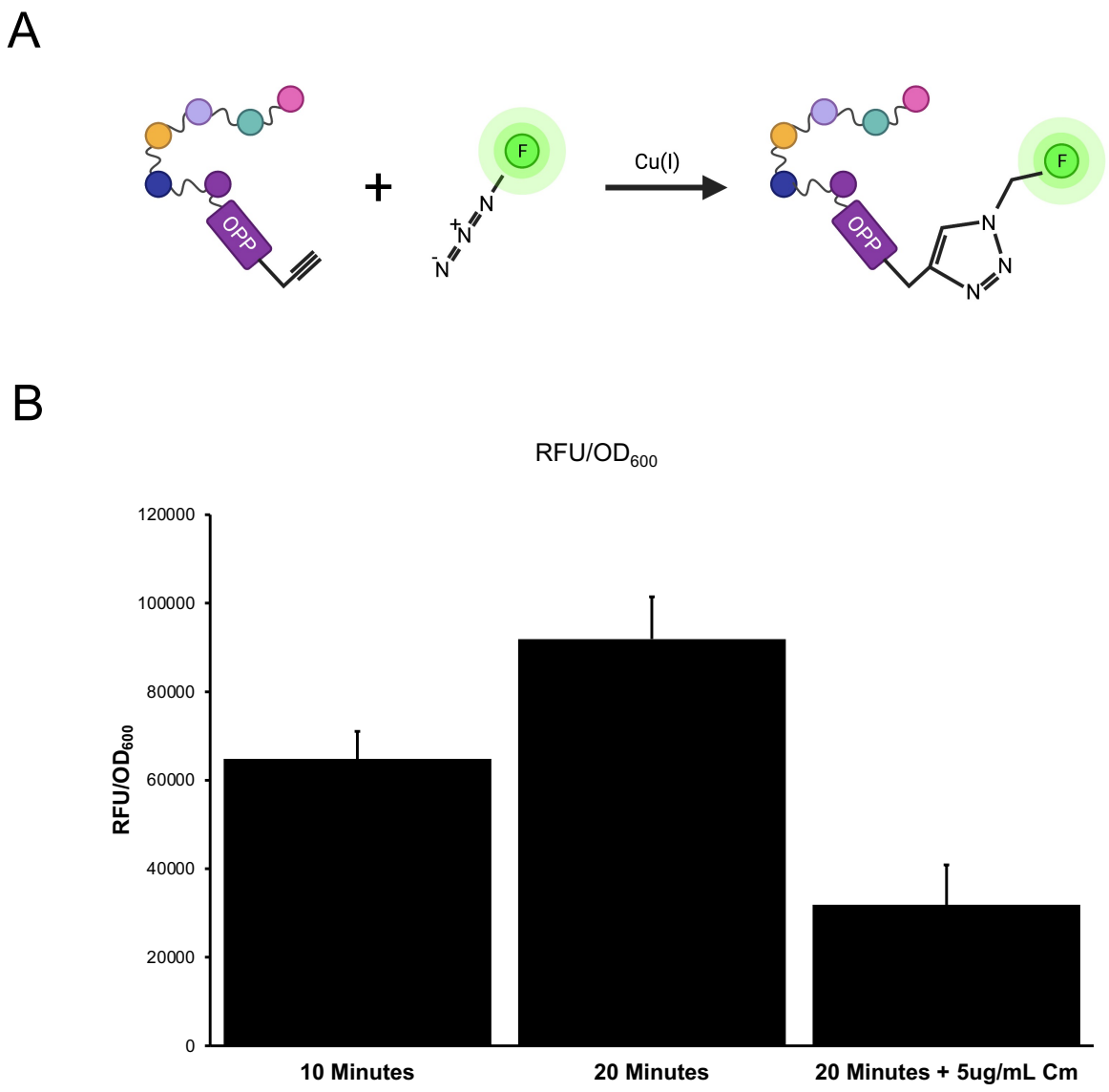

Figure 3.2 OPP labeling of fluorescently tagged nascent polypeptide chains. (A) Schematic description of OPP labeling as a measure of protein synthesis. OPP is incorporated into newly synthesized polypeptide chains. The alkyne modification on OPP allows the tagged polypeptide to be linked to an azide linked fluorescent dye via click chemistry resulting in fluorescent tagging of nascent polypeptide chains. **(B)** OPP does not arrest protein synthesis but is sensitive to inhibition by chloramphenicol (Cm). The effect of OPP addition on protein synthesis was tested during exponential phase. OPP was added to exponentially growing cultures of WT *B. subtilis* and total fluorescence was measured at 10 minutes and 20 minutes post OPP addition. Increased fluorescence was detected 20 minutes after addition compared to 10 minutes after addition indicating continued protein synthesis in the presence of OPP. Chloramphenicol was added to a separate culture in combination with OPP. Decreased fluorescence indicates that OPP is sensitive to translational inhibition (means ± SDs).

I labeled *B. subtilis* cultures with OPP at a series of time points (**Figure 3.1**; dashed black lines). I designated these time points as: exponential (120 minutes of growth), early transition (400 minutes of growth), late transition (750 minutes of growth), and stationary (1200 minutes of growth). These time points will be used throughout the remainder of this thesis. As expected, cells exhibited a progressive decrease in OPP incorporation soon after departure from exponential growth (early transition) that continued as the cells grew slowly in late transition phase **(Figure 3.3A)**. This trend is apparent in the average cellular fluorescence at these time points as well as in stationary phase (**Figure 3.3A).** However, at the late transition time point, the population displayed a noticeable heterogeneity. I used ImageJ to analyze microscope images and quantify protein synthesis in single cells. Approximately 1500 cells per time point were binned based on their fluorescence to generate a population distribution of OPP incorporation **(Figure 3.3B)**. Looking at representative population distributions, it became clear that a substantial fraction of cells in the entire population exhibited little fluorescent signal (**Figure 3.3B "Late transition phase")**. This indicates an absence of protein synthesis, resulting in a population whose distribution of protein synthesis activity is approximately bimodal at the single cell level **(Figure 3.3B "Late transition phase").** Since some cells in the late transition phase culture exhibited a near total inhibition of protein synthesis while others were able to maintain a level of protein synthesis similar to cells in the exponential phase **(Figure 3.3B),** an absence of the nutrients in the extracellular milieu is likely not the cause of the inhibition of protein synthesis. This heterogeneity, therefore, is consistent with the inhibition of protein synthesis being an active process and not simply a passive consequence of amino acid limitation in the growth medium.

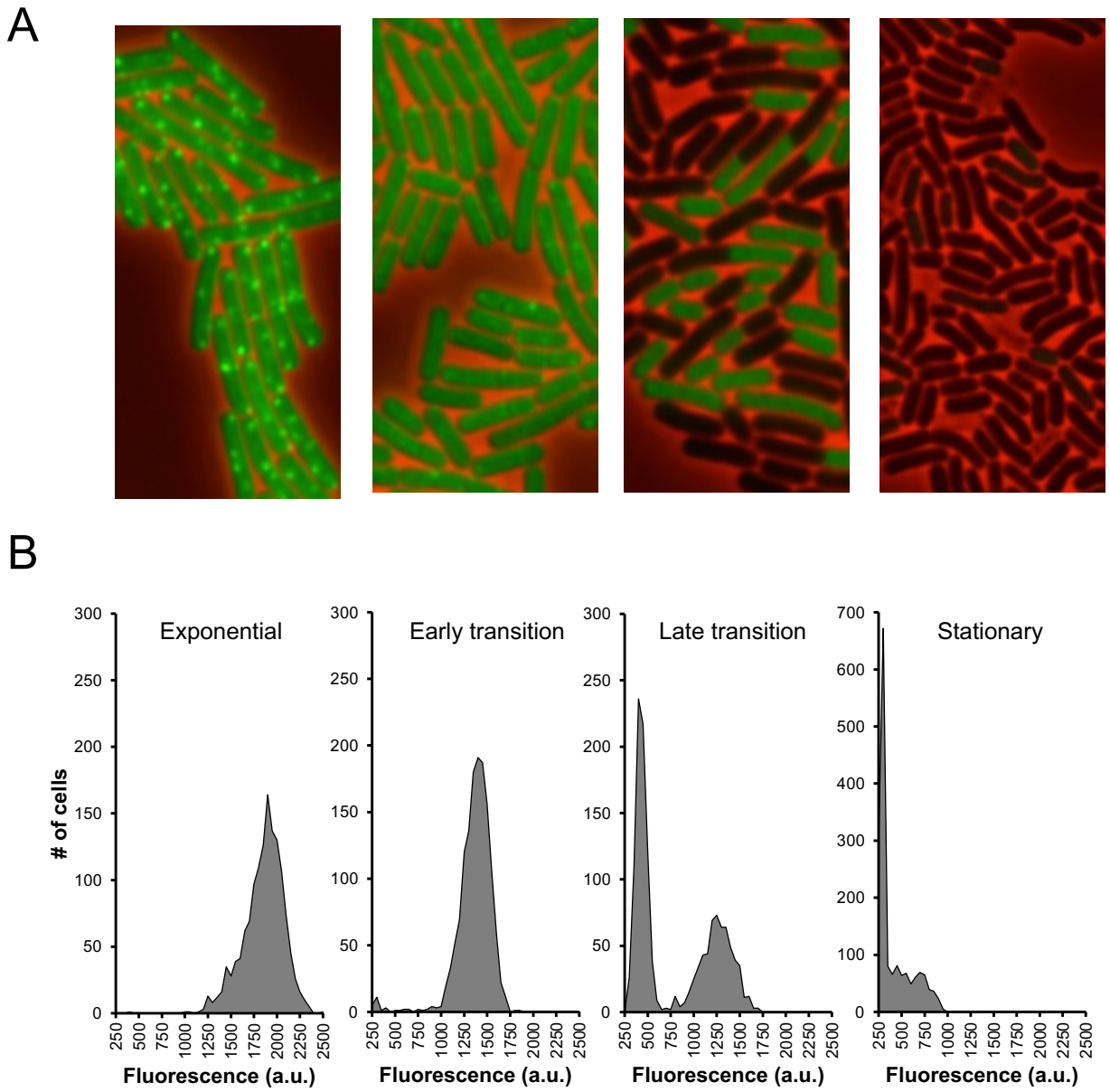

Figure 3.3 Protein synthesis decrease during entry into stationary phase. Wildtype *B. subtilis* cells were labeled with OPP at different time points throughout growth. **(A)** Representative pictures of wildtype *B. subtilis* labelled with OPP at different time points. **(B)** Distributions of mean-cell fluorescence of WT and (pp)pGpp^0 cells.

I quantified this heterogeneity using a cutoff that specifies the population of cells with low protein synthesis activity. I defined the threshold of this cutoff as the magnitude of OPP labeling of a stationary phase wildtype *B. subtilis* culture that captures 95% of the entire population. I determined this threshold (850 RFU) using distributions of three separate cultures of wildtype stationary phase cells **(Figure 3.4A).** I then used this threshold to quantify the percent of the population with low rates of protein synthesis ("OFF") **(Figure 3.4B)**. By convention, the remainder of the population is defined as "ON." Using this cutoff, I quantified the percentage of OPP "OFF" cells throughout growth **(Figure 3.5)**. During late transition phase, when the heterogeneity is most apparent **(Figure 3.3),** the proportion of cells with low rates of protein synthesis ("OFF") is approximately 60 percent **(Figure 3.5)**.

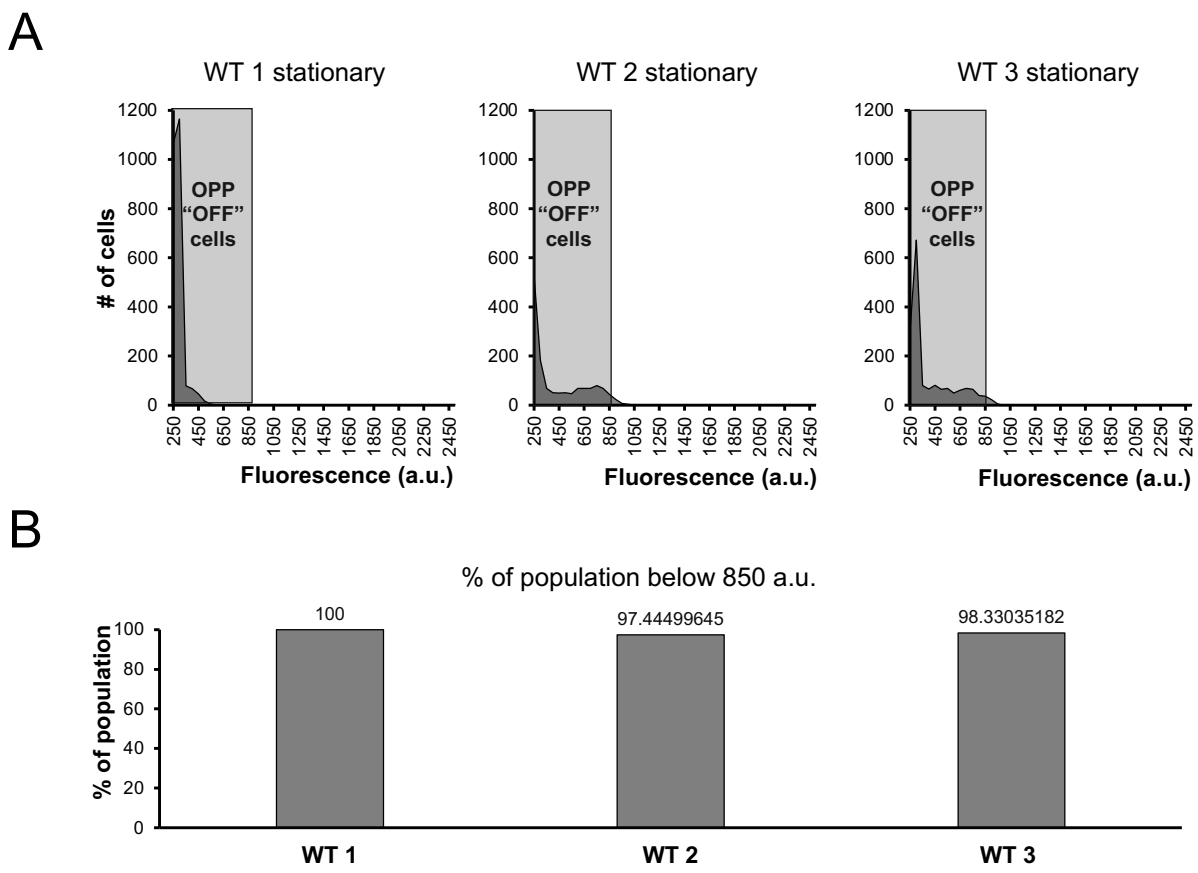

Figure 3.4 Demonstration of method to quantify OPP "OFF" cells. Threshold for OPP "OFF" cells was determined as the fluorescence value (850 a.u.) that is higher than >95% of cells of OPP labeled wildtype *B. subtilis* during stationary phase across three independent experiments. **(A)** Three representative distributions of OPP labeled wildtype *B. subtilis.* Gray box shows cutoff for cells with low rates of protein synthesis ("OFF"). **(B)** Quantitation of % of population below the threshold determined as OPP "OFF" in the three experiments in A (means ± SDs).

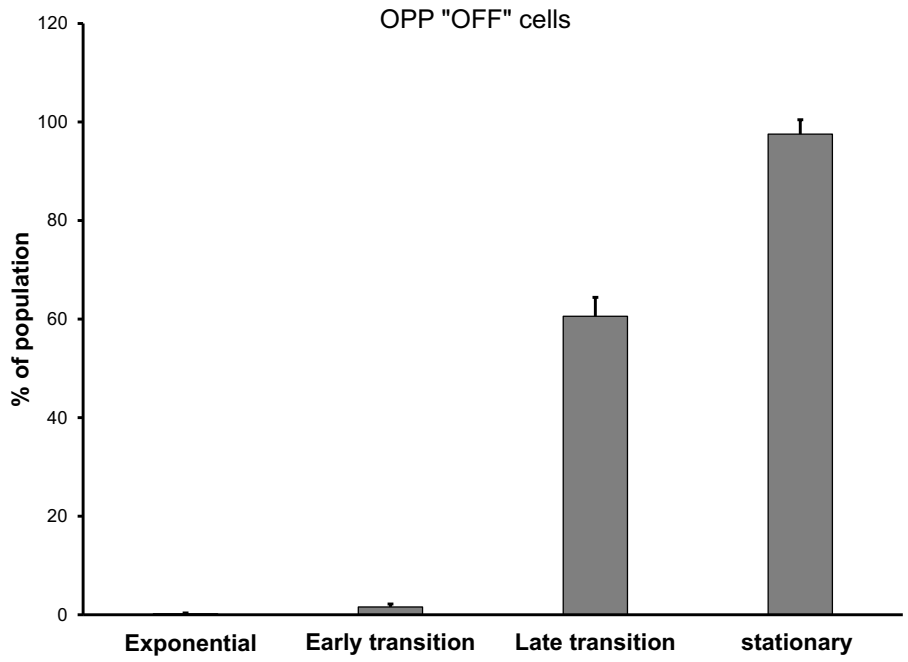

Figure 3.5 Quantitation of OPP "OFF" cells throughout growth in wildtype *B. subtilis.* Percent of the population of wildtype *B. subtilis* below the OPP "OFF" threshold determined in Fig 3.4 throughout all phases of growth (means ± SDs).

3.2 Cell wall sensitive kinase/phosphatase pair is required for down regulation of protein synthesis

The shutoff of protein synthesis in a subpopulation of cells suggests that protein synthesis is inhibited in these cells in a manner not directly related to a significant decrease in amino acid availability **(Figure 3.3)**. What mechanism could account for this inhibition? One possibility is that during the late transition phase, *B. subtilis* senses a change in different cellular process and directly mediates the inhibition of protein synthesis in a subpopulation of cells. I first asked if one of the major sensing systems in *B. subtilis* could mediate this shutoff of protein synthesis. Signaling through eSTK signaling systems has previously been shown to regulate protein synthesis during the transition between growth and dormant phenotypes in *B. subtilis* (65). One of these eSTKs is the PASTA domain containing membrane-bound protein PrkC, which has been shown to directly sense peptidoglycan fragments in the cellular milieu (60, 108). PrkC and its partner phosphatase PrpC have also been shown to affect expression of stationary phase specific genes (63, 108). Specifically, PrkC and PrpC regulate the phosphorylation of WalR (the response regulator of the essential TCS in *B. subtilis*) on Thr-101(63). This phosphorylation in turn, affects expression of a group of stationary phase specific genes (63). One of these genes, *sasA*, is an interesting candidate for mediating the downregulation of protein synthesis because it generates a group of nucleotides ((pp)pGpp) **(Figure 1.2)** that have been previously suggested to directly inhibit protein synthesis (75, 79). Furthermore, expression of *sasA* occurs heterogeneously from cell to cell during exit from exponential phase, and this heterogeneity is affected by PrkC and PrpC (64). Thus, PrkC/PrpC signaling during entry into stationary phase could affect heterogeneity in protein synthesis.

To test this hypothesis, I compared OPP incorporation of strains lacking either PrkC **(Figure 3.6B)** or PrpC **(Figure 3.6C)** during late transition phase to a wildtype strain **(Figure 3.6A)**.

Deletion of PrkC resulted in the loss of cells with low rates of protein synthesis ("OFF") during late transition phase compared to a wildtype strain **(Figure 3.6A, B)**. In contrast, cells with comparatively high rates of protein synthesis are less frequent in a strain lacking PrpC as compared to a wildtype strain **(Figure 3.6A, C**). I quantified these effects over three independent experiments **(Figure 3.6D)** and observed significantly fewer "OFF" cells in the *ΔprkC* strain and significantly more "OFF" cells in the *ΔprpC* strain compared to wildtype**.** These results suggest that sensing through PrkC mediates the inhibition of protein synthesis that is observed during late transition phase. The opposing effects of PrkC and PrpC on protein synthesis also suggest that the mediator of heterogeneity in protein synthesis is a target of PrkC based phosphorylation. As mentioned above, WalR phosphorylation is regulated by PrkC and PrpC during stationary phase, and this phosphorylation affects stationary phase specific gene expression (63). Based on these data, I speculated that PrkC/PrpC based signaling mediated the inhibition of protein synthesis during entry into stationary phase by affecting the expression of certain genes during exit from exponential growth.

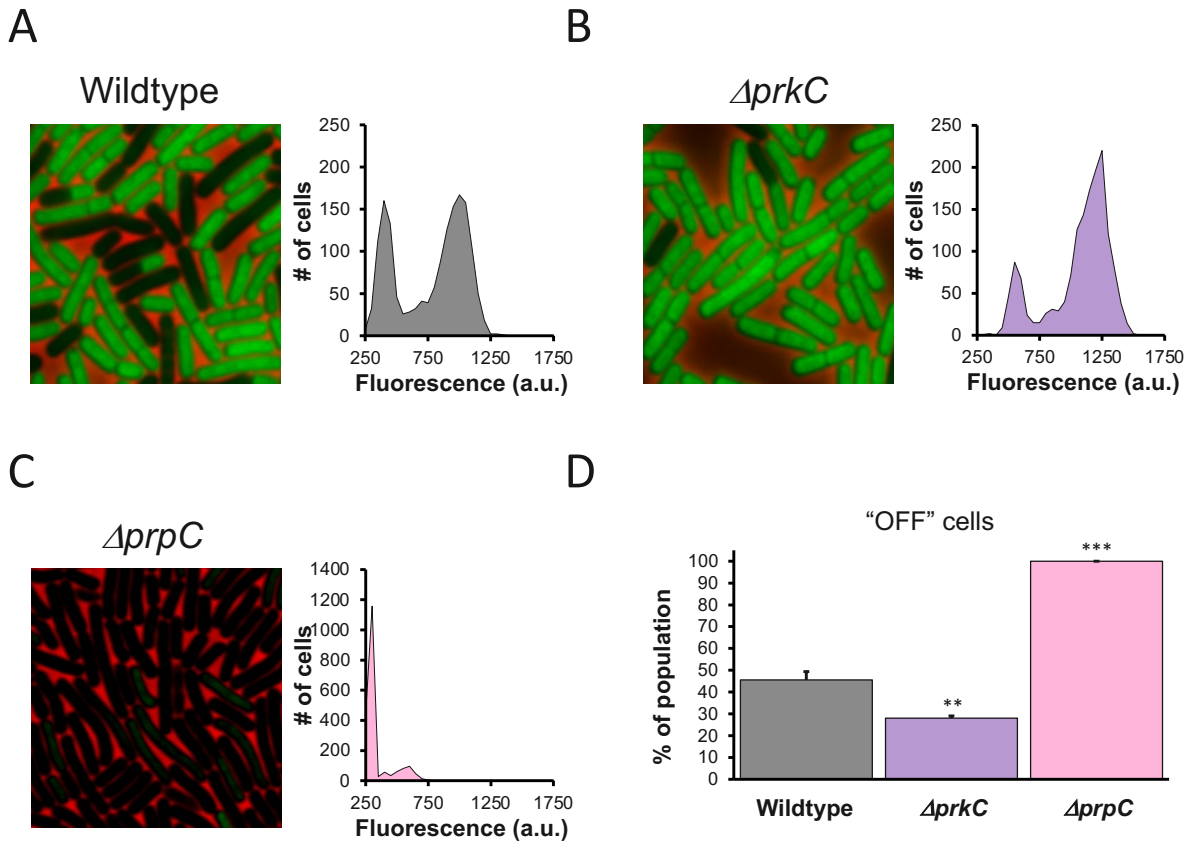

Figure 3.6 Heterogeneity is dependent on signaling via PrkC/PrpC. (A, B, C) Representative picture and population distribution of OPP labeled **(A)** wildtype **(B)** Δ*prkC* and **(C)** Δ*prpC* strains during late transition phase. **(D)** Quantitation of OPP "OFF" cells over three independent experiments for A-C (means ± SDs). n.s. $p > 0.05$, *$p < 0.05$, **$p < 0.01$, ***$p < 0.001$

3.3 (pp)pGpp is required for down regulation of protein synthesis

As previously mentioned, PrkC/PrpC mediated phosphorylation of WalR affects noise in gene expression during the transition from growth to stationary phase (64). Specifically, noise in the expression of *sasA*, a gene previously identified as a (pp)pGppp synthetase in *B. subtilis* is dependent on the phosphorylation status of WalR (63, 64). Expression of *sasA* is interesting for two reasons. Firstly, heterogeneity in *sasA* expression is differentially affected by deletion of PrkC and PrpC (64). Since deletion of either of these signaling proteins also has opposite effects on the heterogeneity in protein synthesis, the heterogeneity in *sasA* expression could be related to the heterogeneity in protein synthesis. I will explore this link in detail in Chapter 4 of this thesis.

Secondly, SasA has been shown to produce a group of molecules that are major regulators of energy intensive-processes in bacteria; the guanosine molecules collectively referred to as (pp)pGpp **(Figure 1.2)** (79). (pp)pGpp is an attractive candidate to directly downregulate protein synthesis during exit from exponential growth because it downregulates diverse processes in cells growing under nutrient limited conditions (109). Furthermore, many bacteria synthesize (pp)pGpp when they depart from exponential phase (110, 111). To investigate the possible role of (pp)pGpp, I asked if (pp)pGpp is necessary for cells with low rates of protein synthesis during exit from growth. To do this, I utilized a strain that lacks (pp)pGpp via a genetic deletion of the three known *B. subtilis* (pp)pGpp synthetases, *relA*, *sasA*, and *sasB* (112, 113), which I will refer to as (pp)pGpp^0. Under the growth conditions used here, the (pp)pGpp^0 strain grows equivalently to the parent wildtype strain during exponential phase as well as early and late transition phase, and based on OD_{600} the cells at these time points do not have any significant difference in viability **(Figure 3.7)**. At approximately 75 minutes after the late transition phase time point, the (pp)pGpp^0 strain begins to lyse **(Figure 3.7).** For this reason, I will only examine protein synthesis in this strain

only at or before the late transition phase time point. As above, I assayed protein synthesis of the (pp)pGpp^0 strain by measuring OPP incorporation. Since (pp)pGpp concentration is low in exponential phase (87), as expected, OPP incorporation of this strain is indistinguishable from the parent **(Figure 3.8A, B "Exponential")**. In contrast, early in transition phase, the distribution of OPP incorporation by (pp)pGpp^0 cells is higher as compared to the wildtype parent **(Figure 3.8A, B "Early Transition")**. This trend continues, and in late transition phase, significantly fewer cells in the (pp)pGpp^0 strain (blue) have decreased their protein synthesis as compared to the wildtype parent (gray) **(Figure 3.8A, B "Late Transition phase")**. The percent of the population with comparatively low rates of protein synthesis "OFF" is significantly different between these two strains during the late transition phase time point (**Figure 3.8 C).**

The results above indicate that (pp)pGpp is required to inhibit protein synthesis in a subpopulation of cells during entry into stationary phase because the population with comparatively lower levels of OPP incorporation ("OFF") is absent in a strain that lacks (pp)pGpp. To confirm that the difference observed between the wildtype and the (pp)pGpp^0 strains was not due to any differences in the OPP reporter that were not directly due to differences in protein synthesis activity, I used methionine incorporation, a more conventional method of measuring protein synthesis activity. The fluorescently tagged methionine analog (HPG) has been previously used as a probe for protein synthesis activity in bacteria (114). Although incorporation of this analog is not efficient in media containing methionine (the (pp)pGpp^0 strain requires methionine to grow (115)), the (pp)pGpp^0 strain incorporated comparatively more HPG during late transition phase, consistent with a higher rate of protein synthesis **(Figure 3.9)**.

For the remainder of this thesis, I will explore the mechanistic basis of this phenomenon. Chapter 4 will investigate how heterogeneity in protein synthesis is derived via (pp)pGpp and the

synthetases responsible for generating these nucleotides. Chapter 5 will investigate how protein synthesis is down-regulated on a biochemical level in the cells with low levels of protein synthesis.

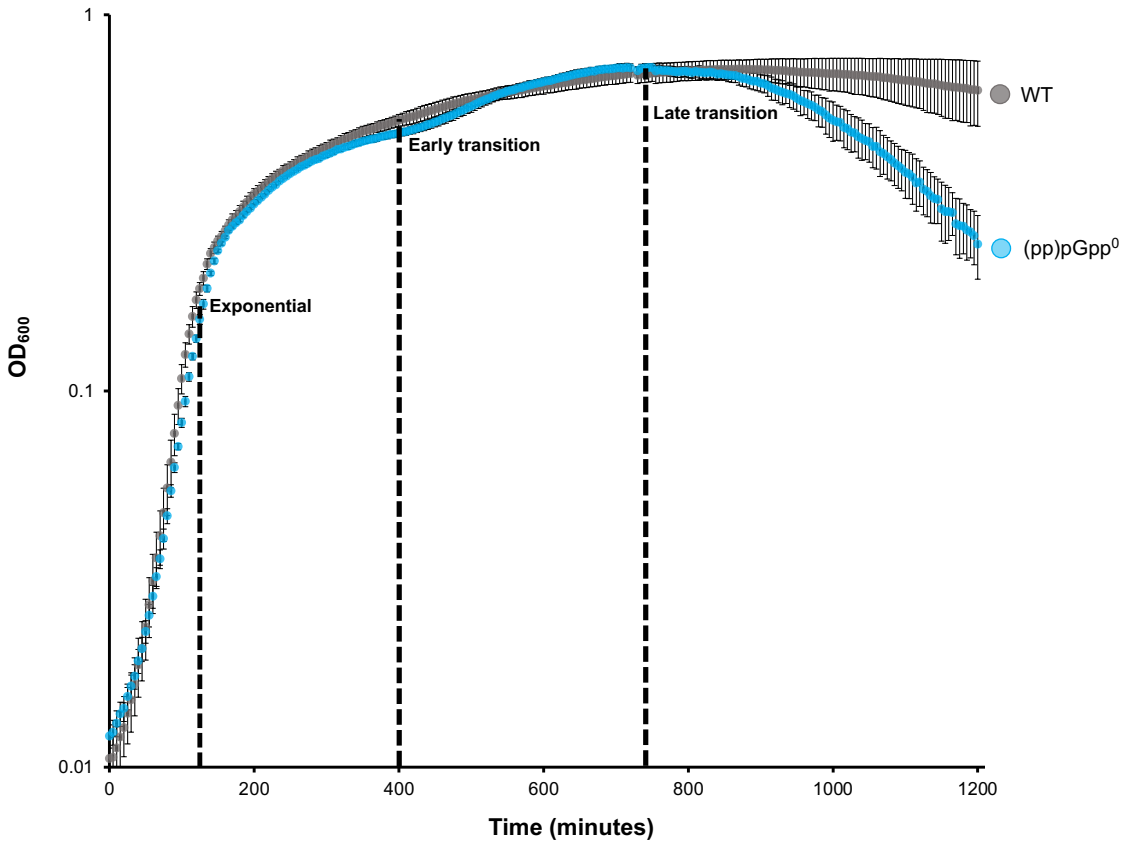

Figure 3.7 Growth curve of *B. subtilis* lacking (pp)pGpp^0. Growth in a strain of *B. subtilis* lacking (pp)pGpp (blue) is comparable to a wildtype (gray) strain during exponential and transition phases, but the (pp)pGpp^0 strain loses viability during entry into stationary phase.

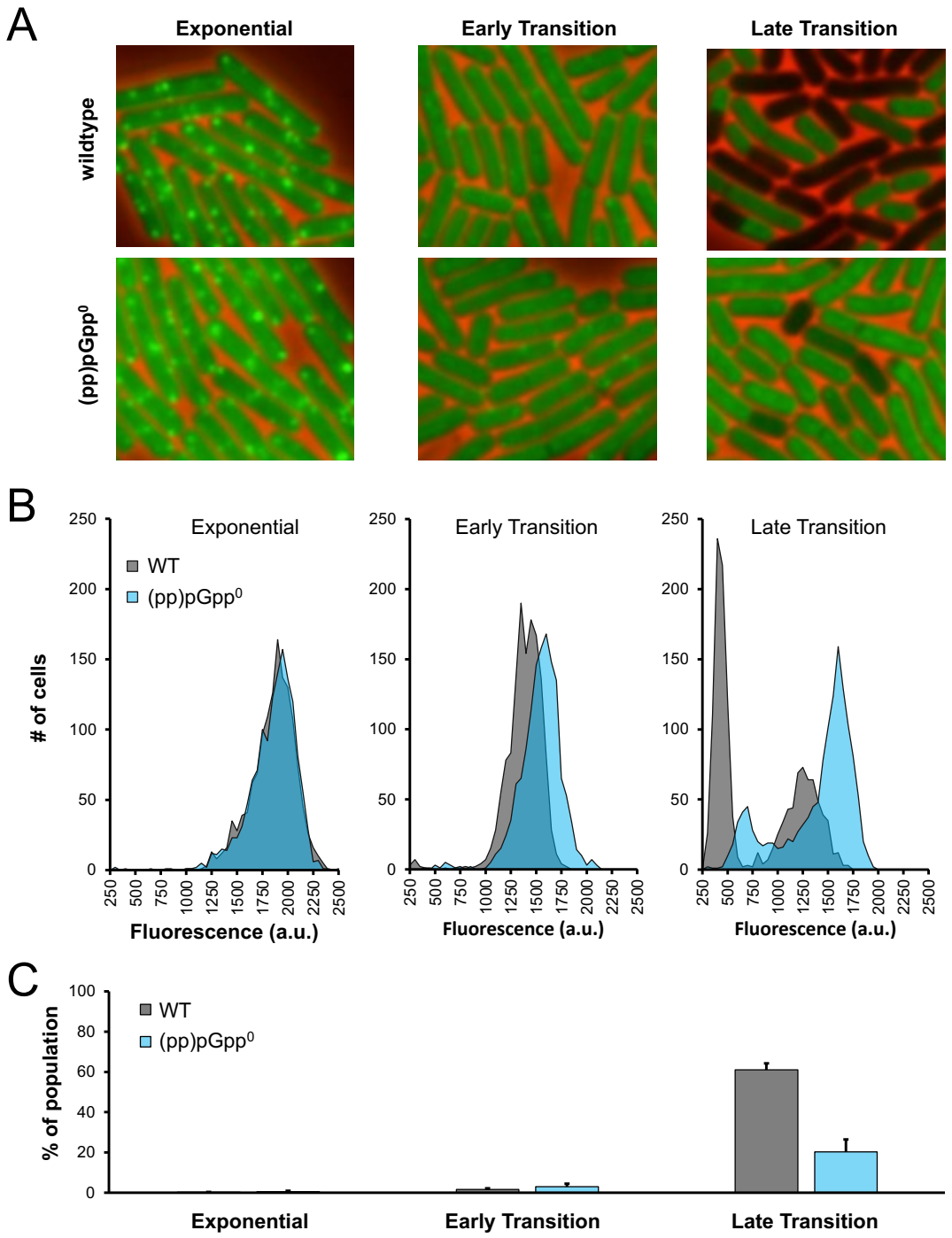

Figure 3.8 (pp)pGpp is required for inhibition of protein synthesis during late transition phase (A) Representative pictures of WT and (pp)pGpp^0 strains labelled with OPP at different time points. **(B)** Distributions of mean-cell fluorescence of WT (gray) and (pp)pGpp^0 (blue) cells. **(C)** Quantitation of OPP "OFF" cells over three independent experiments for A-C (means ± SDs).

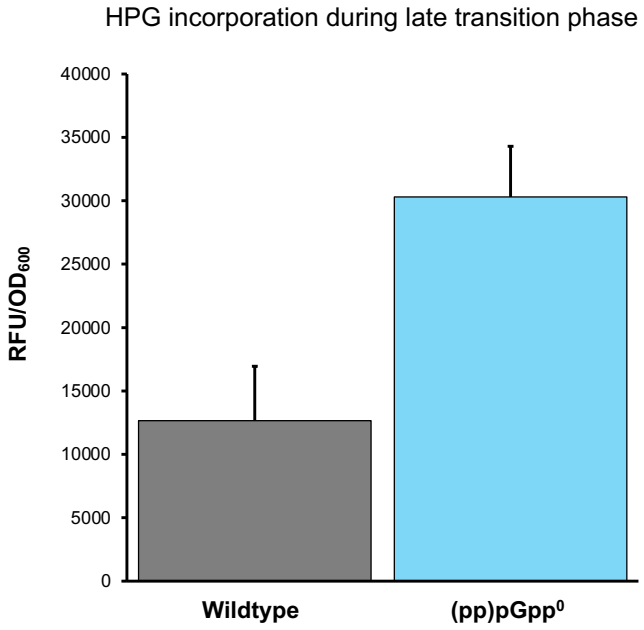

Figure 3.9 (pp)pGpp^0 effect is also observable using HPG labeling. The effect of (pp)pGpp on protein synthesis was confirmed using a fluorescently taggable methionine analog. Rates of protein synthesis during transition phase are higher in the (pp)pGpp^0.

Chapter 4

4 Cross-talk between nucleotide second messengers drives heterogeneity in protein synthesis

4.1 SasA and SasB have opposing effects on heterogeneity

Cellular heterogeneity in protein synthesis as *B. subtilis* cultures exit rapid growth is dependent on the presence of the phosphorylated guanosine nucleotides (pp)pGpp **(Figure 3.8**). *B. subtilis* contains three proteins (RelA, SasA, SasB) that generate the nucleotides (pp)pGpp (82, 112). Whereas RelA is ribosome-associated and requires a starved ribosome to synthesize pppGpp, SasA and SasB are believed to be transcriptionally activated (79, 80). Furthermore, they lack the domains present in RelA that are required for ribosome association and sensing of A-site uncharged tRNAs (80, 81). Additionally, expression of SasA and SasB increases during exit from rapid growth (79). I wanted to investigate the mechanistic basis of heterogeneity in protein synthesis and decided to assess single cell protein synthesis using (OPP) incorporation in strains carrying inactivating mutations in either of the two *B. subtilis* SAS proteins because their expression increases during exit from growth when heterogeneity is observable.

When I analyzed a representative population distribution of a strain lacking SasB (Δ*sasB*), I observed that this strain contained fewer "OFF" cells as compared to the wildtype strain **(Figure 4.1 A, B)**. In contrast, a strain lacking SasA (Δ*sasA*) does not contain the substantial fraction of "ON" cells seen in the wildtype parent strain, and most cells in the population are "OFF" **(Figure 4.1 A, C)**. These differences are quantified across three independent experiments in **Figure 4.1D.** These results indicate that while both SasA and SasB are required for the heterogeneity I observed, SasA and SasB have opposing effect on protein synthesis.

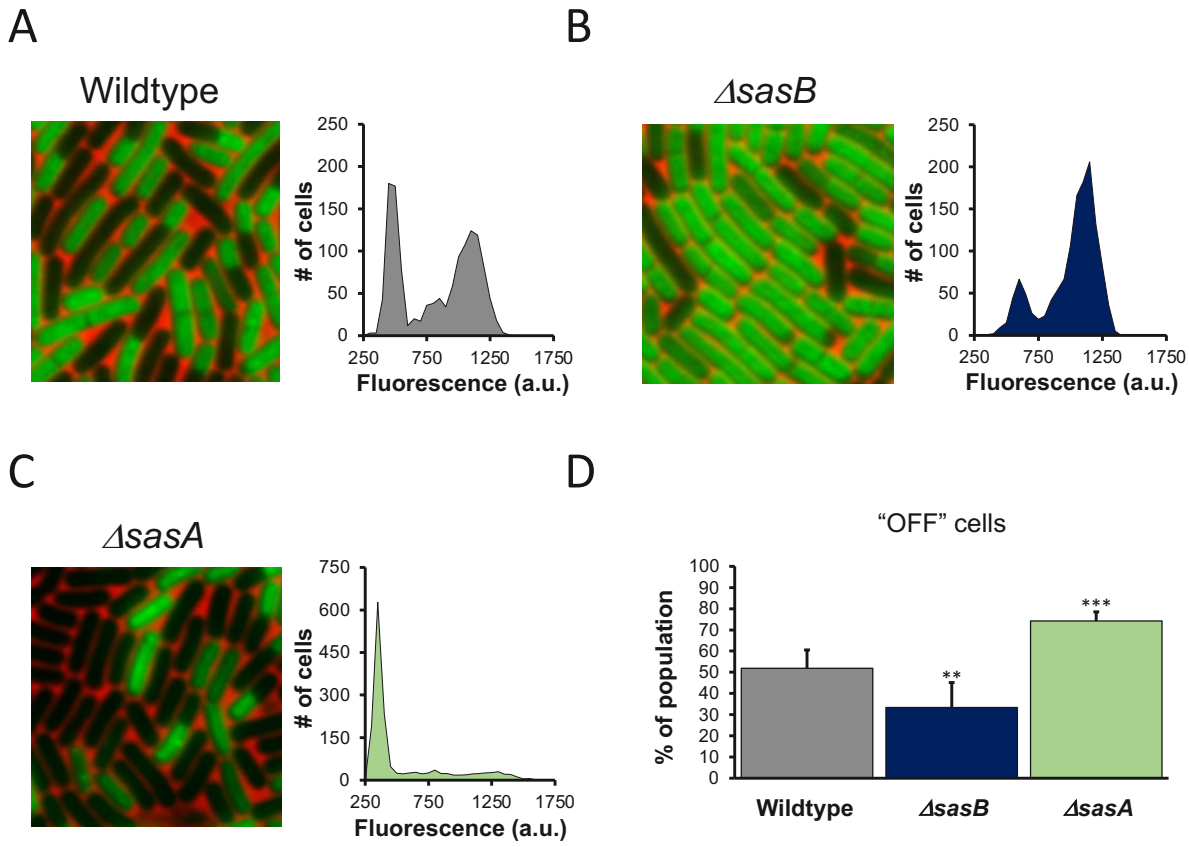

Figure 4.1 SasB and SasA have opposing effects on protein synthesis. (A, B, C) Representative picture and population distribution of OPP labeled **(A)** wildtype, **(B)** *ΔsasB*, and **(C)** *ΔsasA* strains during late transition phase. **(D)** Quantitation of OPP "OFF" cells over three independent experiments for A-C (means ± SDs). n.s. $p > 0.05$, *$p < 0.05$, **$p < 0.01$, ***$p < 0.001$

4.2 *sasA* but not *sasB* expression is correlated with levels of protein synthesis

sasA and *sasB* are believed to be regulated transcriptionally and their expression increases post-exponentially (79, 112) when the heterogeneity is observed **(Figure 3.3)**. I therefore asked if expression of either *sasA* or *sasB* is correlated with protein synthesis using reporters consisting of transcriptional fusions of the *sasA* or the *sasB* promoters to YFP (P_{sasA}-*yfp* or P_{sasB}-*yfp)* integrated at a neutral chromosomal site. As previously observed (79), both *sasA* and *sasB* expression increased during the exit from exponential growth **(Figure 4.2 A, B)**. I examined the relationship between promoter activity and protein synthesis by measuring both YFP expression and OPP incorporation in single cells. Cells with higher *sasA* expression (P_{sasA}-*yfp)* are more likely to have higher levels of protein synthesis than cells with lower *sasA* expression **(Figure 4.2 D)**. If the population is divided into quartiles of *sasA* expression, the average OPP incorporation in the top two quartiles as compared to the bottom quartile is significantly higher **(Figure 4.2 D)**. In comparison, there was no significant difference in OPP incorporation between any quartiles of *sasB* expression **(Figure 4.2 C)**. Thus, differences in *sasA,* but not *sasB*, expression are associated with the observed heterogeneity in protein synthesis.

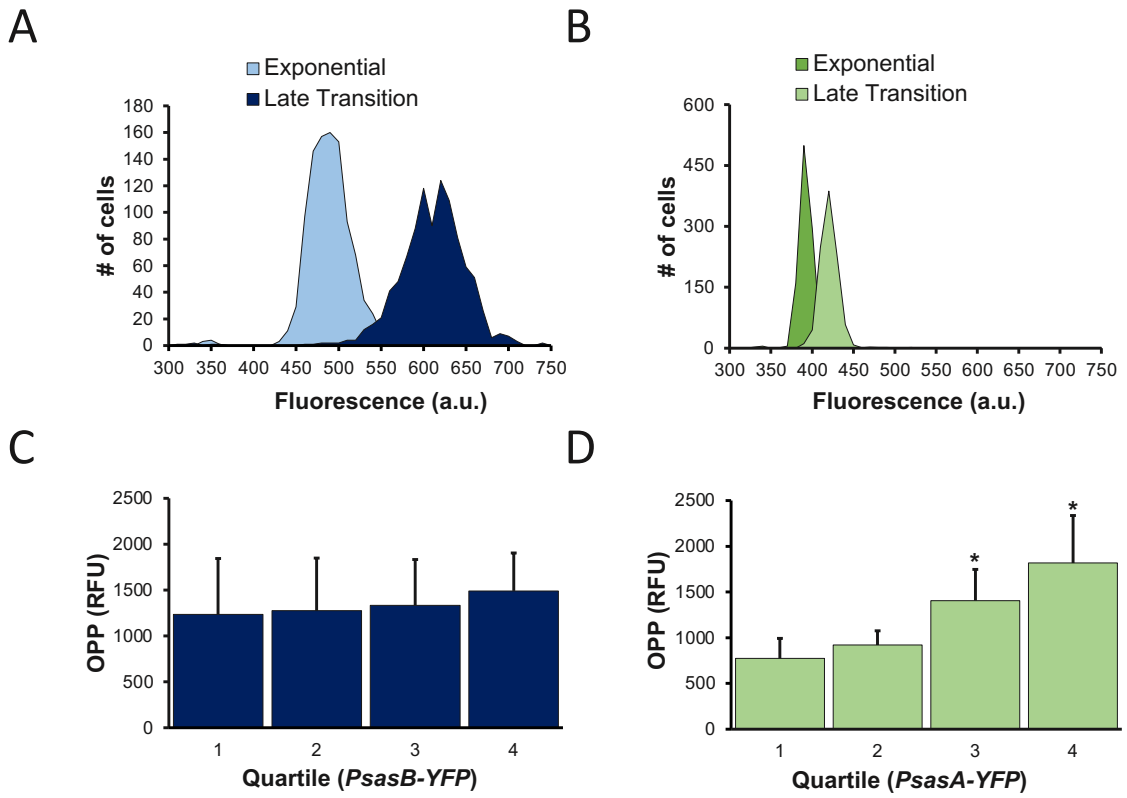

Figure 4.2. Relationship between *sasA* or *sasB* expression and OPP incorporation. (A, B) Representative population distribution of *B. subtilis* carrying a transcriptional reporter of **(A)** *PsasB-yfp* or **(B)** *PsasA-yfp* during exponential and late transition phase. **(C, D)** Average OPP incorporation of each quartile of **(C)** *PsasB-yfp* expression or **(D)** *PsasA-yfp* expression from lowest to highest. Statistical analysis (one tailed t-test) showed no significance ($p > 0.05$) in OPP incorporation between any *PsasB-YFP*, and significantly higher OPP incorporation between quartiles 1 and 3 and quartiles 1 and 4 of *PsasA-yfp* expression. (means ± SDs). n.s. $p > 0.05$, *$p < 0.05$, **$p < 0.01$, ***$p < 0.001$

4.3 SasB allosteric activation is necessary for heterogeneity

If changes in *sasB* transcription are not associated with differences in protein synthesis **(Figure 4.2C)**, but SasB is necessary for the heterogeneity of protein synthesis **(Figure 4.1B),** what mechanism is responsible for differential SasB activity in single cells? *B. subtilis* SasB is subject to allosteric activation by pppGpp, the main product of the *B. subtilis* RSH homolog RelA (85). Phe-42 is a key residue in this activation, and a SasB mutant protein carrying an F42A substitution is no longer allosterically activated by pppGpp (85). I investigated the importance of this allosteric activation for the heterogeneity of protein synthesis activity using a strain expressing an F42A SasB mutant protein. Heterogeneity of this strain is significantly attenuated compared to the WT strain, demonstrating the importance of the allosteric activation of SasB by pppGpp for the bimodality of protein synthesis activity **(Figure 4.3 A, B, D)**.

This result suggests that the enzyme responsible for pppGpp synthesis would also affect the heterogeneity. RelA is the primary source of pppGpp in *B. subtilis* (116), so the loss of *relA* would be predicted to affect SasB activity. I, therefore, generated a strain expressing a RelA mutant protein ($RelA^{Y308A}$) carrying a single amino acid change at a conserved residue essential for synthase but not hydrolysis activity (117, 118) since RelA hydrolytic activity is essential in a strain that retains functional *sasA* and *sasB* genes (113). Labeling of this strain with OPP in late transition phase revealed that it largely lacked the "OFF" population **(Figure 4.3 C, D**), demonstrating that RelA-mediated pppGpp synthesis is important for the bimodality.

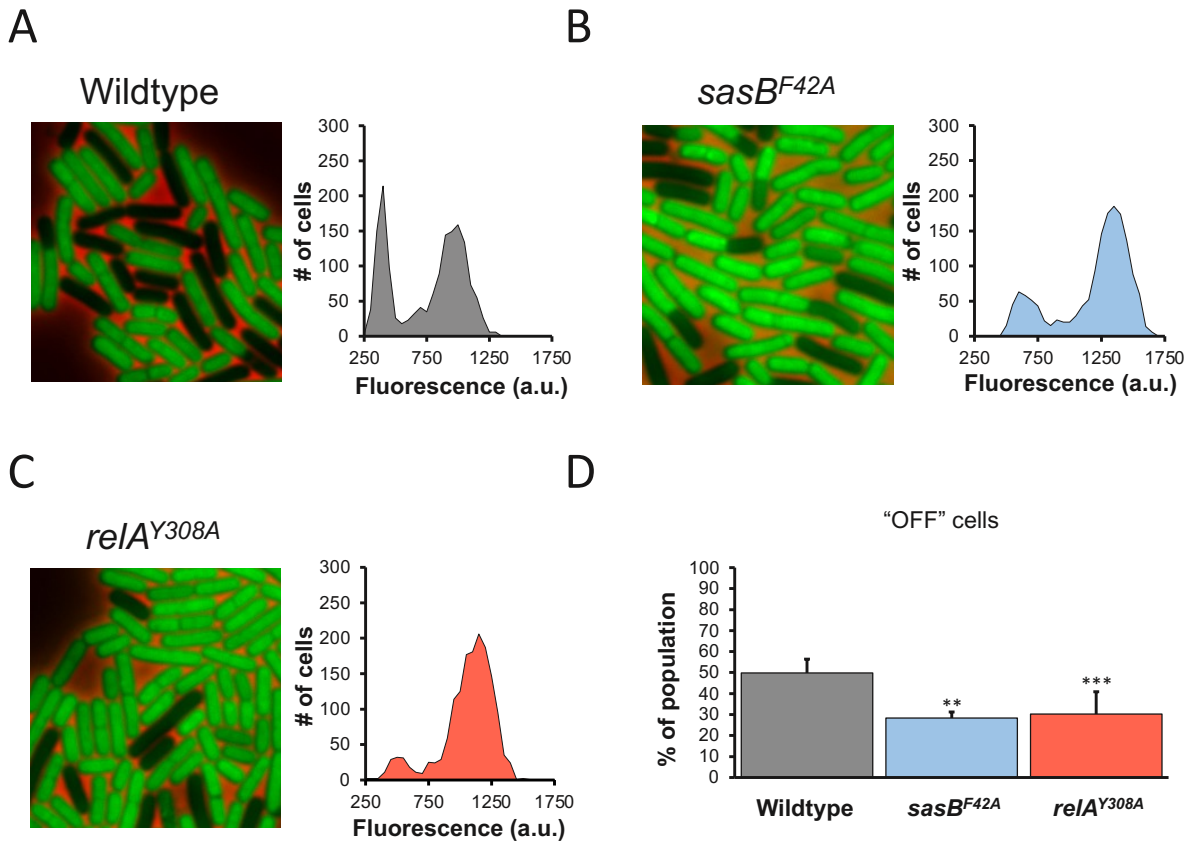

Figure 4.3 Allosteric activation of SasB is required for cells with low protein synthesis. (A, B, C) Representative picture and population distribution of OPP labeled **(A)** wildtype, **(B)** *sasB*^{F42A}, and **(C)** *relA*^{Y308A} strains during late transition phase. **(D)** Quantitation of OPP "OFF" cells over three independent experiments for A-C (means ± SDs). n.s. $p > 0.05$, *$p < 0.05$, **$p < 0.01$, ***$p < 0.001$.

4.4 SasB allosteric activation is inhibited by pGpp

A strain lacking SasA (Δ*sasA*) contains more "OFF" cells as compared to the wildtype parent **(Figure 4.1 C)**. The presence of this sub-population of cells ("OFF") depends on a SasB protein that can be allosterically activated **(Figure 4.3 B)**. Integrating these two observations, I hypothesized that the product of SasA (pGpp) inhibits the allosteric activation of SasB by pppGpp. The similarity of these molecules suggests that they could have an antagonistic interaction since they are likely capable of binding to the same site on SasB, but their differing phosphorylation states could affect their ability to allosterically activate SasB.

I tested this model by assaying *in vitro* whether pGpp inhibits the allosteric activation of SasB. First, I confirmed, as previously reported, that SasB generates more ppGpp when reactions are supplemented with pppGpp (85) and observed a ~2 fold increase in ppGpp production when SasB was incubated with pppGpp **(Figure 4.4 A)**. Using pGpp synthesized *in vitro* by the newly identified (pp)pGpp hydrolase NahA (87), I observed that pGpp attenuates the allosteric activation of SasB in a dose dependent manner **(Figure 4.4 A)**. Since even the highest concentration of pGpp did not decrease production of ppGpp relative to that generated by SasB without the addition of pppGpp **(Figure 4.4 A)**, the inhibition is likely specific to the allosteric activation. I tested this directly by assaying the effect of pGpp on SasB activity in the absence of its allosteric activator (pppGpp). Addition of pGpp did not significantly affect SasB activity within the range of pGpp concentrations I used previously **(Figure 4.4 C)**. I also confirmed the specificity by assaying a SasB F42A mutant protein ($SasB^{F42A}$) that is insensitive to allosteric activation by pppGpp (85). As previously reported, $SasB^{F42A}$ had similar activity to a non-allosterically activated WT SasB in the presence of pppGpp **(Figure 4.4 B)**. However, in contrast with wildtype SasB, pGpp did not affect the activity of $SasB^{F42A}$ even when pppGpp was included **(Figure 4.4 B)**.

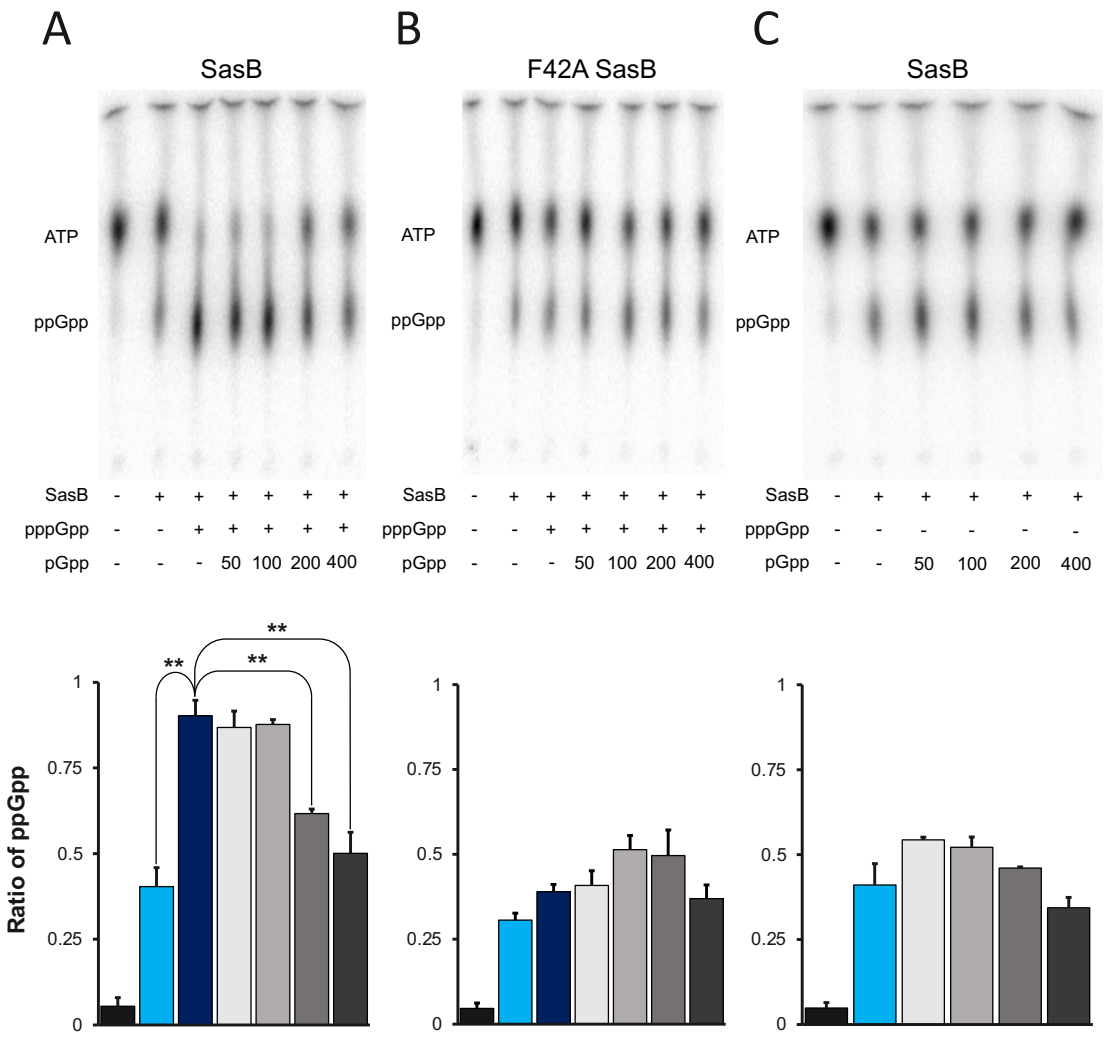

Figure 4.4 pGpp inhibits allosteric activation of SasB by pppGpp
(A) Representative TLC of nucleotides present following incubation of wildtype SasB with [α-^{32}P]-ATP and GDP in the presence or absence of pppGpp and increasing concentrations of pGpp (top). Quantitation of the ratio of ppGpp present in each lane in TLC. Ratio of ppGpp calculated using the formula, ppGpp/ATP + ppGpp (bottom) **(B)** Representative TLC of nucleotides present following incubation of SasB^{F42A} with [α-^{32}P]-ATP and GDP in the presence or absence of pppGpp and increasing concentrations of pGpp (top). Ratio of ppGpp present in each lane in TLC. As determined the formula, ppGpp/ATP + ppGpp (bottom). Statistical analysis (two tailed t-test) showed no significance ($p > 0.05$) between reactions containing SasB whether or not pppGpp and pGpp was included. **(C)** Representative TLC of nucleotides present following incubation of wildtype SasB with [α-^{32}P]-ATP and GDP in the absence of pppGpp and increasing concentrations of pGpp (top). Ratio of ppGpp present in each lane in TLC. As determined the formula, ppGpp/ATP + ppGpp (bottom). Statistical analysis (two tailed t-test) showed no significance ($p > 0.05$) between reactions containing SasB whether or not and pGpp was included. (means ± SDs). n.s. $p > 0.05$, *$p < 0.05$, **$p < 0.01$, ***$p < 0.001$

4.5 Cross-talk between nucleotides is not observed on (pp)pGpp RNA sensor

The allosteric activation of SasB (by pppGpp) is inhibited in the presence of the nucleotide generated by SasA (pGpp) **(Figure 4.4).** These data suggest that, at least *in vitro,* SasB is able to integrate the relative levels of either of these two nucleotides and this results in an either allosterically activated SasB (when pppGpp is bound) that produces comparatively high amounts of ppGpp or an allosterically inactivated SasB (when pGpp is bound) that produces comparatively low amounts of ppGpp. The differential action of these two nucleotides is surprising given that they are structurally similar. It does, however, allow for a more fine-tuned response that presumably relies on the information communicated through either comparatively low or high concentrations of either of these two nucleotides (cell wall metabolism and amino acid availability). I wondered if this kind of cross-talk between phosphorylated guanosine nucleotides also occurred in a different system.

Recently, a new class of riboswitches that bind ppGpp has been identified in Firmicutes (100). Riboswitches are RNA structures within non-coding sections of certain mRNAs that act as regulators of gene expression by directly binding small molecules such as metabolites, coenzymes, signaling molecules, or inorganic ion ligands (119). Upon binding their corresponding small molecule, the riboswitch folding pattern changes, and this change affects the expression of the downstream mRNA (119). Binding of ppGpp to a riboswitch present in the 5'UTR of the *ilvE* gene in *Desulfitobacterium hafniense* (*D. hafniense*) was shown to differentially control transcription termination (100). Specifically, the P3 helix of this aptamer, which acts as a transcriptional anti-terminator, is stabilized in the presence of ppGpp so that when ppGpp is bound, more full-length transcript is generated (100). I wondered if RNA based ppGpp sensors could also be subjected to the crosstalk I observed on SasB. This would not only suggest that this kind of crosstalk between

phosphorylated guanosine nucleotides is a conserved mechanism in bacterial physiology but would also add an interesting level of regulation on riboswitches because it would allow for the integration of multiple signals on one RNA molecule.

I decided to test if transcriptional termination by the *D. hafniense ilvE* 5'UTR encoded riboswitch, which is anti-terminated in the presence of ppGpp was differentially affected by pGpp. To do this, I measured the amount of full-length transcript (FL) and terminated transcript (T) present in single turnover *in vitro* transcription termination assays (100). As previously shown, the expression platform, which contains the natural transcription start site and the ppGpp binding riboswitch of the *D. hafniense ilvE* and ends 28 nucleotides beyond the terminator stem, operates with the *E. coli* RNA polymerase and generates a FL transcript and a T transcript in the absence of ppGpp **(Figure 4.5)**. When I added ppGpp to these reactions, the amount of FL is significantly higher, indicating that ppGpp binding anti-terminated the transcript **(Figure 4.5)**. Next I asked if pGpp had a similar or different effect on anti-termination of this transcript. Inclusion of pGpp in these reactions similarly increased the amount of FL indicating that pGpp also anti-terminates transcription by the *D. hafniense ilvE* riboswitch **(Figure 4.6)**. These results suggest that, unlike SasB, the *D. hafniense ilvE* riboswitch is not subject to cross-talk between phosphorylated guanosine nucleotides because both nucleotides have the same action. At this time however, I cannot rule out that this kind of regulation does occur on a different naturally occurring ppGpp binding riboswitch. Testing this, however, is outside the scope of this thesis.

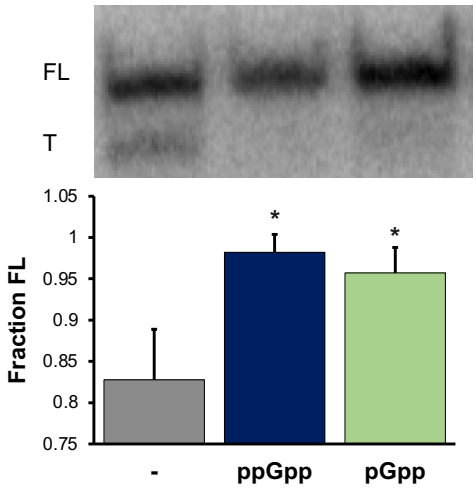

Figure 4.5 ppGpp and pGpp have similar functions on a ppGpp binding riboswitch. Anti-termination of the *D. hafniense ilvE* riboswitch by ppGpp was measured using single turnover *in vitro* transcription termination assays. Termination of the full length (FL) transcript occurs in the absence of any added nucleotide (gray) and a terminated (T) transcript is observable. In the presence of 100 uM ppGpp (navy) the terminated transcript is missing and the fraction of FL transcript generated increases. Similarly to the action of ppGpp, pGpp also antiterminates the *D. hafniense ilvE* riboswitch and reactions with 100 uM pGpp (green) have significantly more FL than reaction without any nucleotide added. (means ± SDs). n.s. $p > 0.05$, *$p < 0.05$, **$p < 0.01$, ***$p < 0.001$

4.6 The effect of *sasA* depends on *sasB* and *relA*

The *in vitro* biochemical experiments in **(Figure 4.4)** suggests that the effect of SasA on the heterogeneity of protein synthesis is dependent on the activity of SasB. If this is true *in vivo*, then a *sasB* deletion should be epistatic to a *sasA* deletion. Consistently, a strain lacking both SasA and SasB (Δ*sasA* Δ*sasB*) exhibits a loss of heterogeneity in comparison to the single *sasA* deletion **(Figure 4.6 A, B, D).** Thus, the effect of SasA is dependent *in vivo* on SasB. Finally, since RelA activates SasB, a Δ*sasA* mutation should be epistatic to a *relA* mutation with respect to protein synthesis. A strain expressing $RelA^{Y308A}$ and carrying a Δ*sasA* mutation exhibits a similar loss of heterogeneity as compared to $relA^{Y308A}$, demonstrating that the effect of the Δ*sasA* mutation depends on a functional RelA synthetase **(Figure 4.6 A, B, D)**. This result is consistent with the hypothesis that *sasA* is epistatic to *relA*.

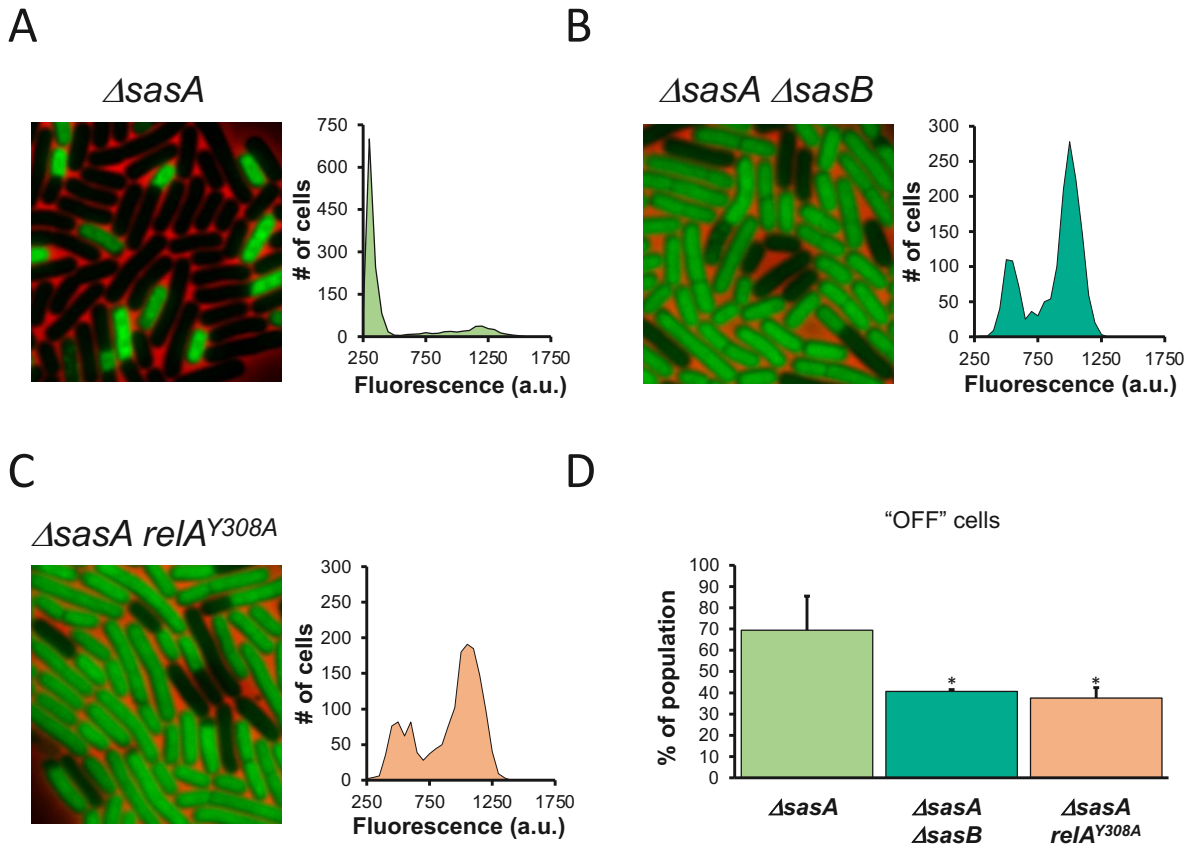

Figure 4.6 The effect of *sasA* depends on *sasA* and *relA*. (A, B, C) Representative picture and population distribution of OPP labeled **(A)** *ΔsasA*, **(B)** *ΔsasA ΔsasB*, and **(C)** *ΔsasA relA*^{Y308A} strains during late transition phase. **(D)** Quantitation of OPP "OFF" cells over three independent experiments for A-C (means ± SDs). n.s. $p > 0.05$, *$p < 0.05$, **$p < 0.01$, ***$p < 0.001$

Chapter 5

5 (pp)pGpp directly regulates translation initiation during entry into quiescence

5.1 ppGpp is sufficient to inhibit protein synthesis

The data provided in Chapter 4 indicates that during entry into stationary phase, a network of (pp)pGpp synthetases regulate heterogeneity of protein synthesis by regulating the allosteric activation of SasB **(Figures 4.3)**. The main activity of SasB in *B. subtilis* is to generate the tetra-phosphorylated guanosine nucleotide, ppGpp (79). I also showed that (pp)pGpp is required for the down-regulation of protein synthesis in a subpopulation of cells during entry into stationary phase **(Figure 3.8 "Late transition").** (pp)pGpp has previously been suggested to directly inhibit translation by binding to and inhibiting the function of translational GTPases, including IF2 and EF-Tu (75, 120). That (pp)pGpp directly inhibits translation and regulates protein synthesis *in vivo* has not been shown, however. These data together address how the heterogeneity is derived and suggest that the accumulation of ppGpp in the subpopulation of cells with comparatively low levels of protein synthesis directly inhibits translation. The biochemical mechanism by which protein synthesis itself is down-regulated is not directly addressed by these data, however. To more closely understand if ppGpp directly inhibits protein synthesis, I first asked if ppGpp on its own can inhibit protein synthesis *in vivo*.

To address this question, I placed the *B. subtilis* (pp)pGpp synthetase *sasB* under the control of a xylose inducible promoter (P_{xyl}) in a strain lacking RelA, the bifunctional (pp)pGpp synthetase and hydrolase, as well the accessory (pp)pGpp synthetases SasA and SasB. The RelA mutation is required for accumulation of ppGpp during *sasB* expression, presumably because it would hydrolyze the ppGpp generated during log phase if it was present (79). The SasA and SasB mutations are required to delete RelA because its hydrolytic activity is essential in a strain with

SasA and SasB (115). As previously observed (79), induction of *sasB* in the presence of these mutations during exponential phase (T_0) results in the accumulation of ppGpp without a noticeable decrease in growth during exponential phase **(Figure 5.1A)**. To determine how ppGpp affects protein synthesis, I labeled cells with OPP following a 60 minute xylose treatment (T_{60}) **(Figure 5.1A)**. At 60 minutes following inducer addition (T_{60}), protein synthesis is significantly reduced in the induced culture as compared to the un-induced culture as can be seen in representative pictures and population distributions of OPP labeling **(Figure 5.1 B, C).** This effect is quantified in **Figure 5.1 D** over three independent experiments, which show that protein synthesis is decreased by 40% in cells expressing *sasB* for 60 minutes during exponential phase **(Figure 5.1 D).** These data indicate that ppGpp is sufficient to inhibit protein synthesis.

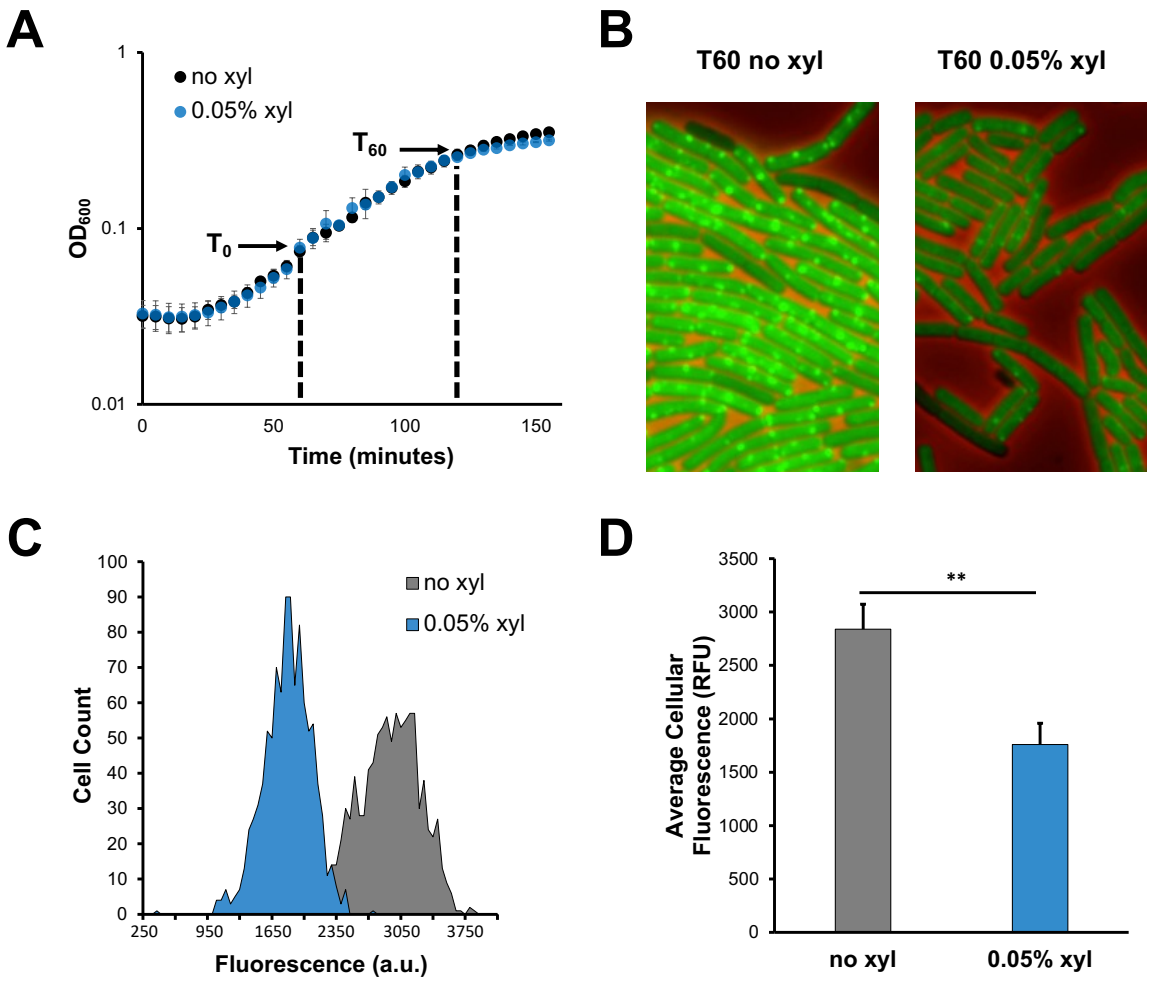

Figure 5.1 *sasB* expression is sufficient to inhibit protein synthesis. The effect of ppGpp on protein synthesis was tested *in vivo* using expression of an inducible ppGpp synthase, *sasB*. **(A)** Growth of a P_{xyl}-*sasB* strain in the presence and absence of induction. Induction of *sasB* occurs during logarithmic growth (T_0) with 0.05% xylose (xyl). Cells growth is monitored throughout exponential phase and labeled with OPP at 60 minutes after xyl addition (T_{60}). **(B)** Representative pictures of OPP-labeled induced and uninduced cultures of a P_{xyl}-*sasB* strain 60 min after induction (T_{60}). **(C)** Representative population distributions of OPP-labled induced and uninduced cultures of a P_{xyl}-*sasB* strain 60 min after induction (T_{60}). **(C)** Average cellular Fluorescence (RFU) of OPP-labeled induced and uninduced cultures of a P_{xyl}-*sasB* strain 60 min after induction (T_{60}) across three independent experiments (means ± SDs). n.s. $p > 0.05$, *$p < 0.05$, **$p < 0.01$, ***$p < 0.001$.

5.2 ppGpp inhibits translation specifically

Given the potential complications in distinguishing indirect effects of (pp)pGpp on global protein synthesis, such as those involving translation of ribosomal proteins, these experiments do not assess a direct effect of (pp)pGpp on translation. To directly address this I utilized the PURExpress *in vitro* reconstituted, coupled transcription-translation system (NEB) that utilizes a defined mix of purified transcription and *E. coli* translation components to transcribe and translate a specific mRNA (121). This purified system is appropriate to study the effects of ppGpp on translation because it utilizes purified components including the T7 RNA polymerase, which has been previously shown to be insensitive to ppGpp (122). Addition of ppGpp to PURExpress reactions inhibited synthesis of a reporter protein (CotE) in a dose-dependent fashion (**Figure 5.2 A**). Concentrations of ppGpp sufficient to significantly inhibit CotE synthesis (~1 mM) are similar to those of (pp)pGpp observed during stringent response induction in *E. coli* (123). qRT-PCR analysis demonstrated that ppGpp had no effect on *cotE* transcription at concentrations where CotE synthesis was significantly impaired (**Figure 5.2 B),** consistent with the known insensitivity of the T7 RNA polymerase used in the PURExpress reaction to ppGpp (122). Thus, ppGpp directly inhibits translation *in vitro*.

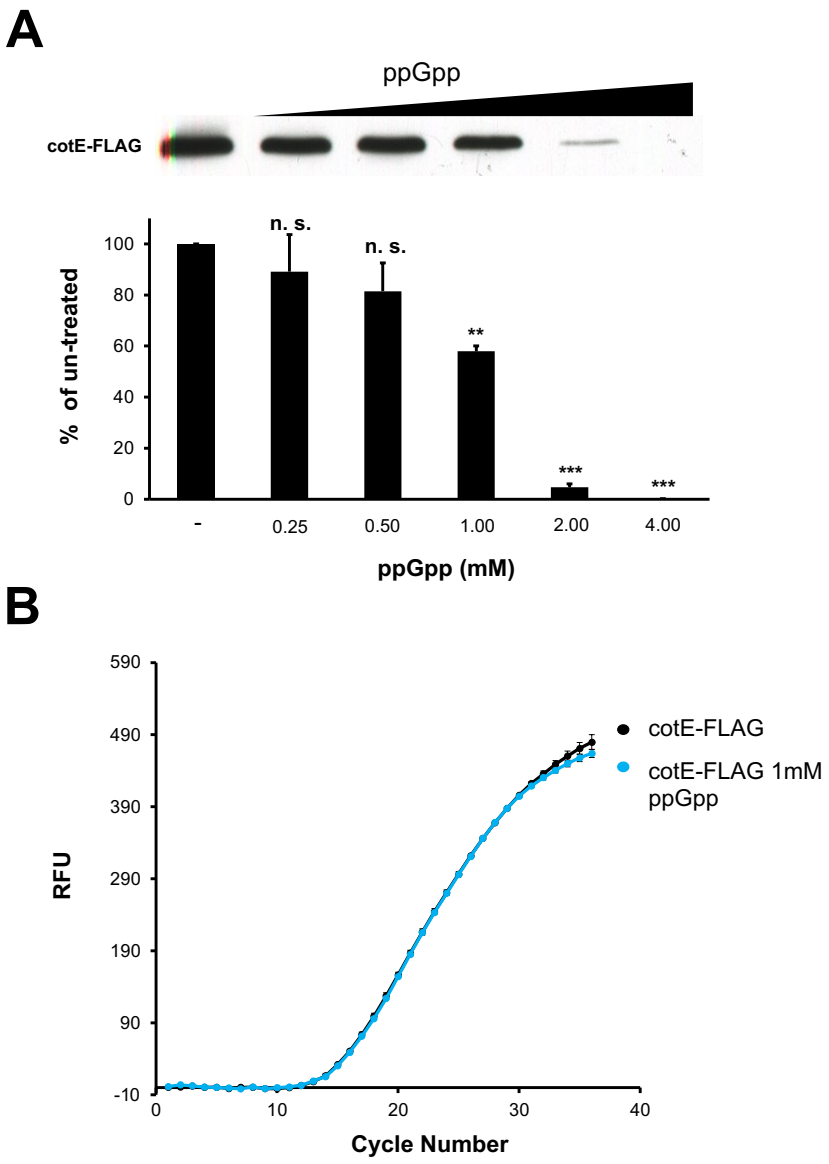

Figure 5.2 ppGpp directly inhibits translation. (A) Protein synthesis activity is monitored using production of CotE-FLAG protein by a PURExpress reaction (NEB) in the absence or presence of ppGpp was assayed via Western blot with α-FLAG. **(B)** Synthesis of *in vitro* transcribed *cotE* mRNA was measured by quantifying total mRNA produced in the presence of a concentration of ppGpp (1mM) that significantly inhibits protein production. RNA was quantified using RT-qPCR (means ± SDs). n.s., not significant; **P < 0.01; ***P < 0.001.

5.3 IF2 is a target of (pp)pGpp

Given these observations, I wished to identify the component(s) of the translation machinery that is (are) targeted by ppGpp *in vivo*. The translational GTPases EF-Tu (124), EF-G (125), and IF2 (126, 127), as well as the ribosome-associated GTPases including Obg (76, 128), RsgA (92, 129), RbgA (92, 130), Era (92), and HflX (92, 129), have all been reported to bind ppGpp. However, since ppGpp inhibits protein synthesis by the PURExpress system (**Figure 5.2 A**), which contains IF2, EF-Tu, and EF-G, but not the other GTPases, inhibition of one or more of these three proteins is likely sufficient to account for the *in vivo* inhibitory effect of (pp)pGpp on translation.

I first investigated whether IF2 was a target under my conditions because it has been proposed to serve as a "metabolic sensor" of (pp)pGpp (127). I therefore attempted to identify mutations in IF2 that would affect (pp)pGpp binding without disrupting GTP binding sufficiently to impair normal function. *E. coli* EF-G and IF2 have a differential affinity for (pp)pGpp (125) and similar but not absolutely conserved G domains. So, if I could identify residue(s) that affect this difference, this information might allow me to construct a *B. subtilis* IF2 allele less sensitive to (pp)pGpp. I focused on those IF2 residues which display a shift in NMR spectra upon binding of ppGpp as compared to GDP (**Figure 5.3 B,** blue residues**)** (127) since GDP interacts with multiple residues in the G domain of IF2 (131). I aligned the region containing those residues (*i.e.*, the G1 motif) with the homologous region in EF-G, which has lower affinity for (pp)pGpp than IF2 (**Figure 5.3 A**). I noted that one of the blue residues in IF2, Gly-226, is an alanine residue (Ala-18) in EF-G (**Figure 5.3 B**, red). In addition, the histidine residue (His-230) in IF2 that is adjacent to the two blue residues is an alanine (Ala-21) in EF-G (**Figure 5.3 B**, red). These differences suggested that substituting the IF2 residues with the corresponding residues found in EF-G would affect the ability of IF2 to bind (pp)pGpp. I therefore used the DRaCALA filter binding assay and observed

that the double mutant IF2 (G226A H230A) bound (pp)pGpp significantly less well than the wildtype protein (**Figure 5.3 C**).

To test the functional consequence of mutating these residues in *B. subtilis* IF2, I used a PURExpress kit that lacks IF2 (ΔIF2). I first confirmed that the ΔIF2 kit, which contains purified *E. coli* translation factors, works equivalently whether the added IF2 is derived from *E. coli* or *B. subtilis* (**Figure 5.4 B**). When supplied as the sole source of IF2 in this reaction, the double mutant *B. subtilis* IF2 produced an equivalent amount of protein as wild type *B. subtilis* IF2 (**Figure 5.4 B**), demonstrating that the slight reduction in GTP binding (**Figure 5.4 A**) did not substantially affect IF2 function in translation. However, the double mutant *B. subtilis* IF2 was significantly less sensitive to ppGpp inhibition than its wild type counterpart (**Figure 5.3 D**). Taken together, these results indicate that ppGpp binding to IF2 accounts for a substantial portion of the inhibition of translation by ppGpp.

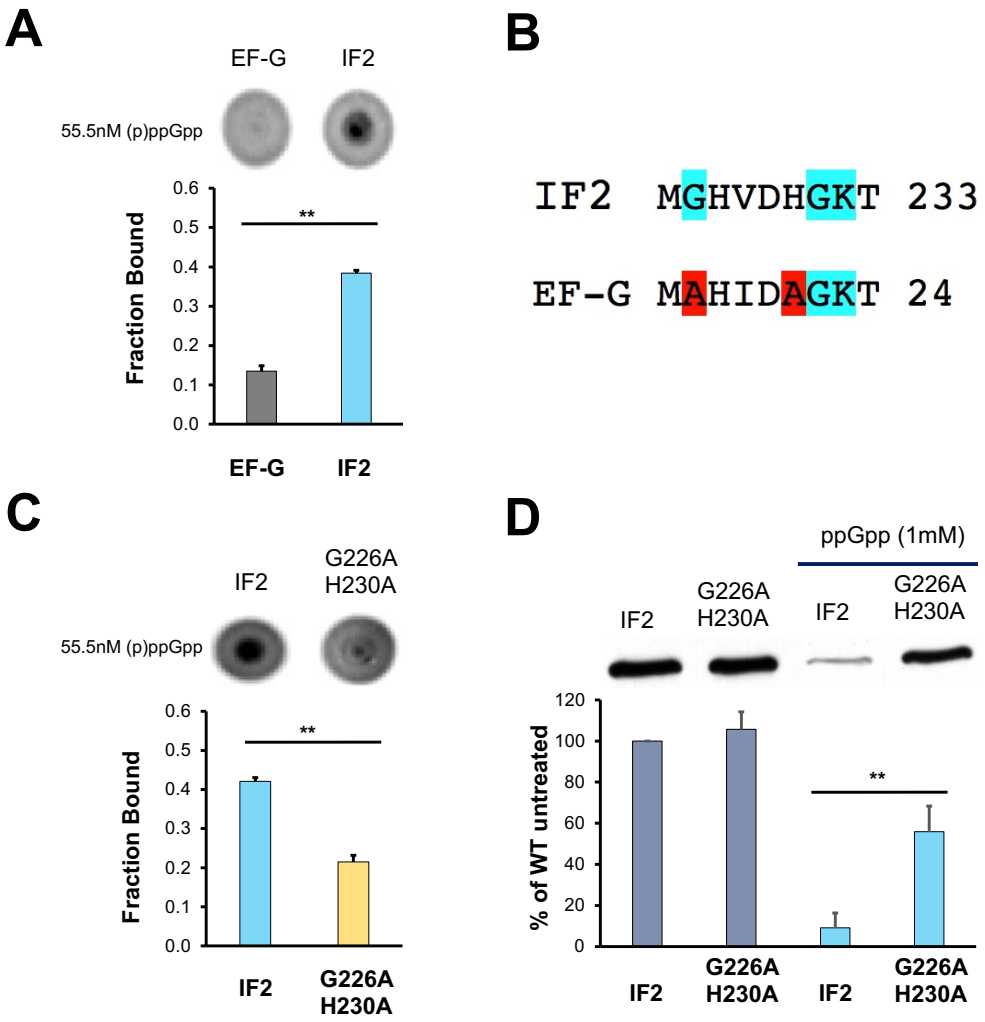

Figure 5.3 IF2 is a target of ppGpp IF2 was validated *in vitro* as a direct target of ppGpp using IF2 mutations that reduce ppGpp binding. **(A)** Affinity of *B. subtilis* EF-G and IF2 for (p)ppGpp was compared using the differential radial capillary action of a ligand assay (DRaCALA) (102). (means ± SDs). **(B)** Alignment of G1 domains of *B. subtilis* IF2 and EF-G. Residues in blue denote those most shifted upon binding of ppGpp *versus* GDP (127). Residues in red are those that differ in EF-G and IF2 and were used to engineer a mutant IF2 with reduced affinity for ppGpp (G226A H230A). **(C)** DRaCALA-based comparison of (p)ppGpp affinity for WT and mutant IF2 (means ± SDs). **(D)** *In vitro* sensitivity of WT and mutant IF2 was assessed using the PURExpress system (NEB). WT and mutant IF2 were added at equimolar amounts to separate PURExpress reactions in the presence of 1mM ppGpp and protein synthesis was monitored by Western blot (means ± SDs). n.s. $p > 0.05$, *$p < 0.05$, **$p < 0.01$, ***$p < 0.001$

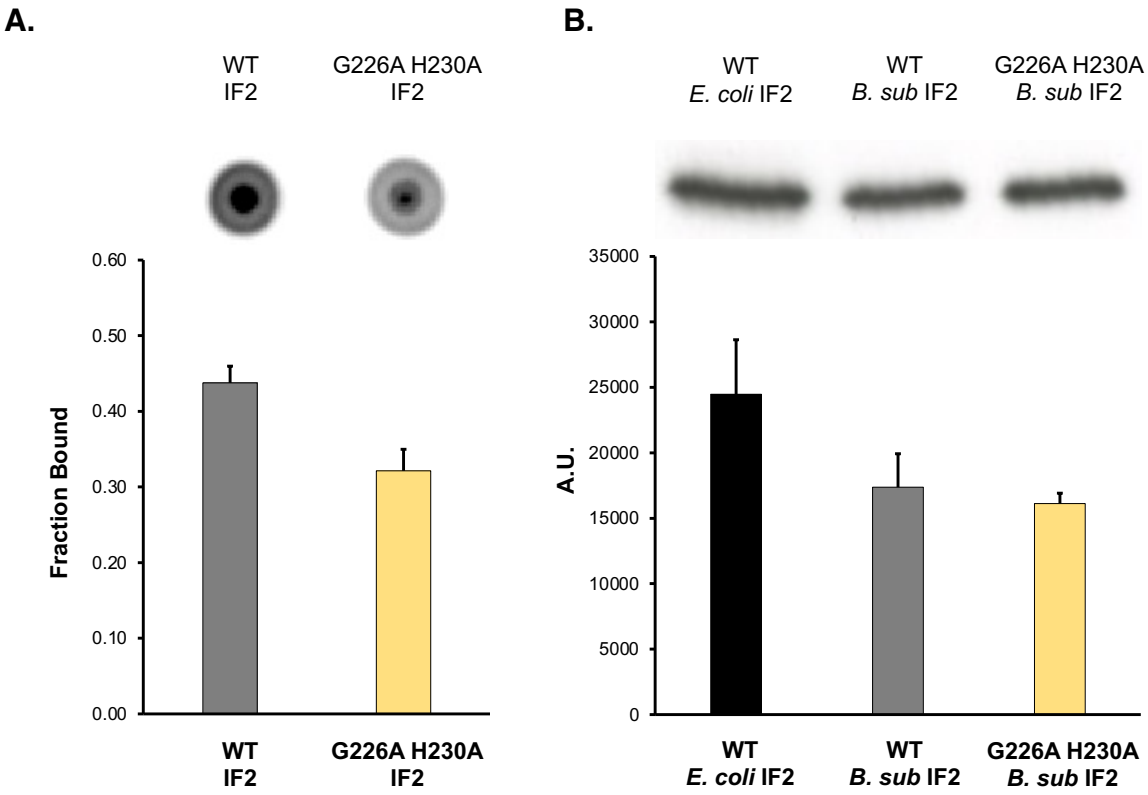

Figure 5.4 G226A H230A IF2 mutant binds GTP less but is not inhibited in function. (A) GTP binding and **(B)** function of G226A H230A IF2 mutant was assayed using DRaCALA assay and *in vitro* transcription-translation assay respectively (means ± SDs).

5.4 ppGpp fails to allosterically activate IF2 for rapid subunit joining

Previously, Milón and colleagues demonstrated that ppGpp inhibits IF2's ability to catalyze 30S IC assembly and subunit joining (127). To elucidate the structural basis of this inhibition, I worked in collaboration with Ruben Gonzalez's lab in the Chemistry department at Columbia to investigate how ppGpp inhibits IF2 function. The Gonzalez lab has previously developed a single molecule FRET method to observe structural aspects of IF2 binding to the 30S IC (132) and has shown that GTP binding allosterically positions IF2 in a confirmation that mediates rapid 50S subunit joining (103). We wished to determine whether and how ppGpp influences the binding of *E. coli* IF2 to the *E. coli* 30S IC and the conformational dynamics of *E. coli* 30S IC-bound IF2. Briefly, IF2 promotes binding of initiator tRNA (fMet-tRNA^{fMet}) to the 30S subunit and uses its domain IV (dIV) to directly contact the *N*-formyl-methionine and aminoacyl acceptor stem of fMet-tRNA^{fMet}, resulting in formation of an IF2-tRNA sub-complex on the intersubunit surface of the 30S IC (133). The presence of GTP in the G domain and recognition of fMet-tRNA^{fMet} by dIV 'activate' 30S IC-bound IF2 for rapid subunit joining (134). We previously used an IF2-tRNA single-molecule fluorescence resonance energy transfer (smFRET) signal (132), to show that activation of IF2 for rapid subunit joining involves a GTP- and fMet-tRNA^{fMet}-dependent conformational change of IF2 that results in an increase in the affinity of IF2 for the 30S IC and an increase in the rate of subunit joining (103). To understand how ppGpp affected this interaction, we began by comparing the affinities of GTP-bound IF2 (IF2(GTP)) and ppGpp-bound IF2 (IF2(ppGpp)) for the 30S IC. As in our previous studies (103, 132), E_{FRET} *versus* time trajectories recorded for individual 30S ICs fluctuate between a zero FRET state (IF2-free 30S IC) and a non-zero FRET state (IF2-bound 30S IC) (**Figure 5.5,** third row). Initial inspection of these trajectories and the corresponding surface contour plots of the post-synchronized time evolution of population

FRET reveals that, while IF2(GTP) exhibits relatively long-lived and stable binding events on the 30S IC, IF2(ppGpp) exhibits significantly shorter-lived and unstable binding events (**Figure 5.5,** third and fourth rows). To quantitatively compare the affinities of IF2(GTP) and IF2(ppGpp) for the 30S IC, we extracted kinetic and thermodynamic parameters from the smFRET data describing the binding of IF2 to the 30S IC. We find that IF2(ppGpp) has a significantly lower affinity for the 30S IC compared to IF2(GTP), with an equilibrium dissociation constant (K_d) that is ~10-fold higher (**Table S1**).

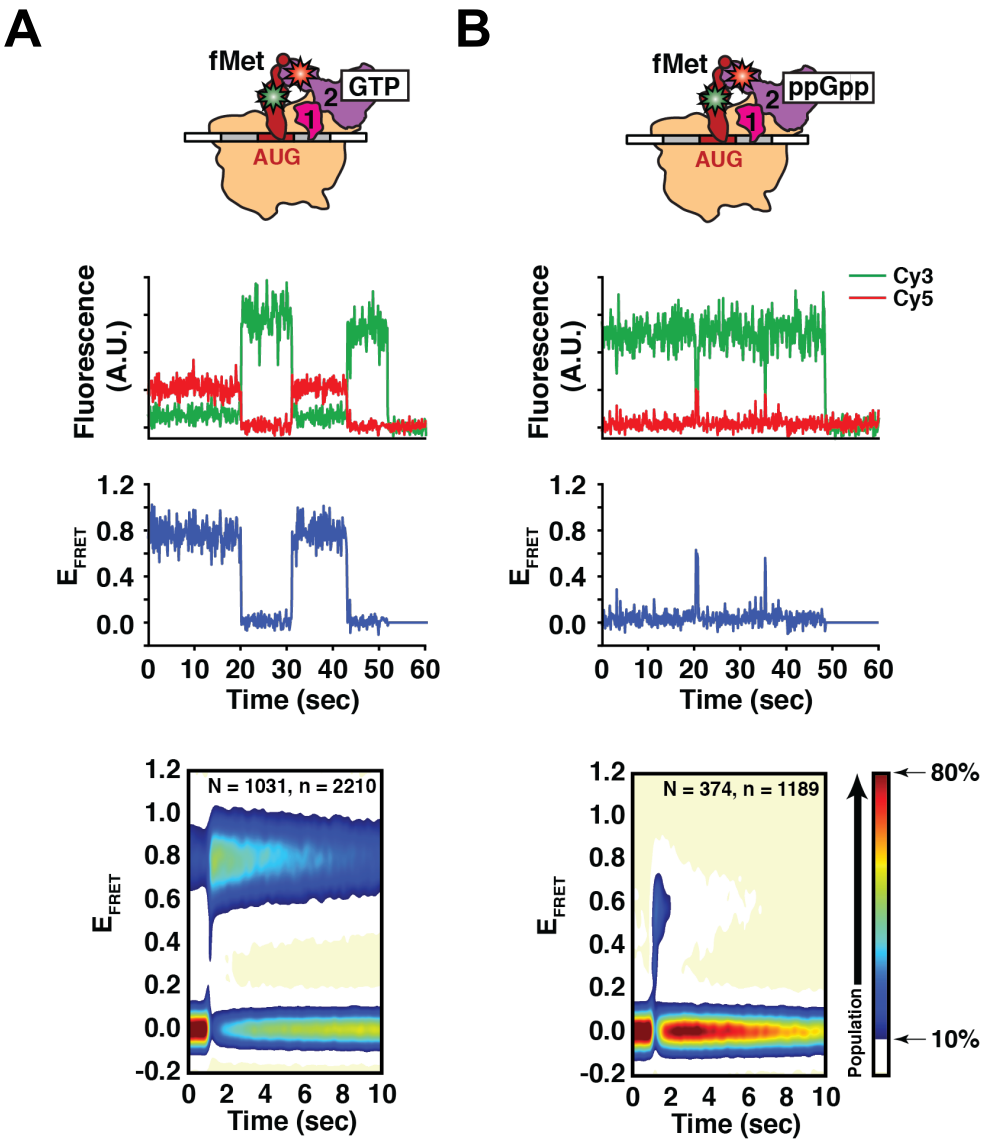

Figure 5.5. ppGpp inhibits IF2 function in catalyzing rapid 50S subunit joining
The binding of IF2 to the 30S IC and the conformation of 30S IC-bound IF2 in the presence of **(A)** GTP and **(B)** ppGpp were directly observed by single-molecule fluorescence resonance energy transfer (smFRET) using an IF2-tRNA smFRET signal. First row: Cartoon representations of 30S ICs assembled using Cy3 FRET donor fluorophore-labeled fMet-tRNA^{fMet} and Cy5 FRET acceptor fluorophore-labeled IF2(GTP) or IF2(ppGpp). Second row: Plots of Cy3 (green) and Cy5 (red) fluorescence emission intensity *versus* time trajectories. Third row: Plots of the E_{FRET} *versus* time trajectories corresponding to the plots of Cy3 and Cy5 fluorescence intensity trajectories in the second row. Fourth row: Surface contour plots of the post-synchronized time evolution of population FRET. These plots are generated by superimposing the E_{FRET} *versus* time trajectories of individual IF2 binding events such that the start of each event is computationally post-synchronized to time = 0 sec, thereby allowing visualization of the time evolution of population FRET for the entire population of IF2 binding events. "N" indicates the total number of individual 30S ICs analyzed and "n" indicates the total number of individual IF2 binding events analyzed.

(The experiments in Figure 5.5 were performed by Jaewook Ryu. Data was analyzed by Jaewook Ryu and Kelvin Caban.)

Table 1. Association rate constant (k_a), dissociation rate constant (k_d), and equilibrium dissociation constant (K_d) for the interaction of IF2(GTP) and IF2(ppGpp) with the 30S IC.

	k_a (μM^{-1} s^{-1})[a]	k_d (s^{-1})[a]	K_d (nM)[a]
IF2(GTP)	4.9 ± 0.2	0.032 ± 0.003[b]	6.5 ± 0.2
IF2(ppGpp)	3.3 ± 0.3	2.0 ± 0.3	616 ± 140

[a] k_a, k_d, and K_d were obtained from three independently collected datasets (mean ± SE)

[b] k_d was corrected for the effects of Cy5 photobleaching as described in Methods

We then compared the conformations of IF2(ppGpp) and IF2(GTP) on the 30S IC by plotting histograms of the E_{FRET} values observed under each condition **(Figure 5.6)**. Consistent with our previous studies, we observed a single non-zero peak centered at an $\langle E_{FRET} \rangle$ of ~0.74 for 30S IC-bound IF2(GTP), corresponding to a distance between our labeling positions of ~46.2 Å (assuming a Förster distance, R_0, of ~55 Å; ref. 58) **(Figure 5.6 A)**. In contrast, we observed a single nonzero peak centered at a significantly lower $\langle E_{FRET} \rangle$ of ~0.53 ($P < 0.005$) for 30S IC-bound IF2(ppGpp), corresponding to a distance between our labeling positions of ~53.9 Å, an increase of ~7.7 A relative to IF2(GTP) **(Figure 5.6 B)**. Notably, the E_{FRET} distribution of 30S IC-bound IF2(ppGpp) closely resembles that of 30S IC-bound IF2(GDP) (57). Thus, the 30S IC-bound IF2(ppGpp) exhibits a conformation that is similar to an IF2 inactive for rapid subunit joining (i.e., IF2(GDP)).

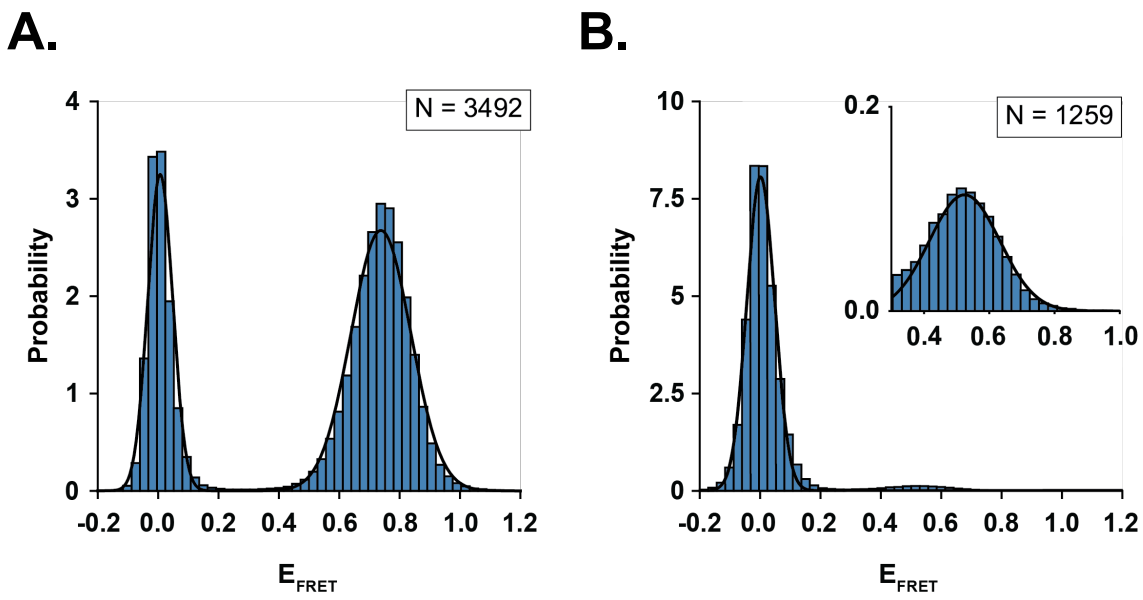

Figure 5.6. IF2(GTP) and IF2(ppGpp) exhibit distinct conformations when bound to the 30S IC

One-dimensional histograms of E_{FRET} value distributions corresponding to the interaction of IF2 with the 30S IC for **(A)** IF2(GTP) and **(B)** IF2(ppGpp). Both histograms were fitted to a two-Gaussian mixture model in which the Gaussian centered at the zero E_{FRET} value corresponds to the IF2-free state of the 30S IC and the Gaussian centered at the non-zero E_{FRET} value corresponds to the IF2-bound state of the 30S IC. However, for the histogram corresponding to IF2(ppGpp), the IF2-bound state was re-fitted to a single Gaussian for datapoints in which $E_{FRET} > 0.2$ (inset). The center of each fitted Gaussian was used to determine the mean E_{FRET} value for the corresponding state ($\langle E_{FRET} \rangle$). The Gaussians corresponding to the IF2-free, IF2(GTP)-bound, and IF2(ppGpp)-bound states of the 30S IC had $\langle E_{FRET} \rangle$s of ~0.0 (in both histograms), ~0.74, and ~0.53, respectively.

(The experiments in Figure 5.6 were performed by Jaewook Ryu. Data was analyzed by Jaewook Ryu and Kelvin Caban.)

5.5 (pp)pGpp binding to IF2 mediates translation inhibition during transition phase

My identification of an IF2 allele that is less sensitive to (pp)pGpp *in vitro* enabled me to test the initial hypothesis that (pp)pGpp accumulation reduces protein synthesis *in vivo* because (pp)pGpp binds IF2 and inhibits its function in translation. To do this, I generated a *B. subtilis* strain expressing, as the sole source of IF2, a mutant protein containing the mutations G226A and H230A that *in vitro* exhibits reduced ppGpp binding without substantially affecting IF2 function (**Figure 5.3 C, Figure 5.4 B**). This strain grows equivalently to the wildtype parent throughout all phases of growth, validating that the mutant IF2 is functional *in vivo* (**Figure 5.8 A**). I tested how these mutations affect protein synthesis during late transition phase since in the wildtype background, protein synthesis is strongly inhibited in a subpopulation of cells during this period (**Figure 5.7 A**). Mutations in IF2 that affect its binding to (pp)pGpp appear to significantly attenuate this phenotype (**Figure 5.7 A, B).** I quantified the effect of these mutations in IF2 by quantifying the number of "OFF" cells in this strain compared to wildtype across three independent experiments before and observe that the G226A H230A IF2 strain has significantly less cells with comparatively low protein synthesis compared to wildtype **(Figure 5.8 B).** This attenuation is similar to that observed in the complete absence of (pp)pGpp (**Fig 3.8**), consistent with it resulting from a direct interaction of (pp)pGpp with IF2. Thus, during transition phase, (pp)pGpp binding to IF2 is sufficient to substantially inhibit translation and thereby reduce protein synthesis.

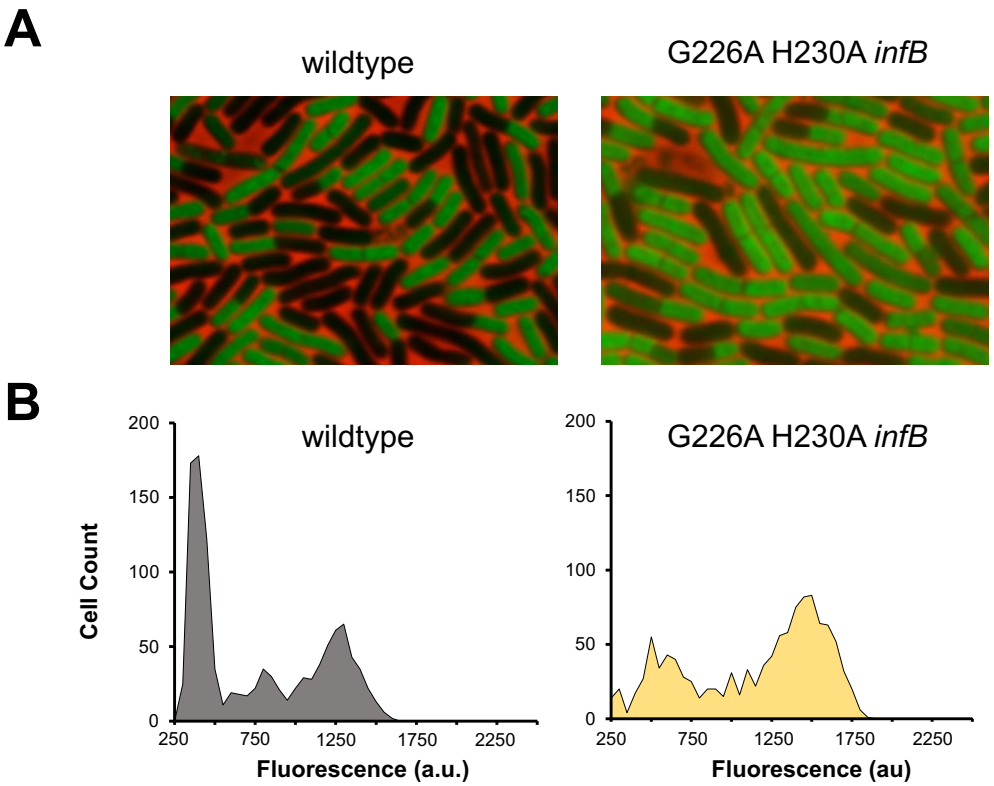

Figure 5.7 IF2 mediates inhibition of protein synthesis by (pp)pGpp during late transition phase. IF2 was validated as an *in vivo* target of (pp)pGpp by measuring protein synthesis in a strain expressing an IF2 G226A H230A double mutant. **(A)** Representative pictures of WT (JDB 1772), (pp)pGpp^0 (JDB 4294), and G226A H230A *infB* (JDB 4297) strains labelled with OPP during late transition phase. **(B)** Distributions of mean cell fluorescence of WT, (pp)pGpp^0 and G226A H230A *infB* strains during late transition phase.

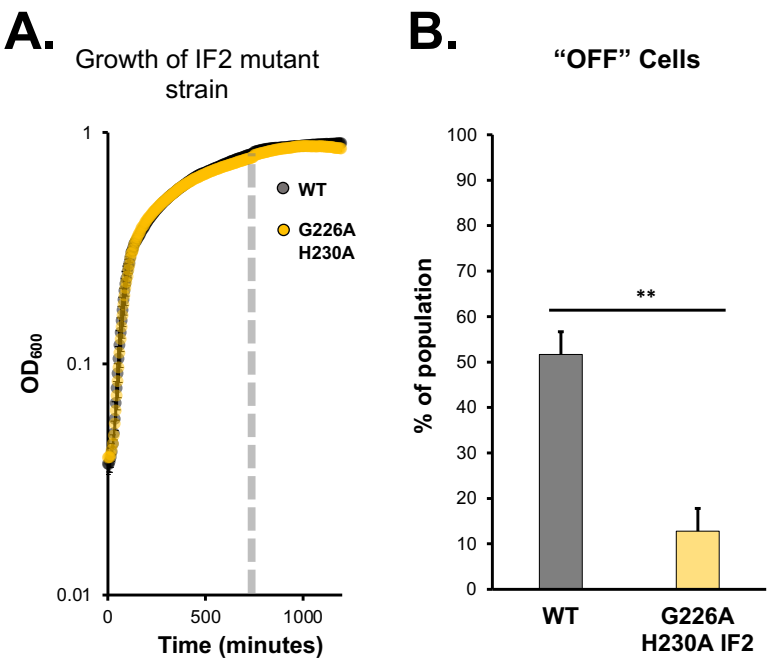

Figure 5.8 Growth curve and % of population "OFF" throughout growth in WT and G226A H230A *infB* strains (A) Growth curve of G226A H230A IF2 strain is equivalent to WT. **(B)** % of population ON were quantified from ~1400 cells in three separate experiments (means ± SDs). n.s. $p > 0.05$, *$p < 0.05$, **$p < 0.01$, ***$p < 0.001$

Chapter 6

6 Summary and future directions

6.1 Summary

6.1.1 Signaling via a cell wall sensitive kinase is essential to downregulation of protein synthesis

The work presented in this thesis identifies a mechanism that mediates the shutdown of protein synthesis, the most energy-intensive process in a growing cell. In Chapter 3, I observed that populations of *B. subtilis* exhibit bimodality in protein synthesis during entry into stationary phase, with one subpopulation that has comparatively low levels of protein synthesis and the other having comparatively high levels **(Figure 3.3)**. Next, I showed that this bimodality is dependent on the presence of an eSTK signaling system that is sensitive to changes in cell wall synthesis **(Figure 3.6)**. I connected signaling through this eSTK with a gene that had been previously suggested to produce a nucleotide second messenger that is involved in the shutdown of energy-intensive processes during bacterial quiescence. I also showed that the bimodality observed was dependent on (pp)pGpp and that these nucleotides are necessary for the shutdown of protein synthesis during entry into stationary phase **(Figure 3.8)**. Following this initial observation, I investigated two questions. Firstly, how is bimodality regulated during entry into stationary phase? Secondly, is protein synthesis down-regulated in a direct manner, and if so, how?

6.1.2 Cross-talk between guanosine nucleotide controls heterogeneity in protein synthesis

In Chapter 4, I first dissected the bimodality in protein synthesis by asking if any of the (pp)pGpp synthetases whose expression increases during exit from rapid growth (SasA and SasB) are responsible on their own for the heterogeneity observed. I show that although both SasA and SasB are necessary for bimodality, they do not all affect bimodality in the same way **(Figure 4.1)**.

Whereas SasB (which primarily makes ppGpp) is important for the population with comparatively low level of protein synthesis, SasA (which makes pGpp) is essential for the other population **(Figure 4.1)**. I showed that the cells with higher SasA expression, but not lower SasB expression, were more likely to have higher rates of protein synthesis, suggesting that SasA is responsible for the heterogeneity **(Figure 4.2)**. I further showed that allosteric activation of SasB by the main product of RelA (pppGpp) is also essential for the bimodality observed **(Figure 4.3)**. Next, I show that SasB allosteric activation by pppGpp is inhibited by pGpp **(Figure 4.4)**. Finally, I provided *in vivo* evidence that the crosstalk between these two nucleotides is responsible for the bimodal distribution of protein synthesis **(Figure 4.6**).

6.1.3 (pp)pGpp directly inhibits translation initiation during entry into stationary phase

Having defined the network of (pp)pGpp synthetases that regulates cellular heterogeneity in protein synthesis, I next investigated how protein synthesis is inhibited in the cells with lower levels of protein synthesis. In Chapter 5, I first showed that ppGpp is sufficient to inhibit protein synthesis *in vitro* and *in vivo* **(Figure 5.1/5.2)**. I further show that this inhibition is due in part via a direct binding of ppGpp to the translational GTPase involved in initiation (IF2) *in vitro* and *in vivo* **(Figure 5.3)**. I also show that the presence of cells with low rates of protein synthesis during entry into stationary phase is dependent on ppGpp binding to IF2 **(Figure 5.7)**. Lastly, in collaboration with Ruben Gonzalez's lab, we showed that ppGpp fails to allosterically activate IF2 in a conformation that allows it rapidly mediate translation initiation **(Figure 5.5)**.

The work presented here, therefore, defines a mechanism by which bacteria heterogeneously regulate protein synthesis during entry into quiescence. The bimodal distribution in protein synthesis is controlled by crosstalk between two nucleotides on SasB **(Figure 6.1).** In response to amino acid limitation, RelA synthesizes pppGpp, which allosterically activates SasB **(Figure 6.1**

A). In response to changes in cell wall metabolism, PrkC regulates noisy expression of *sasA* **(Figure 6.1 A).** The crosstalk of the two molecules that RelA and SasA generate (pppGpp and pGpp respectively) converge on SasB, and pGpp inhibits the allosteric activation of SasB **(Figure 6.1 A)**. The activation of SasB in approximately half the population during late transition phase leads to an accumulation of ppGpp **(Figure 6.1 B)**. In these cells, ppGpp mediates the downregulation of protein synthesis by directly regulating translation initiation. ppGpp achieves this downregulation by directly binding to the essential GTPase IF2. A ppGpp bound IF2 is not allosterically activated compared to a GTP bound IF2 molecule, and a ppGpp bound IF2 is not positioned to mediate rapid subunit joining on the 30S IC **(Figure 6.1B)**.

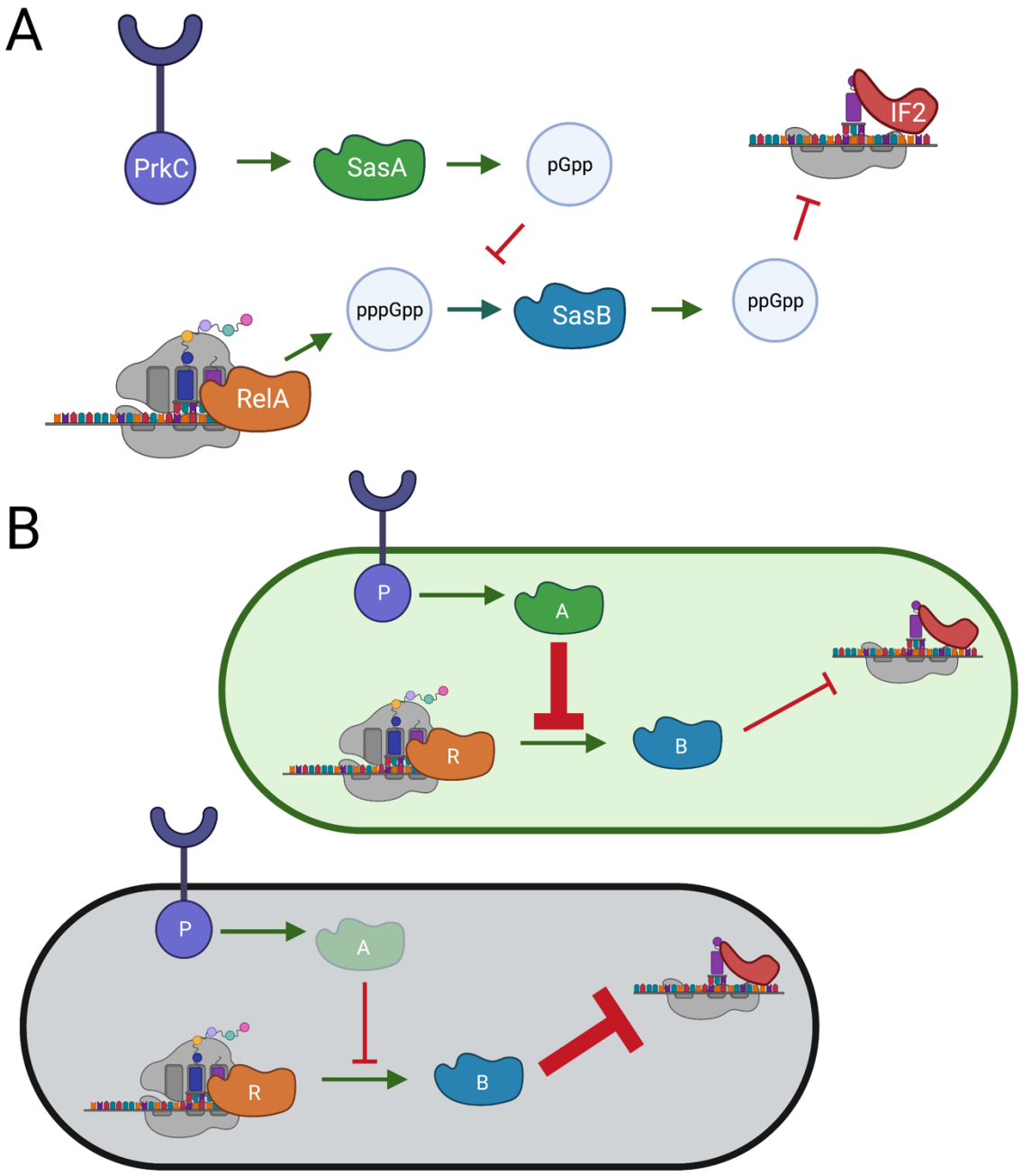

Figure 6.1 Model for heterogenous down-regulation of protein synthesis during entry into quiescence. In response to amino acid limitation, RelA synthesizes pppGpp. In response to changes in cell wall synthesis, PrkC regulates noisy expression of *sasA*. Whereas pppGpp allosterically activates SasB, pGpp (the product of SasA) inhibits this activation. The crosstalk of these two nucleotides, therefore, determines how much ppGpp SasB produces. Lastly, ppGpp accumulation directly inhibits translation initiation by binding to IF2. **(B)** In cells with relatively higher *sasA* ('A') expression, increased inhibition of SasB ('B') allosteric activation by RelA ('R') results in relatively high protein synthesis. In cells with relatively lower *sasA* expression, decreased inhibition of SasB allosteric activation attenuates protein synthesis to a greater extent than in cells with lower *sasA* expression.

6.2 Future directions

6.2.1 What signal(s) mediate down regulation of protein synthesis?

In Chapter 3, I showed that protein synthesis decreases as cells exit from rapid growth **(Figure 3.3)**. I also showed that this down-regulation of protein synthesis depends on signaling through an eSTK signaling system (PrkC/PrpC) **(Figure 3.6)**. The subject of this thesis has been to define the mechanisms that act downstream of PrkC/PrpC signaling. Previous observations show that PrkC/PrpC signaling controls expression of a gene that had previously been shown to have (pp)pGpp synthetase activity (*sasA*) (64). Furthermore, expression of the two small alarmone synthetases (*sasA* and *sasB*) increases during exit from rapid growth in *B. subtilis*. Using this information, I postulated that (pp)pGpp could mediate the shut-down protein synthesis. I then demonstrated that (pp)pGpp is necessary for the shut-down of protein synthesis **(Figure 3.8)**. These initial observations suggest that when cells exit rapid growth, they sense a change in cell wall homeostasis using PrkC. This signal is then communicated to other cellular processes through the accumulation of (pp)pGpp; at this point, however, the exact signals that are sensed have not been experimentally determined. However, PrkC is known to be essential for the resuscitation of *B. subtilis* spores in response to muropeptides released from actively growing cells (60). Furthermore, the PASTA domain of PrkC has been experimentally shown to bind these muropeptides (135). This suggests that part of the signal that cells are sensing during entry into stationary phase heterogeneity is the presence or absence of cell wall homeostasis.

In Chapter 5, I showed that the product of SasB (ppGpp) inhibits IF2 function and inhibits translation **(Figure 5.3/5.7)**. In Chapter 4, I showed that the products of RelA and SasA (pppGpp and pGpp) regulate the activity of SasB **(Figure 4.4)**. This suggests that the signals that cells sense when they are exiting rapid growth are integrated through RelA and SasA. RelA is known to sense

the amino acyl status of tRNAs as a proxy for availability of amino acids (74). It seems, therefore, that part of the signal that cells integrate into the decision to shut off protein synthesis is amino acid availability. The observations that SasB allosteric activation is modulated by the nucleotide generated by SasA **(Figure 4.4)** suggest that the signal that stimulates SasA activity is also important. SasA expression is stimulated during cell wall stress (83). It, therefore, seems that both amino acid availability and cell wall homeostasis are important signals for cells to regulate protein synthesis and potentially other energy-intensive purposes.

How important are either of these signals? I have not made exact measurements of how amino acid availability changes under the conditions I used. I have, however, provided evidence that cell wall synthesis decreases during exit from growth and entry into stationary phase **(Appendix D, Figure 1)**. The probe that I utilized to show this, however, has a low dynamic range during the transition from growth to stationary phase **(Appendix A, Figure 2, 3)**. Due to this, I am not able to correlate rates of cell wall synthesis with rates of protein synthesis on a single cell level during the late transition phase. Such a measurement would provide evidence that individual cells coordinate cell wall synthesis and protein translation.

6.2.2 Does SasB have another physiological stimulus?

The previous observation that SasB is allosterically (85) activated and the data which I have shown in Chapter 4 of this thesis indicates that SasB is only in part transcriptionally activated. This suggests that the activity of SasB is stimulated by the signal that activates its transcription along with any other signal that affects its allosteric activation. Expression of the *sasA* and *sasB* homologs (*relP* and *relQ*) in *E. faecalis* is stimulated in response to treatment with cell wall active antibiotics (84). Furthermore, deletion of both *relP* and *relQ* causes decreases in viability during treatment with the cell wall active antibiotic vancomycin (84). These data together suggest that the

transcription of *sasB* is stimulated in response to changes in cell wall synthesis. This has not been experimentally determined as it has for *sasA* (64, 83). Future experiments would examine this possibility

The allosteric activation of SasB is known to be mediated by the major product of RelA (pppGpp) (85). Here I have shown that this is modulated by the product of SasA (pGpp) (Figure 4.4). SasB allosteric activation has also been shown to be inhibited by ssRNA (86). Specifically, ssRNAs with a sequence with close identity to the consensus Shine-Delgarno sequence (GGAGG) competitively compete with pppGpp (86). This has led to the suggestion that SasB could be a sensor for mRNA (136). This raises the possibility that SasB could serve to sense the presence of mRNA and would integrate this information into the cellular response. For example, SasB activity, which I have shown inhibits protein synthesis (Figure 5.2), would be fine-tuned based on the amino acid availability (through pppGpp made by RelA), cell wall synthesis (by direct competition of pGpp made by SasA and pppGpp), and presence or absence of mRNA (by direct competition of mRNA with pppGpp).

6.2.3 What are the structural aspects that mediate differential guanosine synthesis?

Sequence homology between the SasB and SasA proteins is high (39.11% identity) (137). Furthermore, sequence homology between the synthetase domain of RelA and SasB and SasA is high (29.52% and 33.02% identify, respectively) (85). How do these closely related domains generate different nucleotides? In *B. subtilis,* stimulation of RelA activity during log growth primarily produces pppGpp (82). In contrast, expression of SasB under similar conditions primarily produces ppGpp, and expression of SasA produces pGpp (79). This difference is presumably due to a difference in preferential use of a particular substrate. Specifically, RelA presumably preferentially utilizes GTP and ATP to make pppGpp, whereas SasB utilizes GDP and

ATP to make ppGpp, and SasA utilizes GMP and ATP to make pGpp. Differences in guanosine substrate, therefore, seem to underlie the difference in alarmone production. How is this difference mediated? One possibility is that each enzyme binds a particular nucleotide with greater affinity. Alternatively, catalysis rates by each enzyme could be different depending on guanosine substrate. Biochemical experiments of binding affinity and enzymatic rates using the different nucleotides could answer this question. These nucleotides are structurally similar; they differ from each other only in 1 to 2 phosphate groups on the 3' carbon. What structural aspects of these closely related proteins mediate this? An NMR spectroscopy study looking at how residues shift when each of these proteins is bound to different guanosine substrates could provide candidate residues that mediate this difference. This kind of study previously showed differences in binding of GDP and ppGpp to IF2 (75). I used these differences to identify candidate residues that could affect binding of ppGpp specifically and generated an IF2 protein that bound ppGpp with a lowered affinity(99). Ultimately, engineering a mutant synthetase domain that reverses the substrate specificity of a particular synthetase would definitively demonstrate which residues are important for this phenomenon.

6.2.4 Do other nucleotides (pppGpp and pGpp) affect IF2 function like ppGpp

In Chapter 5, we showed using biochemical and biophysical methods that IF2 function is inhibited by ppGpp (Figure 5.2/5.8). What about the other closely related nucleotides? Chapter 4 of this thesis shows data that suggest that these three nucleotides do not all have the same function. Furthermore, recent work shows that while ppGpp effectively inhibits IF2's ability to form 30S initiation complexes (30S ICs), the closely related pppGpp actually allows IF2 to form 30S ICs (although at a lower efficiency than GTP (138). A biochemical analysis of IF2 function using the in vitro translation reaction used in Chapter 5 in the presence of either pppGpp and pGpp would

answer if IF2 is inhibited by pppGpp and pGpp to the same extent as it is with ppGpp. The structural aspects of the effect of pppGpp and pGpp on IF2 could be elucidated using the single-molecule method developed by Ruben Gonzalez's lab and used in Chapter 4 of this thesis. These experiments require that enough nucleotide is used to fully saturate IF2 with the specific nucleotide in question, and so a binding study to show the affinities of IF2 for pppGpp and pGpp is also required. The single-molecule studies using IF2 and pppGpp have already been initiated in the Gonzalez lab, and preliminary data suggest that pppGpp positions IF2 in a confirmation more similar to GTP than ppGpp. However, these experiments require further validation.

6.2.5 Role of EF-Tu in inhibiting protein synthesis during accumulation of ppGpp

Chapter 5 of this thesis identified IF2 as a target of ppGpp on the translation machinery. It also shows that IF2 binding to ppGpp is necessary for the population of cells with low levels of protein synthesis during entry into stationary phase (Figure 5.6). I showed this by generating an IF2 molecule that has a lower affinity for ppGpp than WT IF2 (Figure 5.3). The residues which are mutated in this IF2 protein are in the G1 domain of the guanosine binding site of IF2 and make the mutant protein have a G1 domain that resembles the G1 domain of EF-G (Figure 5.3). This mutation strategy was designed given the lower binding affinity (approximately 10X lower K_d) of EF-G to ppGpp (125). The other GTPase involved in elongation (EF-Tu) has previously been suggested to also mediate the inhibition of protein synthesis because its binding affinity to ppGpp is similar to IF2 (125). Interestingly, EF-Tu also resembles IF2 in regard to the residues that we identified as being important for binding of ppGpp. During the course of investigating the potential targets for ppGpp, I attempted to generate a mutant EF-Tu protein that carried the homologous mutations that I used to show that IF2 is a target of ppGpp. Unfortunately, I was unable to either express this mutant protein in *E. coli*, or to generate *B. subtilis* strain that carried the mutation in

EF-Tu. I believe that the reason for this has to do with the fact that the changes that affect ppGpp binding also affect GTP binding. I showed that this is true for IF2 but that the difference did not significantly affect IF2 function in the *in vitro* translation reaction, and it apparently does not affect *in vivo* function because the strain carrying these mutations does not have any noticeable growth defect. Unlike IF2, the defect in EF-Tu appears to be more severe and therefore precludes any analysis like the ones performed on IF2. It is possible that additional analysis of the residues which mediate binding of ppGpp specifically to EF-Tu would potentially allow for a more directed mutation strategy that would allow for the generation of an EF-Tu mutant with similar properties to the one that I generated for IF2.

References

1. M. Y. Terzi, M. Izmirli, B. Gogebakan, The cell fate: senescence or quiescence. *Mol Biol Rep* **43**, 1213-1220 (2016).

2. K. Masutomi *et al.*, Telomerase Maintains Telomere Structure in Normal Human Cells. *Cell* **114**, 241-253 (2003).

3. I. Sagot, D. Laporte, Quiescence, an individual journey. *Curr Genet* **65**, 695-699 (2019).

4. C. T. J. van Velthoven, T. A. Rando, Stem Cell Quiescence: Dynamism, Restraint, and Cellular Idling. *Cell Stem Cell* **24**, 213-225 (2019).

5. J. B. Russell, G. M. Cook, Energetics of Bacterial Growth- Balance of Anabolic and Catabolic Reactions *Microbiological Reviews* **59**, 48-62 (1995).

6. J. R. Valcourt *et al.*, Staying alive: metabolic adaptations to quiescence. *Cell Cycle* **11**, 1680-1696 (2012).

7. A. G. Chapman, L. Fall, D. E. Atkinson, Adenylate Energy Charge in Escherichia coli During Growth and Starvation. *Journal of Bacteriology* **108**, 1072-1086 (1971).

8. C. A. Reeve, A. T. Bockman, A. Matin, Role of Protein Degradation in the Survival of Carbon-Starved Escherichia coli and Salmonella typhimurium. *Journal of Bacteriology* **157** (1984).

9. R. Kolter, D. A. Siegele, A. Tormo, THE STATIONARY PHASE OF THE BACTERIAL LIFE CYCLE. *Annual Reviews of Microbiology* **47**, 855-874 (1993).

10. M. Choder, A general topoisomeraseI-dependent transcriptional repressionin the stationary phasein yeast. *Genes & Development* **5**, 2315-2326 (1991).

11. E. K. Fuge, E. L. Braun, M. Werner-Washburne, Protein Synthesis in Long-Term Stationary-Phase Cultures of Saccharomyces cerevisiae. *Journal of Bacteriology* **176**, 5802-5813 (1994).

12. C. Allen *et al.*, Isolation of quiescent and nonquiescent cells from yeast stationary-phase cultures. *J Cell Biol* **174**, 89-100 (2006).

13. C. A. Reeve, P. S. Amy, A. Matin, Role of Protein Synthesis in the Survival of Carbon-Starved EscherichiacoliK-12. *Journal of Bacteriology* **160**, 1041-1046 (1984).

14. P. H. O'Farrell, Quiescence: early evolutionary origins and universality do not imply uniformity. *Philos Trans R Soc Lond B Biol Sci* **366**, 3498-3507 (2011).

15. L. Li, H. Clevers, Coexistence of Quiescent and Active Adult Stem Cells in Mammals. *Science* **327**, 542-545 (2010).

16. S. J. Buczacki *et al.*, Intestinal label-retaining cells are secretory precursors expressing Lgr5. *Nature* **495**, 65-69 (2013).

17. M. Ito *et al.*, Stem cells in the hair follicle bulge contribute to wound repair but not to homeostasis of the epidermis. *Nat Med* **11**, 1351-1354 (2005).

18. M. Ahmad, A. U. Khan, Global economic impact of antibiotic resistance: A review. *J Glob Antimicrob Resist* **19**, 313-316 (2019).

19. D. R. Dodds, Antibiotic resistance: A current epilogue. *Biochem Pharmacol* **134**, 139-146 (2017).

20. K. Bush, P. A. Bradford, beta-Lactams and beta-Lactamase Inhibitors: An Overview. *Cold Spring Harb Perspect Med* **6** (2016).

21. A. Zapun, C. Contreras-Martel, T. Vernet, Penicillin-binding proteins and beta-lactam resistance. *FEMS Microbiol Rev* **32**, 361-385 (2008).

22. J. W. Bigger, TREATMENT OF STAPHYLOCOCCAL INFECTIONS WITH PENICILLIN. *The Lancet* **244**, 497-500 (1944).

23. G. L. Hobby, K. Meyer, C. Eleanor, Observations on the mechanism of action of penicillin. *Proceedings of the Society of Experimental Biology and Medicine* **50**, 281-285 (1942).

24. A. D. Gardner, Morphological Effects of Penicillin on Bacteria *Nature* **146**, 837-838 (1940).

25. N. H. Albertson, T. Nystrom, S. Kjelleberg, Macromolecular synthesis during recovery of the marine Vibrio sp. S14 from starvation. *Journal of General Microbiology* **136**, 2201-2207 (1990).

26. M. H. Pontes, E. A. Groisman, Slow growth determines nonheritable antibiotic resistance in Salmonella enterica. *Science Signaling* **12** (2019).

27. R. A. Fisher, B. Gollan, S. Helaine, Persistent bacterial infections and persister cells. *Nat Rev Microbiol* **15**, 453-464 (2017).

28. S. S. Grant, D. T. Hung, Persistent bacterial infections, antibiotic tolerance, and the oxidative stress response. *Virulence* **4**, 273-283 (2013).

29. M. Huemer *et al.*, Molecular reprogramming and phenotype switching in Staphylococcus aureus lead to high antibiotic persistence and affect therapy success. *Proc Natl Acad Sci U S A* **118** (2021).

30. R. A. Proctor, J. M. Balwit, O. Vesga, Variant subpopulations of Staphylococcus aureus as cause of persistent and recurrent infections. *Infectious Agents and Disease* **3**, 302-312 (1994).

31. I. Levin-Reisman *et al.*, Antibiotic tolerance facilitates the evolution of resistance. *Science* **355** (2017).

32. P. S. Stewart, M. J. Franklin, Physiological heterogeneity in biofilms. *Nat Rev Microbiol* **6**, 199-210 (2008).

33. E. Drenkard, F. M. Ausubel, Pseudomonas biofilm formation and antibiotic resistance are linked to phenotypic variation. *Nature* **416**, 740-743 (2002).

34. H. Maamar, D. Dubnau, Bistability in the Bacillus subtilis K-state (competence) system requires a positive feedback loop. *Mol Microbiol* **56**, 615-624 (2005).

35. M. Thattai, A. van Oudenaarden, Stochastic Gene Expression in Fluctuating Environments. *Genetics* **167**, 523-530 (2003).

36. I. R. Booth, Stress and the single cell- Intrapopulation diversity is a mechanism to ensure survival upon exposure to stress. *International Journal of Food Microbiology* **78**, 19-30 (2002).

37. A. Aertsen, C. W. Michiels, Diversify or die: generation of diversity in response to stress. *Crit Rev Microbiol* **31**, 69-78 (2005).

38. M. Kaern, T. C. Elston, W. J. Blake, J. J. Collins, Stochasticity in gene expression: from theories to phenotypes. *Nat Rev Genet* **6**, 451-464 (2005).

39. N. Q. Balaban, J. Merrin, R. Chait, L. Kowalik, S. Leibler, Bacterial Persistence as a Phenotypic Switch. *Science* **305** (2004).

40. J. E. Ferrell, Self-perpetuating states in signal transduction: positive feedback, double-negative feedback and bistability. *Current Opinion in Cell Biology* **14**, 140-148 (2002).

41. D. Dubnau, R. Losick, Bistability in bacteria. *Mol Microbiol* **61**, 564-572 (2006).

42. A. Becskei, B. Seraphin, L. Serrano, Positive feedback in eukaryotic gene networks: cell differentiation by graded to binary response conversion. *The EMBO Journal* **20**, 2528-2535 (2001).

43. M. Ptashne, A Genetic Switch: Phage Lambda Revisited, Third Edition. *Cold Spring Harbor Laboratory Press* (2004).

44. E. Kussell, S. Leibler, Phenotypic Diversity, Population Growth, and Information in Fluctuating Environments. *Science* **309**, 2075-2078 (2005).

45. P. Guptasarma, Does replication-induced transcription regulate synthesis of the myriad low copy number proteins of Escherichia coli? *BioEssasys* **17**, 987-997 (1995).

46. M. B. Elowitz, A. J. Levine, E. D. Siggia, P. S. Swain, Stochastic Gene Expression in a Single Cell. *Science* **297** (2002).

47. H. H. McAdams, A. Arkin, Stochastic mechanisms in gene expression. *Proc Natl Acad Sci U S A* **94**, 814-819 (1997).

48. H. H. McAdams, A. Arkin, It's a noisy business! Genetic regulation at the nanomolar scale. *Trends in Genetics* **15**, 65-69 (1999).

49. M. Delbruck, The burst size distribution in the growth of bacterial viruses (bacteriophages). *Journal of Bacteriology* **50**, 131-135 (1945).

50. A. Novick, M. Weiner, Enzyme induction as an all-or-none phenomenon. *Proceedings of The National Academy of Sciences of The United States of America* **43**, 553-566 (1957).

51. J. L. Spudich, D. E. Koshland Jr., Non-genetic individuality- chance in the single cell. *Nature* **262**, 467-471 (1976).

52. P. S. Swain, M. B. Elowitz, E. D. Siggia, Intrinsic and extrinsic contributions to stochasticity in gene expression. *Proc Natl Acad Sci U S A* **99**, 12795-12800 (2002).

53. O. K. Silander *et al.*, A genome-wide analysis of promoter-mediated phenotypic noise in Escherichia coli. *PLoS Genet* **8**, e1002443 (2012).

54. A. M. Stock, V. L. Robinson, P. N. Goudreau, TWO-COMPONENT SIGNAL TRANSDUCTION. *Annual Reviews of Biochemistry* **69**, 183-215 (2000).

55. J. Munoz-Dorado, S. Inouye, M. Inouye, A gene encoding a protein serine:threonine kinase is required for normal development of M. xanthus, a gram-negative bacterium. *Cell* **67**, 995-1006 (1991).

56. C. M. Kang *et al.*, The Mycobacterium tuberculosis serine/threonine kinases PknA and PknB: substrate identification and regulation of cell shape. *Genes Dev* **19**, 1692-1704 (2005).

57. L. Novakova *et al.*, Characterization of a eukaryotic type serine/threonine protein kinase and protein phosphatase of Streptococcus pneumoniae and identification of kinase substrates. *FEBS J* **272**, 1243-1254 (2005).

58. A. J. F. Egan, J. Errington, W. Vollmer, Regulation of peptidoglycan synthesis and remodelling. *Nat Rev Microbiol* **18**, 446-460 (2020).

59. R. J. Doyle, J. Chaloupka, V. Vinter, Turnover of Cell Walls in Microorganisms. *Microbiological Reviews* **52**, 554-567 (1988).

60. I. M. Shah, M. H. Laaberki, D. L. Popham, J. Dworkin, A eukaryotic-like Ser/Thr kinase signals bacteria to exit dormancy in response to peptidoglycan fragments. *Cell* **135**, 486-496 (2008).

61. P. Hardt *et al.*, The cell wall precursor lipid II acts as a molecular signal for the Ser/Thr kinase PknB of Staphylococcus aureus. *Int J Med Microbiol* **307**, 1-10 (2017).

62. P. Bisicchia *et al.*, The essential YycFG two-component system controls cell wall metabolism in Bacillus subtilis. *Mol Microbiol* **65**, 180-200 (2007).

63. E. A. Libby, L. A. Goss, J. Dworkin, The Eukaryotic-Like Ser/Thr Kinase PrkC Regulates the Essential WalRK Two-Component System in Bacillus subtilis. *PLoS Genet* **11**, e1005275 (2015).

64. E. A. Libby, S. Reuveni, J. Dworkin, Multisite phosphorylation drives phenotypic variation in (p)ppGpp synthetase-dependent antibiotic tolerance. *Nat Commun* **10**, 5133 (2019).

65. S. F. Pereira, R. L. Gonzalez, Jr., J. Dworkin, Protein synthesis during cellular quiescence is inhibited by phosphorylation of a translational elongation factor. *Proc Natl Acad Sci U S A* **112**, E3274-3281 (2015).

66. T. W. Rall, E. W. Sutherland, J. Berthet, The Relationship of Epinephrine and Glucagon to Liver Phosphorylase. *Journal of Biological Chemistry* **224**, 463-475 (1957).

67. E. W. Sutherland, T. W. Rall, Fractionation and Characterization of a Cyclic Adenine Ribonucleotide Formed by Tissue Particles. *Journal of Biological Chemistry* **232**, 1077-1091 (1958).

68. T. W. Rall, E. W. Sutherland, Formation of a Cyclic Adenine Ribonucleotide by Tissue Particles. *Journal of Biological Chemistry* **232**, 1065-1076 (1958).

69. A. Ullmann, J. Monod, Cyclic AMP as an antagonist of catabolite repression in Escherichia coli. *FEBS letters* **2**, 57-60 (1968).

70. M. K. Sands, R. B. Roberts, The effects of a tryptophan-histidine deficiency in a mutant of Escherichia coli. . *Journal of Bacteriology* **63**, 505-511 (1952).

71. E. Borek, J. Rockenbach, A. Ryan, Studies on a mutant of Escherichia coli with unbalanced ribonucleic acid synthesis. *Journal of Bacteriology* **71**, 318-323 (1956).

72. G. S. Stent, S. Brenner, A genetic locus for the regulation of ribonucleic acid synthesis. *Proceedings of The National Academy of Sciences of The United States of America* **47** (1961).

73. M. Cashel, J. Gallant, Two compounds implicated in the function of the RC gene of Escherichia. coli. *Nature* **221** (1969).

74. M. Cashel, B. Kalbacher, The Control of Ribonucleic Acid Synthesis in Escherichia coli *The Journal of Biological Chemistry* **245** (1970).

75. P. Milon *et al.*, The nucleotide-binding site of bacterial translation initiation factor 2 (IF2) as a metabolic sensor. *Proc Natl Acad Sci U S A* **103**, 13962-13967 (2006).

76. B. Feng *et al.*, Structural and functional insights into the mode of action of a universally conserved Obg GTPase. *PLoS Biol* **12**, e1001866 (2014).

77. T. Tosa, L. Pizer, I., Biochemical Bases for the Antimetabolite Action ofL-SerineHydroxamate. *Journal of Bacteriology* **106** (1971).

78. L. Pizer, I., J. Merlie, P., Effect of Serine Hydroxamate on Phospholipid Synthesis in Escherichia coli. *Journal of Bacteriology* **114** (1973).

79. K. Tagami *et al.*, Expression of a small (p)ppGpp synthetase, YwaC, in the (p)ppGpp(0) mutant of Bacillus subtilis triggers YvyD-dependent dimerization of ribosome. *MicrobiologyOpen* **1**, 115-134 (2012).

80. S. Ronneau, R. Hallez, Make and break the alarmone: regulation of (p)ppGpp synthetase/hydrolase enzymes in bacteria. *FEMS Microbiol Rev* **43**, 389-400 (2019).

81. A. Brown, I. S. Fernandez, Y. Gordiyenko, V. Ramakrishnan, Ribosome-dependent activation of stringent control. *Nature* **534**, 277-280 (2016).

82. T. M. Wendrich, M. A. Marahiel, Cloning and characterization of a relA spoT homologue from Bacillus subtilis. *Molecular Microbiology* **26** (1997).

83. M. A. D'Elia *et al.*, Probing teichoic acid genetics with bioactive molecules reveals new interactions among diverse processes in bacterial cell wall biogenesis. *Chemistry & Biology* **16**, 548-556 (2009).

84. T. Geiger, B. Kastle, F. L. Gratani, C. Goerke, C. Wolz, Two small (p)ppGpp synthases in Staphylococcus aureus mediate tolerance against cell envelope stress conditions. *J Bacteriol* **196**, 894-902 (2014).

85. W. Steinchen *et al.*, Catalytic mechanism and allosteric regulation of an oligomeric (p)ppGpp synthetase by an alarmone. *Proc Natl Acad Sci U S A* **112**, 13348-13353 (2015).

86. J. Beljantseva *et al.*, Negative allosteric regulation of Enterococcus faecalis small alarmone synthetase RelQ by single-stranded RNA. *Proc Natl Acad Sci U S A* **114**, 3726-3731 (2017).

87. J. Yang *et al.*, The nucleotide pGpp acts as a third alarmone in Bacillus, with functions distinct from those of (p) ppGpp. *Nat Commun* **11**, 5388 (2020).

88. I. Artsimovitch *et al.*, Structural Basis for Transcription Regulation by Alarmone ppGpp. *Cell* **117** (2004).

89. W. Ross *et al.*, ppGpp Binding to a Site at the RNAP-DksA Interface Accounts for Its Dramatic Effects on Transcription Initiation during the Stringent Response. *Mol Cell* **62**, 811-823 (2016).

90. A. Kriel *et al.*, Direct regulation of GTP homeostasis by (p)ppGpp: a critical component of viability and stress resistance. *Mol Cell* **48**, 231-241 (2012).

91. J. D. Wang, G. M. Sanders, A. D. Grossman, Nutritional control of elongation of DNA replication by (p)ppGpp. *Cell* **128**, 865-875 (2007).

92. R. M. Corrigan, L. E. Bellows, A. Wood, A. Grundling, ppGpp negatively impacts ribosome assembly affecting growth and antimicrobial tolerance in Gram-positive bacteria. *Proc Natl Acad Sci U S A* **113**, E1710-1719 (2016).

93. E. Hamel, M. Cashel, Guanine nucleotides in protein synthesis. Utilization of pppGpp and dGTP by initiation factor 2 and elongation factor Tu. *Archives of Biochemistry and Biophysics* **162** (1973).

94. T. Laffler, J. A. Gallant, Stringent Control of Protein Synthesis in E. coli. *Cell* **3** (1974).

95. P. H. O'Farrell, The suppression of defective translation by ppGpp and its role in the stringent response. *Cell*, 545-557 (1978).

96. D. W. Tempest, O. M. Neijssel, The status of YATP and maintenance energy as biologically interpretable phenomena. *Annual Reviews of Microbiology* **38**, 459-486 (1984).

97. T. E. Dever, T. G. Kinzy, G. D. Pavitt, Mechanism and Regulation of Protein Synthesis in Saccharomyces cerevisiae. *Genetics* **203**, 65-107 (2016).

98. M. V. Rodnina, Translation in Prokaryotes. *Cold Spring Harb Perspect Biol* **10** (2018).

99. S. Diez, J. Ryu, K. Caban, R. L. Gonzalez, Jr., J. Dworkin, The alarmones (p)ppGpp directly regulate translation initiation during entry into quiescence. *Proc Natl Acad Sci U S A* **117**, 15565-15572 (2020).

100. M. E. Sherlock, N. Sudarsan, R. R. Breaker, Riboswitches for the alarmone ppGpp expand the collection of RNA-based signaling systems. *Proc Natl Acad Sci U S A* **115**, 6052-6057 (2018).

101. J. Fei *et al.*, "A Highly Purified, Fluorescently Labeled In Vitro Translation System for Single-Molecule Studies of Protein Synthesis" in Single Molecule Tools: Fluorescence Based Approaches, Part A. (2010), 10.1016/s0076-6879(10)72008-5, pp. 221-259.

102. K. G. Roelofs, J. Wang, H. O. Sintim, V. T. Lee, Differential radial capillary action of ligand assay for high-throughput detection of protein-metabolite interactions. *Proc Natl Acad Sci U S A* **108**, 15528-15533 (2011).

103. K. Caban, M. Pavlov, M. Ehrenberg, R. L. Gonzalez, Jr., A conformational switch in initiation factor 2 controls the fidelity of translation initiation in bacteria. *Nat Commun* **8**, 1475 (2017).

104. B. J. Desai, R. L. Gonzalez, 10.1101/730465 (2019).

105. J. E. Bronson, J. Fei, J. M. Hofman, R. L. Gonzalez, Jr., C. H. Wiggins, Learning rates and states from biophysical time series: a Bayesian approach to model selection and single-molecule FRET data. *Biophys J* **97**, 3196-3205 (2009).

106. J. Hon, R. L. Gonzalez, Jr., Bayesian-Estimated Hierarchical HMMs Enable Robust Analysis of Single-Molecule Kinetic Heterogeneity. *Biophys J* **116**, 1790-1802 (2019).

107. J. Liu, Y. Xu, D. Stoleru, A. Salic, Imaging protein synthesis in cells and tissues with an alkyne analog of puromycin. *Proc Natl Acad Sci U S A* **109**, 413-418 (2012).

108. I. M. Shah, J. Dworkin, Induction and regulation of a secreted peptidoglycan hydrolase by a membrane Ser/Thr kinase that detects muropeptides. *Mol Microbiol* **75**, 1232-1243 (2010).

109. K. Potrykus, H. Murphy, N. Philippe, M. Cashel, ppGpp is the major source of growth rate control in E. coli. *Environ Microbiol* **13**, 563-575 (2011).

110. H. D. Murray, D. A. Schneider, R. L. Gourse, Control of rRNA expression by small molecules is dynamic and nonredundant. *Mol Cell* **12**, 125-134 (2003).

111. N. Boes, K. Schreiber, M. Schobert, SpoT-triggered stringent response controls usp gene expression in Pseudomonas aeruginosa. *J Bacteriol* **190**, 7189-7199 (2008).

112. H. Nanamiya *et al.*, Identification and functional analysis of novel (p)ppGpp synthetase genes in Bacillus subtilis. *Mol Microbiol* **67**, 291-304 (2008).

113. A. Srivatsan *et al.*, High-precision, whole-genome sequencing of laboratory strains facilitates genetic studies. *PLoS Genet* **4**, e1000139 (2008).

114. S. Atwal *et al.*, Clickable methionine as a universal probe for labelling intracellular bacteria. *J Microbiol Methods* **169**, 105812 (2020).

115. A. Kriel *et al.*, GTP dysregulation in Bacillus subtilis cells lacking (p)ppGpp results in phenotypic amino acid auxotrophy and failure to adapt to nutrient downshift and regulate biosynthesis genes. *J Bacteriol* **196**, 189-201 (2014).

116. T. M. Wendrich, M. A. Marahiel, Cloning and characterization of a relA/spoT homologue from Bacillus subtilis *Molecular Microbiology* **26**, 65-79 (1997).

117. T. Hogg, U. Mechold, H. Malke, M. Cashel, R. Hilgenfeld, Conformational antagonism between opposing active sites in a bifunctional RelA/SpoT homolog modulates (p)ppGpp metabolism during the stringent response. *Cell* **117**, 57-68 (2004).

118. M. C. Manav *et al.*, Structural basis for (p)ppGpp synthesis by the Staphylococcus aureus small alarmone synthetase RelP. *J Biol Chem* **293**, 3254-3264 (2018).

119. R. R. Breaker, Riboswitches and Translation Control. *Cold Spring Harb Perspect Biol* **10** (2018).

120. A. Rojas, M. Ehrenberg, S. G. E. Andersson, C. G. Kurland, ppGpp inhibition of elongation factors Tu, G and Ts during polypeptide synthesis. *Mol Gen Genet* **197**, 36-45 (1984).

121. Y. Shimizu, Y. Kuruma, T. Kanamori, T. Ueda, The PURE system for protein production. *Methods in molecular biology* **1118**, 275-284 (2014).

122. J. D. Friesen, N. Fiil, Accumulation of Guanosine Tetraphosphate in T7 Bacteriophage-Infected Escherichia coli *J Bacteriol* **113**, 697-703 (1973).

123. M. H. Buckstein, J. He, H. Rubin, Characterization of nucleotide pools as a function of physiological state in Escherichia coli. *J Bacteriol* **190**, 718-726 (2008).

124. A. M. Rojas, M. Ehrenberg, S. G. Andersson, C. G. Kurland, ppGpp inhibition of elongation factors Tu, G and Ts during polypeptide synthesis. *Molecular & general genetics : MGG* **197**, 36-45 (1984).

125. V. A. Mitkevich *et al.*, Thermodynamic characterization of ppGpp binding to EF-G or IF2 and of initiator tRNA binding to free IF2 in the presence of GDP, GTP, or ppGpp. *J Mol Biol* **402**, 838-846 (2010).

126. L. Legault, C. Jeantet, F. Gros, Inhibition of in vitro protein synthesis by ppGpp. *FEBS Lett* **27**, 71-75 (1972).

127. P. Milon *et al.*, The nucleotide-binding site of bacterial translation initiation factor 2 (IF2) as a metabolic sensor. *Proc Natl Acad Sci U S A* **103**, 13962–13967 (2006).

128. J. Buglino, V. Shen, P. Hakimian, C. D. Lima, Structural and biochemical analysis of the Obg GTP binding protein. *Structure* **10**, 1581-1592 (2002).

129. Y. Zhang, E. Zbornikova, D. Rejman, K. Gerdes, Novel (p)ppGpp Binding and Metabolizing Proteins of Escherichia coli. *MBio* **9** (2018).

130. P. Pausch *et al.*, Structural basis for (p)ppGpp-mediated inhibition of the GTPase RbgA. *J Biol Chem* **293**, 19699-19709 (2018).

131. H. Wienk *et al.*, Structural dynamics of bacterial translation initiation factor IF2. *J Biol Chem* **287**, 10922-10932 (2012).

132. J. Wang, K. Caban, R. L. Gonzalez, Jr., Ribosomal initiation complex-driven changes in the stability and dynamics of initiation factor 2 regulate the fidelity of translation initiation. *J Mol Biol* **427**, 1819-1834 (2015).

133. A. Simonetti *et al.*, Structure of the 30S translation initiation complex. *Nature* **455**, 416-420 (2008).

134. M. Y. Pavlov, A. Zorzet, D. I. Andersson, M. Ehrenberg, Activation of initiation factor 2 by ligands and mutations for rapid docking of ribosomal subunits. *EMBO J* **30**, 289-301 (2011).

135. F. Squeglia *et al.*, Chemical basis of peptidoglycan discrimination by PrkC, a key kinase involved in bacterial resuscitation from dormancy. *J Am Chem Soc* **133**, 20676-20679 (2011).

136. V. Hauryliuk, G. C. Atkinson, Small Alarmone Synthetases as novel bacterial RNA-binding proteins. *RNA Biol* **14**, 1695-1699 (2017).

137. W. Steinchen *et al.*, Structural and mechanistic divergence of the small (p)ppGpp synthetases RelP and RelQ. *Sci Rep* **8**, 2195 (2018).

138. D. S. Vinogradova *et al.*, How the initiating ribosome copes with ppGpp to translate mRNAs. *PLoS Biol* **18**, e3000593 (2020).

139. N. Mirouze, Y. Desai, A. Raj, D. Dubnau, Spo0A~P imposes a temporal gate for the bimodal expression of competence in Bacillus subtilis. *PLoS Genet* **8**, e1002586 (2012).

140. T. A. Gaidenko, T. J. Kim, C. W. Price, The PrpC serine-threonine phosphatase and PrkC kinase have opposing physiological roles in stationary-phase Bacillus subtilis cells. *J Bacteriol* **184**, 6109-6114 (2002).

141. N. Mirouze, P. Prepiak, D. Dubnau, Fluctuations in spo0A transcription control rare developmental transitions in Bacillus subtilis. *PLoS Genet* **7**, e1002048 (2011).

142. J. E. Patrick, D. B. Kearns, MinJ (YvjD) is a topological determinant of cell division in Bacillus subtilis. *Mol Microbiol* **70**, 1166-1179 (2008).

143. E. Kuru *et al.*, In Situ probing of newly synthesized peptidoglycan in live bacteria with fluorescent D-amino acids. *Angew Chem Int Ed Engl* **51**, 12519-12523 (2012).

144. O. Irazoki, S. B. Hernandez, F. Cava, Peptidoglycan Muropeptides: Release, Perception, and Functions as Signaling Molecules. *Front Microbiol* **10**, 500 (2019).

145. S. Sharifzadeh, F. Dempwolff, D. B. Kearns, E. E. Carlson, Harnessing beta-Lactam Antibiotics for Illumination of the Activity of Penicillin-Binding Proteins in Bacillus subtilis. *ACS Chem Biol* **15**, 1242-1251 (2020).

Appendix A

Table 2. Strains used in this thesis

168 trpC2 (WT)	Lab stock	JDB 1772
trpC2 ΔsasA::kan	(139)	JDB 4310
trpC2 ΔsasB::tet	(139)	JDB 4311
sacA::P_{sasB}-YFP (cm)	unpublished	JDB 4341
sacA::P_{sasA}-YFP (cm)	(64)	JDB 4030
trpC2 sasB^{F42A}	unpublished	JDB 4340
trpC2 relA^{Y308A}	unpublished	JDB 4300
trpC2 ΔsasA::kan ΔsasB::tet	(139)	JDB 4312
trpC2 ΔsasA::kan relA^{Y308A}	unpublished	JDB 4301
168 trpC2 Δ*prpC*	(140)	JDB 1773
168 trpC2 Δ*prkC*	(140)	JDB 1774
trpC2 ΔywaC::kan ΔyjbM::tet ΔrelA::erm	(141)	JDB 4294
trpC2 amyE:P_{xyl}-yjbM spc ΔywaC::kan ΔyjbM::tet ΔrelA::erm	unpublished	JDB 4295
trpC2 subtilis infB$^{G226A\ H230A}$	(99)	JDB 4297
MG1655	Lab stock	JDE 1497
BL21 pETPHOS B. subtilis infB	(99)	JDE 3077
BL21 pETPHOS B. subtilis infB$^{G226A\ H230A}$	(99)	JDE 3078
BL21 pETPHOS B. subtilis fusA	(99)	JDE 3075
BL21 pETPHOS E. coli 1-455 relA	(99)	JDE 3079
DH5α pMINIMAD2 *B. subtilis relA*^{Y308A}	unpublished	JDE 3115
DH5α pMINIMAD2 *B. subtilis sasB^{F42A}*	unpublished	JDE 3135
DH5α AEC 127 B. subtilis P_{sasB}	unpublished	
BL21 pETPHOS *B. subtilis sasB*	unpublished	JDE 3136
BL21 pETPHOS *B. subtilis sasB^{F42A}*	unpublished	JDE 3137
BL21 pETPHOS *B. subtilis yvcI*	unpublished	JDE 3138

Appendix B

Table 3. Oligos used in this thesis

GGCTAGAATTCTGATGCTCTTCCTTTCCG	This study	yjbM operon promoter EcoRI F
GGCTAGGATCCACAAAGTACAGATTCATTTT	This study	yjbM operon promoter BamHI R
GGGCCCGAATTCGATGACAAACAATGGGAG	This study	F42A yjbM EcoRI F pMINIMAD2
GGGCCCGTCGACTTGTTGCTCGCTTCCT	This study	F42A yjbM SalI R pMINIMAD2
TTCACCGATCGAAGCTGTGACCGGACGCG	This study	yjbM F42A F
CGCGTCCGGTCACAGCTTCGATCGGTGAA	This study	yjbM F42A R
CATCTTTCGTTTTTTTCTTG	This study	Y308A relA EcoRI F pMINIMAD2
TGGGCTTCATTCGTTTTG	This study	Y308A relA BamHI R pMINIMAD2
AGCCGAATATGGCTCAATCGCTTCA	This study	Y308A relA F
TGAAGCGATTGAGCCATATTCGGCT	This study	Y308A relA R
CCGGGCATATGGATGACAAACAATGG	This study	yjbM NdeI F
GGGAAAACTAGTCTATTGTTGCTCGCTTCC	This study	yjbM SpeI R
GGGCCCCATATGGTGACGTACTTGCAAAGA	This study	yvcI NdeI F
GGGCCCACTAGTCTATTTGATGTGCTGCGG	This study	yvcI SpeI R
GGGAAAGAATTCATGGCTAAAATGAGAGTATACG	This study	*infB* EcoRI F
GGGAAAGGATCCATTCAAACCGGTAATTTCAACC	This study	*infB* BamHI R
GACAATCATGGCTCACGTTGACC	This study	*infB* G226A F
GGTCAACGTGAGCCATGATTGTC	This study	*infB* G226A R
CCACGTTGACGCTGGGAAAACAA	This study	*infB* H230A F
TTGTTTTCCCAGCGTCAACGTGG	This study	*infB* H230A R
GGGAAACATATGGCTAAAATGAGAGTATACG	This study	*infB* NdeI F
GGGAAAGGATCCGCAAATCCGATCACGTTCTTTCAATTTCTTGC	This study	*infB* BamHI R
GGAAGTCGACAAGGAGGGCGAAAAATGGATTTATCTGTAACACATA	This study	*fusA* NdeI F
CCCAAAGGATCCTTAATCCACTTCTTTCTTAATC	This study	*fusA* BamHI R
GATCGGATCCGCGGCCGCTTCTAGAGGGAGTTCTGAGAATTGGTATGC	This study	*E. coli relA* NdeI F
GATCAAGCTTAACTACATTTATTGTACAACACGAGC	This study	*E. coli relA* N-terminal domain R BamHI

Appendix C

Table 4. Plasmids used in this thesis

pETPHOS	Lab stock
pMINIMAD2	(142)
AEC 127	(64)
pETPHOS WT *sasB*	unpublished
pETPHOS *sasB*^{F42A}	unpublished
pETPHOS *yvcI*	unpublished
pMINIMAD2 *relA*^{Y308A}	unpublished
pMINIMAD2 *sasB*^{F42A}	unpublished
AEC 127 PsasB	unpublished
pDR150	Lab stock
pSac-cm	Lab stock
pDR150 *yjbM*	unpublished
pMINIMAD2 *G226A H230A B. subtilis infB*	(99)
pETPHOS *B. subtilis infB*	(99)
pETPHOS *G226A H230A B. subtilis infB*	(99)
pETPHOS *B. subtilis fusA*	(99)
pETPHOS *E.coli 1-455 relA*	(99)

Appendix D

Cell wall synthesis decreases during exit from rapid growth.

The data provided in this thesis sets up a model for the down-regulation of protein synthesis in a heterogenous manner during entry into stationary phase **(Figure 6.1).** Specifically, this model describes how during entry into stationary phase, one subpopulation of cells downregulates protein synthesis to a greater extent than the rest of the population. This thesis dissects the molecular mechanism by which heterogeneity is regulated in chapter 4 and the mechanism that directly downregulates protein synthesis in the cells with comparatively low levels of protein synthesis in chapter 5. Importantly, the mechanism that regulates heterogeneity in protein synthesis is dependent on the activity of both RelA (whose activity is stimulated by amino acid availability) and SasA (whose expression is regulated by the cell wall sensitive kinase, PrkC). The regulation of *sasA* expression is particularly interesting because it is subject to extrinsic noise that is dependent on PrkC (64). In chapter 4, I also showed that cells with higher *sasA* expression are more likely to have higher protein synthesis, suggesting that noise in *sasA* expression could be directly responsible for the heterogeneity I observed. The extracellular PASTA domain of PrkC is known to directly bind peptidoglycan fragments (61), and PrkC is essential for muropeptide mediated spore germination (60), indicating that PrkC directly senses changes in cell wall synthesis. Because of this, I wished to directly ask if changes in cell wall synthesis could be mediating the difference between cells with comparatively low and high levels of protein synthesis.

To do this, I first observed how cell wall synthesis changed throughout growth by using the fluorescent D-amino acid (FDAA) 7-hydroxycoumarincarbonylamino-D-alanine (HADA) that covalently labels newly synthesized peptidoglycan (143). HADA is a structural analog of the D-

alanine residues that are part of the peptides that cross-link glycan strands in peptidoglycan (143). Incorporation of HADA occurs efficiently during exponential phase and is most visible at the division septum in *B. subtilis* as previously observed (143) **(Appendix D Figure 1)**. During exit from rapid growth (early transition phase) HADA incorporation decreases dramatically, and during late transition phase, most cells have HADA incorporation that is no higher than the background (visible in the single red line at 200-210 a.u bin) **(Appendix D Figure 1)**. Given that the range in HADA incorporation is low even during early transition phase (99% of the population is between 200 and 250 a.u.) compared to OPP incorporation (99% of the population is between 1000 and 2000 a.u.), it is unlikely that a meaningful correlation can be derived between these two probes **(Appendix Figure 2 A)**. Indeed the correlation between both of these probes is low (R^2 0.2263) **(Appendix Figure 2 C** left**).**

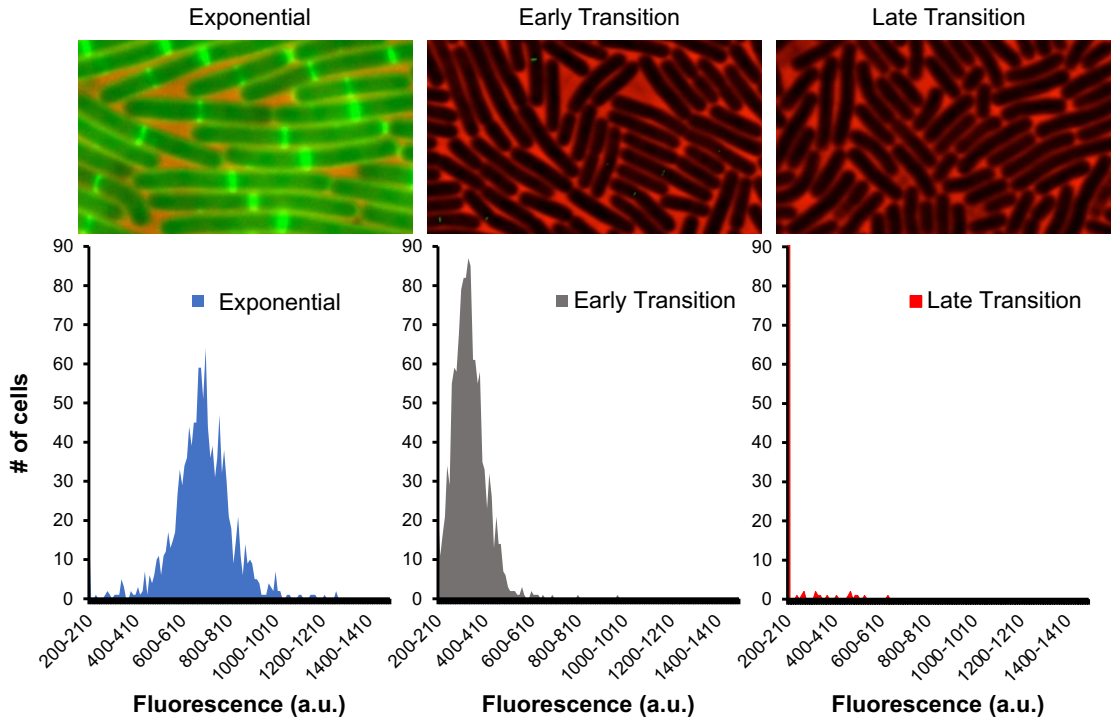

Appendix D Figure 1. Cell wall synthesis decreases during entry into stationary phase. Top row. Microscopy images of HADA incorporation depicted in green and phase contrast in red. **Bottom row.** Population distribution of HADA incorporation throughout growth

I wanted to explore the possibility that under certain conditions, I could increase HADA signal in order to correlate it with OPP in single cells. Peptidoglycan is a mesh-like polymer made up of glycan strains that are cross-linked to each other by short peptides (144). These peptides extend from the glycan strand typically in this order; an L-alanine, a D-glutamic acid, a dibasic amino acid (typically a meso-diaminopimelic acid (*m*DAP) or an L-lysine), a D-alanine, and another D-alanine. In *B. subtilis*, this pentapeptide is cleaved between the two D-alanine residues by the carboxypeptidase PBP 5 (encoded by the gene *dacA*). I reasoned that if I could somehow inhibit this enzyme, it would increase the signal from HADA because the last HADA molecule incorporated would not be cleaved. Recently, the penicillin like drug 6-aminopenicillanic acid (6-APA) was shown to selectively inhibit PBP 5 (145). Consistently, addition of 6-APA to cells during early transition phase increased HADA incorporation without any apparent effect on OPP incorporation **(Appendix Figure 2 A, B).** Although HADA incorporation increases in the presence of 6-APA, the range of signal is still low compared to OPP 99% of the population is between 250 and 330 a.u) next asked if addition of 6-APA affected the correlation observed between HADA and OPP incorporation. I did not observe any difference in R^2 when OPP and HADA are correlated between cells treated with or without 6-APA **(Appendix Figure 2 C)**. Consistently, a *ΔdacA* mutant also does not have increased correlation between OPP and HADA incorporation **(Appendix Figure 3).**

At this point, I am not able to correlate OPP incorporation with HADA. However, I cannot definitively say that this lack of correlation is not due to the low signal provided by HADA incorporation during transition phase, even in the presence of 6-APA.

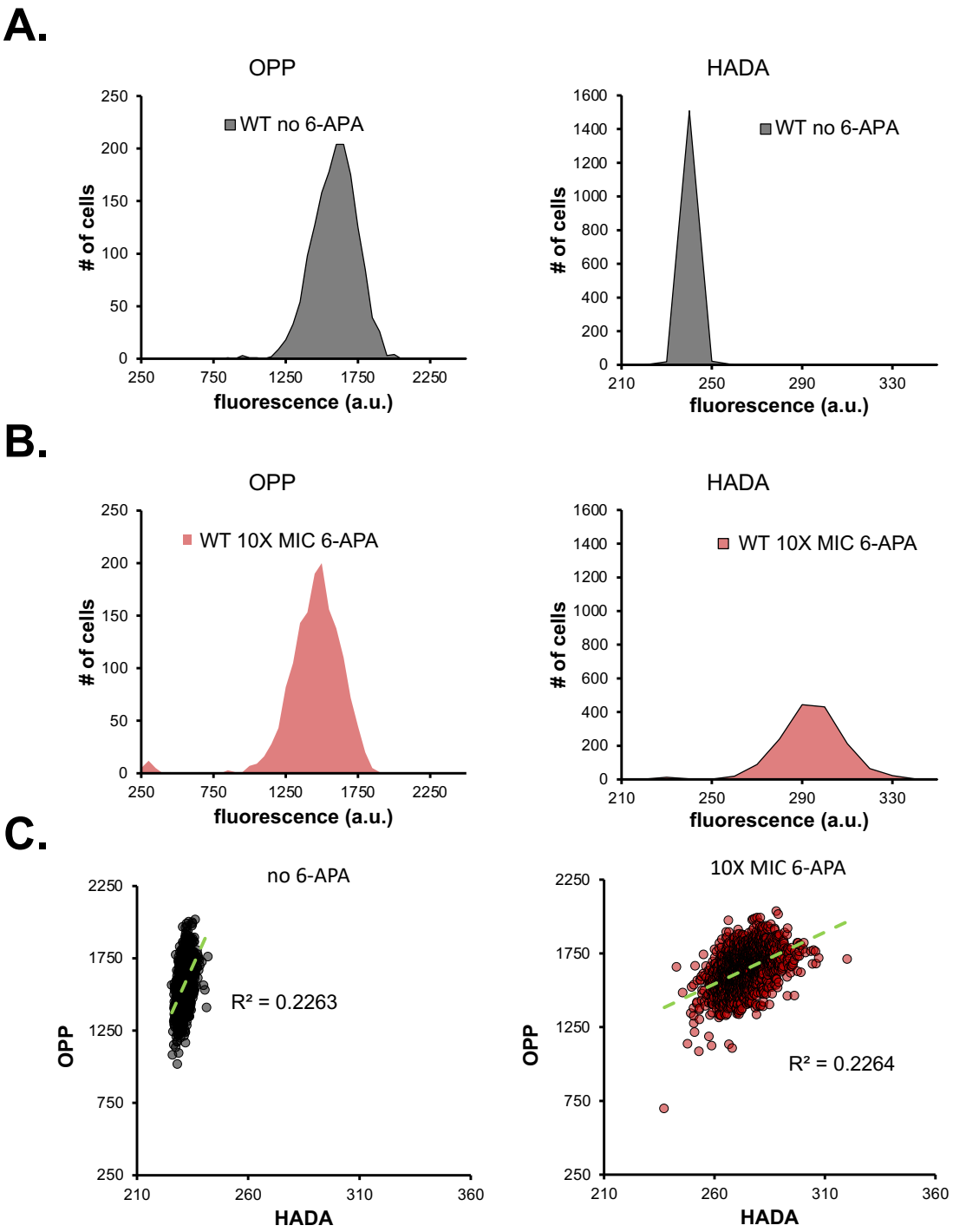

Appendix D Figure 2. Cell wall synthesis in the presence of 6-APA during early transition phase. Population distributions of OPP (left) and HADA (right) incorporation in the absence **(A)** of 6-APA and presence of 10X the MIC of 6-APA **(B). (C)** Plots depicting correlation of single cells labeled with OPP (Y-axis) and HADA (X-axis) during early transition phase in the absence (left) and presence (right) of 6-APA.

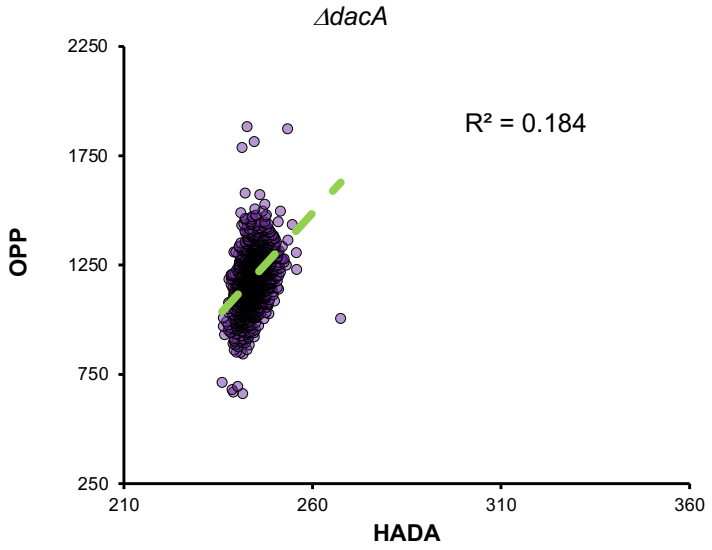

Appendix D Figure 3. Correlation between OPP and HADA incorporation in a *ΔdacA* mutant. Plot depicting correlation of single cells labeled with OPP (Y-axis) and HADA (X-axis) during early transition phase.